Pisias, N.G., Mayer, L.A., Janecek, T.R., Palmer-Julson, A., and van Andel, T.H. (Eds.), 1995
Proceedings of the Ocean Drilling Program, Scientific Results, Vol. 138

19. BIOGENIC SEDIMENTATION AT SITE 847, EASTERN EQUATORIAL PACIFIC OCEAN, DURING THE PAST 3 M.Y.[1]

D.W. Murray,[2] J.W. Farrell,[2,3] and V. McKenna[2]

ABSTRACT

Site 847, located on the equator beneath the region of divergent-driven upwelling in the eastern tropical Pacific Ocean, provides a continuous record of biogenic sedimentation spanning the past 3 m.y. Sediments at the site are primarily composed of carbonate and opal microfossils, with secondary amounts of detrital material that was transported to the site by means of winds. The cyclic changes in the relative abundance of carbonate and opal during the past 1 m.y. exhibit a strong 100-k.y. variability, which generally corresponds to late Pleistocene climatic oscillations. A distinct, carbonate-poor interval is evident from the last major interglacial and has been attributed to a decrease in production rather than to dissolution. The long-term changes in $CaCO_3$ mass accumulation rates (MARs) also are driven by production rather than dissolution. High rates near 2.8 Ma are followed by a distinct minima near 1.8 Ma. $CaCO_3$ MARs increase to a maxima near 0.4 Ma, followed by the decrease in production that occurred during the last interglacial period. Opal accumulations exhibit distinct maxima between 1.7 and 2.0 Ma, 1.1 and 1.3 Ma, and during glacial stages 6 and 2. These increases by more than a factor of 2 in opal accumulation tentatively have been attributed to opal production.

Site 847 provides the eastern anchor of three sites studied from the central (near 140°W) to eastern (near 95°W) equatorial Pacific Ocean to evaluate spatial changes in carbonate and opal sedimentation in an area of strong divergence during the past 3 m.y. Modern oceanographic studies show a west to east gradient in surface productivity across this region. Analysis of the carbonate sedimentation for the past 3 m.y. and the opal sedimentation for the past 1 m.y. at the three sites reveals distinct differences in the respective gradients of accumulation. The west to east gradient in carbonate accumulation is small despite the fact that the eastern site is shallower and has better carbonate preservation. However, the gradient in opal accumulation is steep and shows a four- to fivefold increase from the central to the eastern equatorial Pacific sites. Thus, the surface gradient in primary production is reflected by bulk opal accumulation, not by carbonate accumulation.

INTRODUCTION

The eastern equatorial Pacific Ocean is an area of high biological productivity fueled by the divergence-driven upwelling of nutrient-rich waters associated with the regional trade-wind systems. Chavez and Barber (1987) indicated that this region is responsible for as much as 50% of the global "new" production. An understanding of the response of this biological production to perturbations in climate will provide insights about the role of this area in the transfer of carbon from the surface waters to the deep sea over geologic time. Long continuous records of sediment deposition obtained from the eastern equatorial Pacific during Ocean Drilling Program (ODP) Leg 138 offer the potential to unravel the response of this area to major regional tectonic events (the closing of the Panamanian seaway) and global climate changes that occurred during the late Neogene (Mayer, Pisias, Janecek, et al, 1992).

Sediments recovered at equatorial sites during Leg 138 are largely a mixture of biogenic calcite and opal. Carbonate and opal shells of microplankton that accumulate beneath the equatorial upwelling zone provide an opportunity to quantify past changes in surface production. However, differential preservation of calcite and opal complicates the relationship between production of these microfossils and their accumulation in deep-sea sediments. Careful site selection was necessary to minimize these potential biases when interpreting the geological record. Calcite preservation is dependent upon the carbonate and organic carbon rain, water depth, and carbonate ion concentrations in the water column and pore waters (see Broecker and Peng, 1982; Archer, 1991a, 1991b, and references therein). The relationships between production and accumulation are more reliable at shallow sites that exhibit little depth-dependent dissolution. Seawater is undersaturated with respect to opal at all depths of the ocean; therefore, only a small portion (<10%) of the original rain has been preserved beneath the zone of equatorial upwelling (Broecker and Peng, 1982; Lyle et al., 1988; Archer et al., 1993). Broecker and Peng (1982) suggested that opal preservation is enhanced during periods with high rain rates. Archer et al. (1993) questioned this relationship and suggested that opal preservation in tropical regions reflects the solubility and dissolution kinetics of the opal raining to the seafloor rather than production. Despite this claim, opal concentration does exhibit a match to the global distribution of surface productivity (Leinen et al., 1986), the latitudinal changes in productivity in the eastern Pacific Ocean (Murray and Leinen, 1993), and is a reliable monitor of monsoonal upwelling in the Arabian Sea (Clemens et al., 1991). Although the relationship between opal production and preservation may be complex, sufficient evidence exists to suggest that opal accumulation in some regions at least may be a qualitative measure of surface production.

The goal of this study is to quantify the accumulation of carbonate and opal in a longitudinal transect along the equator so that spatial and temporal changes in surface production can be evaluated for this region during the late Pliocene to Pleistocene. This time interval includes the initiation of Northern Hemisphere glaciation, but it is after the closing of the Isthmus of Panama (Keigwin, 1982). Thus, the regional current patterns that are evident today (Fig. 1) are likely to have existed throughout the time interval considered. Changes in biogenic sediment accumulation should reflect regional to global perturbations in climate and oceanic properties. This study focuses on results from Site 847 (0°11.6′N, 95°19.2′W, water depth of 3334 m), which is the eastern anchor of a transect along the equator beginning in the central Pacific near 140°W (Fig. 1). We use data from the studies of Lyle et al. (1988), Farrell and Prell (1991), and Rea et al. (1991) for the area near 140°W, and Farrell (1991) and Farrell and Prell (1991) for the middle location, Deep Sea Drilling Project (DSDP) Site 572 near 114°W.

[1] Pisias, N.G., Mayer, L.A., Janecek, T.R., Palmer-Julson, A., and van Andel, T.H. (Eds.), 1995. *Proc. ODP, Sci. Results,* 138: College Station, TX (Ocean Drilling Program).
[2] Department of Geological Sciences, Brown University, Providence, RI 02912, U.S.A.
[3] Present address: Department of Oceanography, University of British Columbia, Vancouver, B.C., Canada, V6T 1Z4.

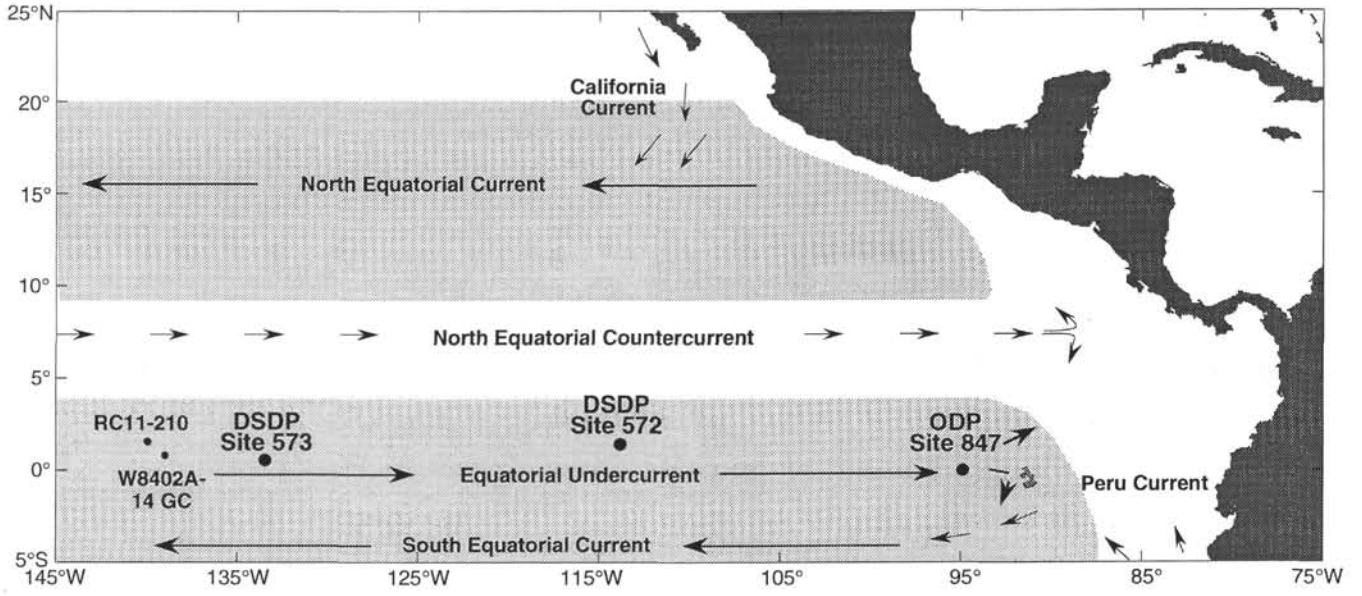

Figure 1. Location map of sites used in this study within the major regional current system. The shaded areas are the annual extent of the North and South Equatorial Current systems.

METHODS

The mean sedimentation rate for Site 847 over the past 3 m.y. is near 35 m/m.y. Samples were taken at 15-cm intervals in Cores 138-847C-1H to -9H, which provide a temporal spacing close enough to resolve precessional-scale variability (23 k.y.) in biogenic sedimentation (Table 1). Additional samples were taken in discrete sections from Holes 847B and 847D to account for disturbed or missing sections that were recognized in Hole 847C (see below). Companion samples were taken at these same depths for foraminiferal and stable isotope studies, and the washing and counting procedures along with faunal and stable isotope data for the top 1 m.y. are presented in chapters by Farrell et al. (this volume) and McKenna et al. (this volume). Included in Table 2 are the dry weight percentage of the sample that is >150-µm, as well as the percentage of whole foraminifers [100 × whole planktonic foraminifers/(whole planktonic foraminifers + fragments)] and the percentage of radiolarians [100 × radiolarians/(whole planktonic foraminifers + radiolarians)] in the >150-µm portion of selected samples.

Composite Depth Section

One of the first tasks in a study of 10^4- to 10^5-yr scale of variability from deep-sea cores is to ensure that the stratigraphic section reflects a continuous record of sediment deposition spanning the period of interest. The existence of sediment recovery gaps between successive cores using the advanced hydraulic piston corer (APC) from DSDP and ODP sites is well documented (Ruddiman et al., 1989; Robinson, 1990; Murray and Prell, 1991; Farrell and Janecek, 1991). These missing sections are evident even with consistent recovery of more than 9.5 m for each 9.5 m drilled, which indicates that the cored material is somehow expanded in the recovery processes. Multiple offset holes drilled at a single site provide a means to construct a continuous stratigraphic section as material from adjacent holes can be "spliced" together to construct a continuous depth section for the site. One of the primary objectives of the Leg 138 Shipboard Scientific Party was to construct composite depth sections for each of the sites drilled (Hagelberg et al., 1992). Each composite depth section considered the stratigraphies from all holes at a site to create a continuous section. Cores from adjacent holes were moved relative to one another by a fixed amount to provide a high interhole correlation for gamma-ray attenuation porosity evaluator (GRAPE), magnetic susceptibility, and color reflectance data. These data were measured in each core soon after recovery at a sample spacing of approximately 2 to 5 cm. The composite stratigraphic section for Site 847, based on the shipboard work, consists of cored intervals from Holes 847B, 847C, and 847D (Hagelberg et al., this volume). Samples used in this study came primarily from Hole 847C, with splices from Holes 847B and 847D. Thus, only a portion of the samples were taken from the sections included in the shipboard spliced composite record. Because significant stretching and squeezing of sections is apparent among the holes at a given site (Hagelberg et al., this volume), a simple transfer of the shipboard meters composite depth (mcd) to Hole 847C will yield offsets in the structure of Hole 847C data relative to other holes and the composite. As shown in Figure 2A, GRAPE data in Holes 847C and 847D can be offset by as much as 0.5 m; the GRAPE maxima at points A, B, and C for Hole 847C are offset in composite depth from the same events in Hole 847D labeled A′, B′, and C′.

A revision is needed to account for the offsets that arise when shipboard mcd is assigned to sections other than those used in the composite. Hagelberg et al. (this volume) derived a revised meters composite depth (rmcd) scale, which stretched and squeezed the composite depth sections within each core to align structure in GRAPE records among holes (Fig. 2B). However, this rmcd (Table 1) assumes a common GRAPE structure for a site and adjusts depths in each hole to fit that structure. For the 579 sample intervals from Hole 847C, which measured approximately 15 cm in ODP depth, 98 were stretched or squeezed by at least 5 cm (Fig. 3). In the extreme case, a 15-cm sample interval within one core, between Samples 138-847C-1H-1, 77 cm, and -1H-1, 92 cm, was stretched by 34 cm using this method. Sedimentation rates derived from the adjusted depth scale may not reflect the true sedimentation rate for an interval within a given hole. Because we develop an isotope stratigraphy from measurements on samples from Holes 847C and 847D, including sections other than the ones used in the final composite for the site, and we use this chronostratigraphy in calculating sedimentation rates and mass accumulation rates (MARs) for each sample, the rmcd scale does not meet the needs of our project. Therefore, a composite depth stratigraphy for Cores 1H to 9H (~0 to 3 Ma) was developed for Site 847 by selecting Hole 847C as the primary record and using sections from Holes 847B and 847D to fill in coring gaps or disturbed intervals. This composite depth reconstruction for Site 847 is summarized in Figure 4 and Table 3. We

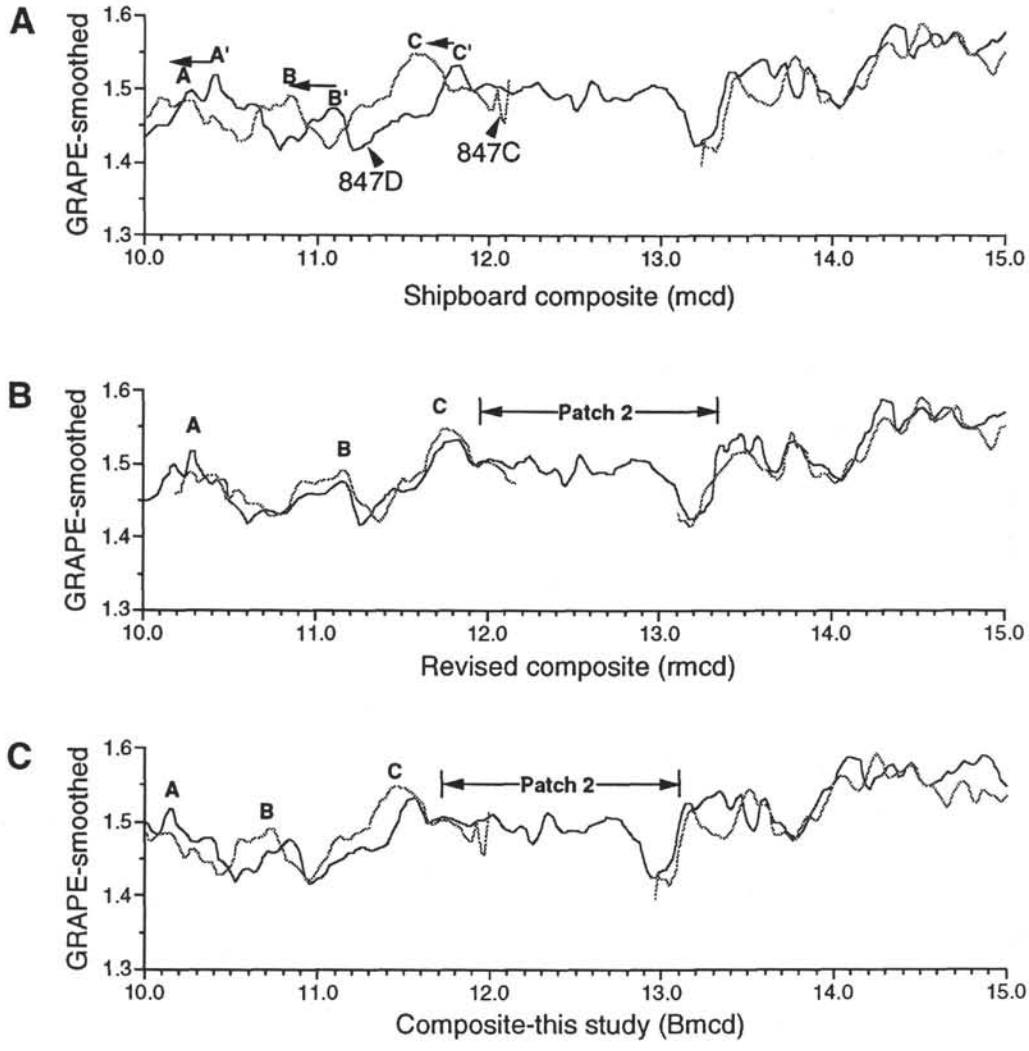

Figure 2. Composite depth reconstruction using smoothed (nine-point Gaussian filter) GRAPE data from Holes 847C and 847D between 10 and 15 m. **A.** Shipboard composite depths (mcd) and applied to data from Holes 847C and 847D. Note offsets in GRAPE structure at events A–A′, B–B′, and C–C′. **B.** Revised composite depth for Site 847 after Hagelberg et al. (this volume). **C.** Meters composite depth (Bmcd) constructed for this study. The reconstruction is similar to that in Figure 2A, but choosing Hole 847C as the primary record and patches and core breaks coming mostly from Hole 847D.

use the notation "Bmcd" (Brown mcd) to distinguish these depths from other composite reconstructions. The new stratigraphy has the same limitations noted above for the shipboard mcd when using an alternative hole as the primary record (Fig. 2C). Care was taken to ensure that GRAPE events adjacent to the patches were aligned to avoid replication and to ensure representation of these events in the composite section.

Chronostratigraphy and Sedimentation Rates

Shackleton et al. (1992) showed that GRAPE density records can be correlated among the Leg 138 sites and that these cycles have a high correlation to solar insolation variations. Shackleton et al. (this volume) use this correlation to assign a chronostratigraphy to the GRAPE records by matching insolation maxima of known age with GRAPE maxima. A total of 89 events between 0 and 3 Ma were used in the age model for Site 847 (Table 4). The ages based on Shackleton et al.'s (this volume) chronology were assigned to samples in this study (Table 1) through interpolation by assuming a linear sedimentation rate of rmcd between datums. Sedimentation rates were assigned to each sample by the rmcd and age difference between a sample and the adjacent younger sample:

$$\text{Sedimentation rate}_{(i)} = [\text{Depth}_{(i)} - \text{Depth}_{(i-1)}]/[\text{Age}_{(i)} - \text{Age}_{(i-1)}].$$

Farrell et al. (this volume) provide an independent chronostratigraphy for Site 847 spanning the top 1.14 m.y., based on oxygen isotope stratigraphy for the composite depth section developed in this study, using the planktonic foraminifer *Globigerinoides sacculifer* (Table 1). A total of 58 events were used for this age model. Farrell et al. (this volume) discuss the differences between the oxygen isotope and GRAPE-based chronologies. Because the oxygen isotope age model is independent of the carbonate changes, we have used this chronology for our time-series analysis and the discussion of the glacial to interglacial variations over the past 1 m.y. Shackleton et al. (this volume) incorporated data from the oxygen isotope studies of Leg 138 sites and presents a revision of the GRAPE-based age model over the past 1 m.y., in addition to that derived by using GRAPE records alone.

Chemical Data

Calcium carbonate and opal concentrations were measured in 5-cm^3 samples of bulk sediment (Table 2). All samples were freeze-dried and two-thirds of the dried sample was removed and ground with a mortar and pestle. Before being analyzed, the ground samples were

Table 1. Site 847 samples and corresponding depths, ages, and sedimentation rates.

Core, section, interval (cm)	ODP depth (mbsf)	Shipboard composite depth (mcd)	Revised composite depth (rmcd)	Composite depth, this study (Bmcd)	Ages		Sedimentation rates	
					Shackleton age model (Ma)	Isotope age model (Ma)	Shackleton ages (m/m.y.)	Isotope ages (m/m.y.)
138-847B-								
1H-1, 2	0.02[a]	0.02	0.02	0.02	0.0010	0.0060	—	—
1H-1, 19	0.19	0.19	0.19	0.19	0.0096	0.0093	19.82	50.77
1H-1, 30	0.30	0.30	0.30	0.30	0.0151	0.0115	19.82	50.77
1H-1, 47	0.47	0.47	0.47	0.47	0.0237	0.0149	19.82	50.77
1H-1, 59	0.59	0.59	0.59	0.59	0.0298	0.0172	19.82	50.77
1H-1, 77	0.77	0.77	0.77	0.77	0.0388	0.0205	19.82	55.46
1H-1, 92	0.92	0.92	0.92	0.92	0.0464	0.0229	19.82	61.11
1H-1, 107	1.07	1.07	1.07	1.07	0.0540	0.0254	19.82	61.11
1H-1, 123	1.23	1.23	1.24	1.23	0.0579	0.0280	40.57	61.11
1H-1, 137	1.37	1.37	1.40	1.37	0.0602	0.0317	62.31	37.60
1H-2, 2	1.52	1.52	1.55	1.52	0.0626	0.0357	62.31	37.60
1H-2, 24	1.74	1.74	1.75	1.74	0.0661	0.0416	62.31	37.60
1H-2, 37	1.87	1.87	1.87	1.87	0.0682	0.0450	62.31	37.60
1H-2, 52	2.02	2.02	2.02	2.02	0.0706	0.0490	62.31	37.60
1H-2, 67	2.17	2.17	2.17	2.17	0.0730	0.0530	62.31	37.60
1H-2, 80	2.30	2.30	2.30	2.30	0.0751	0.0592	62.31	20.83
1H-2, 92	2.42	2.42	2.42	2.42	0.0770	0.0650	62.31	20.83
1H-2, 107	2.57	2.57	2.57	2.57	0.0794	0.0700	62.31	30.00
1H-2, 123	2.73	2.73	2.73	2.73	0.0820	0.0753	62.31	30.00
1H-2, 137	2.87	2.87	2.87	2.87	0.0860	0.0800	35.24	30.00
1H-3, 2	3.02	3.02	3.02	3.02	0.0902	0.0855	35.24	27.50
1H-3, 17	3.17	3.17	3.17	3.17	0.0945	0.0909	35.24	27.50
1H-3, 30	3.30	3.30	3.30	3.30	0.0982	0.0956	35.24	27.50
1H-3, 47	3.47	3.47	3.47	3.47	0.1030	0.1018	35.24	27.50
138-847C-								
1H-1, 122	3.22	3.62	3.60	3.50	0.1042	0.1029	25.65	27.50
1H-1, 137	3.37	3.77	3.74	3.65	0.1100	0.1084	25.65	27.50
1H-2, 2	3.52	3.92	3.87	3.80	0.1159	0.1138	25.65	27.50
1H-2, 17	3.67	4.07	4.00	3.95	0.1217	0.1193	25.65	27.50
1H-2, 32	3.82	4.22	4.14	4.10	0.1271	0.1239	28.04	32.72
1H-2, 47	3.97	4.37	4.30	4.25	0.1310	0.1276	37.72	40.38
1H-2, 65	4.15	4.55	4.51	4.43	0.1358	0.1320	37.72	40.38
1H-2, 77	4.27	4.67	4.67	4.55	0.1390	0.1350	37.72	40.38
1H-2, 92	4.42	4.82	4.87	4.70	0.1430	0.1382	37.72	46.88
1H-2, 107	4.57	4.97	5.05	4.85	0.1469	0.1414	37.72	46.88
1H-2, 122	4.72	5.12	5.20	5.00	0.1509	0.1446	37.72	46.88
1H-2, 137	4.87	5.27	5.32	5.15	0.1549	0.1478	37.72	46.88
1H-3, 2	5.02	5.42	5.44	5.30	0.1589	0.1510	37.72	46.88
1H-3, 17	5.17	5.57	5.57	5.45	0.1629	0.1560	37.72	30.00
1H-3, 32	5.32	5.72	5.71	5.60	0.1668	0.1610	37.72	30.00
1H-3, 47	5.47	5.87	5.87	5.75	0.1708	0.1660	37.72	30.00
1H-3, 62	5.62	6.02	6.03	5.90	0.1748	0.1710	37.72	30.00
1H-3, 77	5.77	6.17	6.19	6.05	0.1788	0.1750	37.72	37.50
1H-3, 92	5.92	6.32	6.34	6.20	0.1827	0.1790	37.72	37.50
1H-3, 107	6.07	6.47	6.48	6.35	0.1867	0.1830	37.72	37.50
1H-3, 122	6.22	6.62	6.61	6.50	0.1907	0.1861	37.72	47.73
1H-3, 137	6.37	6.77	6.76	6.65	0.1947	0.1893	37.72	47.73
1H-4, 2	6.52	6.92	6.91	6.80	0.1986	0.1924	37.72	47.73
1H-4, 17	6.67	7.07	7.07	6.95	0.2026	0.1977	37.72	28.64
1H-4, 32	6.82	7.22	7.22	7.10	0.2066	0.2050	37.72	20.45
1H-4, 47	6.97	7.37	7.36	7.25	0.2106	0.2160	37.72	13.64
1H-4, 62	7.12	7.52	7.51	7.40	0.2146	0.2220	37.72	25.00
1H-4, 77	7.27	7.67	7.67	7.55	0.2188	0.2280	35.14	25.00
1H-4, 92	7.42	7.82	7.84	7.70	0.2250	0.2313	24.32	45.00
1H-4, 107	7.57	7.97	8.03	7.85	0.2312	0.2347	24.32	45.00
1H-4, 122	7.72	8.12	8.20	8.00	0.2373	0.2380	24.32	45.00
1H-4, 137	7.87	8.27	8.36	8.15	0.2435	0.2417	24.32	40.91
1H-5, 2	8.02	8.42	8.52	8.30	0.2497	0.2453	24.32	40.91
1H-5, 17	8.17	8.57	8.68	8.45	0.2558	0.2490	24.32	40.91
1H-5, 32	8.32	8.72	8.83	8.60	0.2620	0.2557	24.32	22.50
1H-5, 47	8.47	8.87	8.98	8.75	0.2666	0.2623	32.68	22.50
1H-5, 62	8.62	9.02	9.11	8.90	0.2712	0.2690	32.68	22.50
1H-5, 77	8.77	9.17	9.24	9.05	0.2758	0.2730	32.68	37.50
1H-5, 92	8.92	9.32	9.39	9.20	0.2804	0.2770	32.68	37.50
1H-5, 107	9.07	9.47	9.56	9.35	0.2850	0.2810	32.68	37.50
1H-5, 122	9.22	9.62	9.77	9.50	0.2895	0.2850	32.68	37.50
1H-5, 137	9.37	9.77	9.97	9.65	0.2958	0.2894	23.79	34.09
1H-6, 2	9.52	9.92	10.12	9.80	0.3023	0.2942	23.10	31.25
1H-6, 17	9.67	10.07	10.25	9.95	0.3088	0.2990	23.10	31.25
1H-6, 32	9.82	10.22	10.37	10.10	0.3141	0.3030	28.26	37.50
1H-6, 47	9.97	10.37	10.51	10.25	0.3189	0.3085	31.82	27.08
1H-6, 62	10.12	10.52	10.70	10.40	0.3236	0.3141	31.82	27.08
1H-6, 77	10.27	10.67	10.93	10.55	0.3283	0.3196	31.82	27.08
1H-6, 92	10.42	10.82	11.13	10.70	0.3330	0.3252	31.82	27.08
1H-6, 107	10.57	10.97	11.28	10.85	0.3368	0.3307	39.05	27.08
1H-6, 122	10.72	11.12	11.41	11.00	0.3407	0.3362	39.05	27.08
1H-6, 137	10.87	11.27	11.52	11.15	0.3445	0.3407	39.05	33.62
1H-7, 2	11.02	11.42	11.63	11.30	0.3484	0.3441	39.05	44.31
1H-7, 17	11.17	11.57	11.75	11.45	0.3522	0.3475	39.05	44.31
1H-7, 32	11.32	11.72	11.88	11.60	0.3570	0.3508	31.30	44.31
1H-7, 47	11.47	11.87	12.02	11.75	0.3626	0.3542	26.67	44.31

Table 1 (continued).

Core, section, interval (cm)	ODP depth (mbsf)	Shipboard composite depth (mcd)	Revised composite depth (rmcd)	Composite depth, this study (Bmcd)	Ages		Sedimentation rates	
					Shackleton age model (Ma)	Isotope age model (Ma)	Shackleton ages (m/m.y.)	Isotope ages (m/m.y.)
138-847D-								
2H–3, 62	10.22	12.02	12.04	11.76	0.3630	0.3545	26.67	44.31
2H–3, 77	10.37	12.17	12.16	11.91	0.3686	0.3578	26.67	44.31
2H–3, 92	10.52	12.32	12.28	12.06	0.3734	0.3612	31.21	44.31
2H–3, 107	10.67	12.47	12.41	12.21	0.3770	0.3646	41.94	44.31
2H–3, 122	10.82	12.62	12.55	12.36	0.3806	0.3680	41.94	44.31
2H–3, 137	10.97	12.77	12.68	12.51	0.3842	0.3750	41.94	21.43
2H–4, 2	11.12	12.92	12.82	12.66	0.3877	0.3802	41.94	29.00
2H–4, 17	11.27	13.07	13.00	12.81	0.3913	0.3853	41.94	29.00
2H–4, 32	11.42	13.22	13.20	12.96	0.3949	0.3905	41.94	29.00
138-847C-								
2H–1, 17	11.67	13.35	13.23	13.08	0.3977	0.3947	41.94	29.00
2H–1, 30	11.82	13.48	13.57	13.21	0.4008	0.3991	41.94	29.00
2H–1, 47	11.97	13.65	13.70	13.38	0.4049	0.4050	41.94	29.00
2H–1, 62	12.12	13.80	13.78	13.53	0.4088	0.4114	38.81	23.28
2H–1, 77	12.27	13.95	13.92	13.68	0.4145	0.4179	26.11	23.28
2H–1, 92	12.42	14.10	14.11	13.83	0.4203	0.4243	26.11	23.28
2H–1, 107	12.57	14.25	14.25	13.98	0.4260	0.4308	26.11	23.28
2H–1, 122	12.72	14.40	14.39	14.13	0.4317	0.4374	26.11	22.78
2H–1, 137	12.87	14.55	14.56	14.28	0.4375	0.4441	26.11	22.30
2H–2, 2	13.02	14.70	14.70	14.43	0.4432	0.4508	26.11	22.30
2H–2, 17	13.17	14.85	14.85	14.58	0.4490	0.4575	26.11	22.30
2H–2, 30	13.30	14.98	14.98	14.71	0.4540	0.4634	26.11	22.30
2H–2, 47	13.47	15.15	15.15	14.88	0.4605	0.4710	26.11	22.30
2H–2, 64	13.64	15.32	15.32	15.05	0.4653	0.4750	35.00	42.86
2H–2, 77	13.77	15.45	15.45	15.18	0.4687	0.4780	39.09	42.86
2H–2, 92	13.92	15.60	15.60	15.33	0.4725	0.4823	39.09	34.62
2H–2, 107	14.07	15.75	15.75	15.48	0.4763	0.4867	39.09	34.62
2H–2, 122	14.22	15.90	15.90	15.63	0.4802	0.4910	39.09	34.62
2H–2, 137	14.37	16.05	16.05	15.78	0.4840	0.4984	39.09	20.15
2H–3, 2	14.52	16.20	16.20	15.93	0.4887	0.5059	31.70	20.15
2H–3, 17	14.67	16.35	16.35	16.08	0.4935	0.5133	31.70	20.15
2H–3, 30	14.82	16.48	16.48	16.21	0.4976	0.5198	31.70	20.15
2H–3, 47	14.97	16.65	16.65	16.38	0.5029	0.5267	31.70	24.53
2H–3, 62	15.12	16.80	16.80	16.53	0.5077	0.5315	31.70	31.34
2H–3, 77	15.27	16.95	16.96	16.68	0.5124	0.5363	31.70	31.34
2H–3, 92	15.42	17.10	17.10	16.83	0.5171	0.5411	31.70	31.34
2H–3, 107	15.57	17.25	17.24	16.98	0.5218	0.5459	31.70	31.34
2H–3, 122	15.72	17.40	17.40	17.13	0.5266	0.5506	31.70	31.34
2H–3, 137	15.87	17.55	17.57	17.28	0.5346	0.5554	18.81	31.34
2H–4, 2	16.02	17.70	17.71	17.43	0.5439	0.5602	16.02	31.34
2H–4, 17	16.17	17.85	17.85	17.58	0.5533	0.5650	16.02	31.34
2H–4, 32	16.32	18.00	17.99	17.73	0.5626	0.5686	16.02	41.67
2H–4, 47	16.47	18.15	18.14	17.88	0.5720	0.5722	16.02	41.67
2H–4, 62	16.62	18.30	18.31	18.03	0.5794	0.5768	20.38	32.97
2H–4, 77	16.77	18.45	18.46	18.18	0.5844	0.5823	29.58	27.27
2H–4, 92	16.92	18.60	18.60	18.33	0.5895	0.5878	29.58	27.27
2H–4, 107	17.07	18.75	18.76	18.48	0.5946	0.5933	29.58	27.27
2H–4, 122	17.22	18.90	18.91	18.63	0.5997	0.5988	29.58	27.27
2H–4, 137	17.37	19.05	19.05	18.78	0.6047	0.6043	29.58	27.27
2H–5, 2	17.52	19.20	19.20	18.93	0.6098	0.6103	29.58	24.66
2H–5, 17	17.67	19.35	19.36	19.08	0.6149	0.6170	29.58	22.50
2H–5, 30	17.82	19.48	19.49	19.21	0.6193	0.6210	29.58	32.14
2H–5, 47	17.97	19.65	19.65	19.38	0.6250	0.6263	29.58	32.14
2H–5, 62	18.12	19.80	19.79	19.53	0.6301	0.6310	29.58	32.14
2H–5, 77	18.27	19.95	19.95	19.68	0.6352	0.6366	29.58	26.61
2H–5, 92	18.42	20.10	20.10	19.83	0.6402	0.6423	29.58	26.61
2H–5, 107	18.57	20.25	20.25	19.98	0.6453	0.6479	29.58	26.61
2H–5, 122	18.72	20.40	20.40	20.13	0.6509	0.6535	26.87	26.61
2H–5, 137	18.87	20.55	20.55	20.28	0.6570	0.6592	24.32	26.61
2H–6, 2	19.02	20.70	20.70	20.43	0.6632	0.6648	24.32	26.61
2H–6, 17	19.17	20.85	20.87	20.58	0.6694	0.6705	24.32	26.61
2H–6, 30	19.32	20.98	21.00	20.71	0.6747	0.6753	24.32	26.61
2H–6, 47	19.47	21.15	21.14	20.88	0.6817	0.6817	24.32	26.61
2H–6, 64	19.62	21.32	21.35	21.05	0.6887	0.6881	24.32	26.61
2H–6, 77	19.77	21.45	21.55	21.18	0.6970	0.6930	15.68	26.61
2H–6, 92	19.92	21.60	21.71	21.33	0.7120	0.6984	10.00	27.78
2H–6, 107	20.07	21.75	21.84	21.48	0.7174	0.7038	27.57	27.78
2H–6, 122	20.22	21.90	22.02	21.63	0.7229	0.7092	27.57	27.78
2H–6, 137	20.37	22.05	22.19	21.78	0.7283	0.7146	27.57	27.78
2H–7, 2	20.52	22.20	22.34	21.93	0.7338	0.7200	27.57	27.78
2H–7, 17	20.67	22.35	22.46	22.08	0.7392	0.7264	27.57	23.33
2H–7, 30	20.82	22.48	22.54	22.21	0.7439	0.7320	27.57	23.33
138-847D-								
3H–3, 62	19.72	22.72	22.72	22.38	0.7497	0.7385	29.62	26.11
3H–3, 77	19.87	22.87	22.86	22.53	0.7530	0.7443	45.39	26.11
3H–3, 92	20.02	23.02	23.01	22.68	0.7563	0.7500	45.39	26.11
3H–3, 107	20.17	23.17	23.17	22.83	0.7596	0.7553	45.39	28.18
3H–3, 122	20.32	23.32	23.32	22.98	0.7629	0.7606	45.39	28.18
3H–3, 137	20.47	23.47	23.47	23.13	0.7662	0.7660	45.39	28.18

Table 1 (continued).

Core, section, interval (cm)	ODP depth (mbsf)	Shipboard composite depth (mcd)	Revised composite depth (rmcd)	Composite depth, this study (Bmcd)	Ages		Sedimentation rates	
					Shackleton age model (Ma)	Isotope age model (Ma)	Shackleton ages (m/m.y.)	Isotope ages (m/m.y.)
138-847C-								
3H–1, 17	21.17	23.57	23.48	23.31	0.7701	0.7724	45.39	28.18
3H–1, 32	21.32	23.72	23.62	23.46	0.7735	0.7777	45.39	28.18
3H–1, 47	21.47	23.87	23.72	23.61	0.7768	0.7830	45.39	28.18
3H–1, 62	21.62	24.02	23.84	23.76	0.7801	0.7880	45.39	30.00
3H–1, 77	21.77	24.17	24.01	23.91	0.7834	0.7930	45.39	30.00
3H–1, 92	21.92	24.32	24.27	24.06	0.7867	0.7980	45.39	30.00
3H–1, 107	22.07	24.47	24.47	24.21	0.7931	0.8028	23.22	31.54
3H–1, 122	22.22	24.62	24.62	24.36	0.7999	0.8075	22.03	31.54
3H–1, 137	22.37	24.77	24.77	24.51	0.8067	0.8123	22.03	31.54
3H–2, 2	22.52	24.92	24.92	24.66	0.8136	0.8170	22.03	31.54
3H–2, 17	22.67	25.07	25.07	24.81	0.8204	0.8218	22.03	31.54
3H–2, 30	22.82	25.20	25.20	24.94	0.8254	0.8259	25.84	31.54
3H–2, 47	22.97	25.37	25.37	25.11	0.8302	0.8313	35.71	31.54
3H–2, 65	23.12	25.55	25.55	25.29	0.8352	0.8370	35.71	31.54
3H–2, 77	23.27	25.67	25.67	25.41	0.8386	0.8411	35.71	29.33
3H–2, 92	23.42	25.82	25.82	25.56	0.8428	0.8462	35.71	29.33
3H–2, 107	23.57	25.97	25.97	25.71	0.8470	0.8513	35.71	29.33
3H–2, 122	23.72	26.12	26.12	25.86	0.8512	0.8564	35.71	29.33
3H–2, 137	23.87	26.27	26.27	26.01	0.8554	0.8615	35.71	29.33
3H–3, 2	24.02	26.42	26.42	26.16	0.8596	0.8667	35.71	29.33
3H–3, 17	24.17	26.57	26.57	26.31	0.8638	0.8718	35.71	29.33
3H–3, 32	24.32	26.72	26.72	26.46	0.8680	0.8769	35.71	29.33
3H–3, 47	24.47	26.87	26.87	26.61	0.8722	0.8820	35.71	29.33
3H–3, 62	24.62	27.02	27.02	26.76	0.8764	0.8868	35.71	31.25
3H–3, 76	24.76	27.16	27.16	26.90	0.8803	0.8913	35.71	31.25
3H–3, 92	24.92	27.32	27.32	27.06	0.8848	0.8964	35.71	31.25
3H–3, 107	25.07	27.47	27.47	27.21	0.8890	0.9012	35.71	31.25
3H–3, 122	25.22	27.62	27.61	27.36	0.8932	0.9060	35.71	31.25
3H–3, 137	25.37	27.77	27.75	27.51	0.8974	0.9100	35.71	37.50
3H–4, 2	25.52	27.92	27.91	27.66	0.9016	0.9140	35.71	37.50
3H–4, 17	25.67	28.07	28.06	27.81	0.9058	0.9180	35.71	37.50
3H–4, 32	25.82	28.22	28.22	27.96	0.9114	0.9233	26.80	28.13
3H–4, 47	25.97	28.37	28.37	28.11	0.9185	0.9287	20.86	28.13
3H–4, 62	26.12	28.52	28.52	28.26	0.9257	0.9340	20.86	28.13
3H–4, 76	26.26	28.66	28.66	28.40	0.9325	0.9390	20.86	28.13
3H–4, 92	26.42	28.82	28.82	28.56	0.9401	0.9447	20.86	28.13
3H–4, 107	26.57	28.97	28.97	28.71	0.9473	0.9500	20.86	28.13
3H–4, 122	26.72	29.12	29.12	28.86	0.9545	0.9543	20.86	35.00
3H–4, 137	26.87	29.27	29.27	29.01	0.9617	0.9586	20.86	35.00
3H–5, 2	27.02	29.42	29.42	29.16	0.9689	0.9629	20.86	35.00
3H–5, 17	27.17	29.57	29.57	29.31	0.9761	0.9694	20.86	22.93
3H–5, 32	27.32	29.72	29.72	29.46	0.9810	0.9782	30.81	17.05
3H–5, 47	27.47	29.87	29.87	29.61	0.9850	0.9870	37.27	17.05
3H–5, 62	27.62	30.02	30.02	29.76	0.9890	0.9900	37.27	50.00
3H–5, 76	27.76	30.16	30.16	29.90	0.9928	0.9928	37.27	50.00
3H–5, 92	27.92	30.32	30.32	30.06	0.9970	0.9960	37.27	50.00
3H–5, 107	28.07	30.47	30.47	30.21	1.0018	0.9990	31.45	50.00
3H–5, 122	28.22	30.62	30.62	30.36	1.0086	1.0020	22.00	50.00
3H–5, 137	28.37	30.77	30.77	30.51	1.0155	1.0050	22.00	50.00
3H–6, 2	28.52	30.92	30.92	30.66	1.0223	1.0100	22.00	30.29
3H–6, 17	28.67	31.07	31.07	30.81	1.0291	1.0149	22.00	30.29
3H–6, 30	28.82	31.20	31.20	30.94	1.0350	1.0192	22.00	30.29
3H–6, 47	28.97	31.37	31.37	31.11	1.0427	1.0255	22.00	26.98
3H–6, 65	29.12	31.55	31.55	31.29	1.0504	1.0329	23.43	24.32
3H–6, 77	29.27	31.67	31.66	31.41	1.0529	1.0378	48.64	24.32
3H–6, 92	29.42	31.82	31.81	31.56	1.0560	1.0440	48.64	24.32
3H–6, 107	29.57	31.97	31.99	31.71	1.0590	1.0474	48.64	43.75
3H–6, 122	29.72	32.12	32.17	31.86	1.0621	1.0509	48.64	43.75
3H–6, 137	29.87	32.27	32.34	32.01	1.0652	1.0543	48.64	43.75
3H–7, 2	30.02	32.42	32.48	32.16	1.0683	1.0577	48.64	43.75
3H–7, 17	30.17	32.57	32.59	32.31	1.0714	1.0611	48.64	43.75
3H–7, 30	30.30	32.70	32.68	32.44	1.0747	1.0641	39.19	43.75
3H–7, 47	30.47	32.87	32.84	32.61	1.0793	1.0680	37.03	43.75
3H–7, 62	30.62	33.02	33.05	32.76	1.0833	1.0728	37.03	31.48
138-847D-								
4H–3, 47	29.07	33.07	33.07	32.86	1.0860	1.0759	37.03	31.48
4H–3, 62	29.22	33.22	33.22	33.01	1.0901	1.0807	37.03	31.48
4H–3, 77	29.37	33.37	33.37	33.16	1.0941	1.0855	37.03	31.48
4H–3, 92	29.52	33.52	33.51	33.31	1.0982	1.0902	37.03	31.48
4H–3, 107	29.67	33.67	33.66	33.46	1.1022	1.0950	37.03	31.48
4H–3, 122	29.82	33.82	33.82	33.61	1.1063	1.0993	37.03	35.00
4H–3, 137	29.97	33.97	33.97	33.76	1.1103	1.1036	37.03	35.00
138-847C-								
4H–1, 32	30.82	34.12	34.22	33.94	1.1152	1.1087	37.03	35.00
4H–1, 47	30.97	34.27	34.58	34.09	1.1193	1.1130	37.03	35.00
4H–1, 61	31.11	34.41	34.68	34.23	1.1230	1.1174	37.03	32.14
4H–1, 77	31.27	34.57	34.76	34.39	1.1274	1.1223	37.03	32.14
4H–1, 92	31.42	34.72	34.85	34.54	1.1314	1.1270	37.03	32.14
4H–1, 107	31.57	34.87	34.95	34.69	1.1355	1.1323	37.03	28.13
4H–1, 122	31.72	35.02	35.08	34.84	1.1395	1.1377	37.03	28.12
4H–1, 137	31.87	35.17	35.22	34.99	1.1436	1.1430	37.03	28.13

Table 1 (continued).

Core, section, interval (cm)	ODP depth (mbsf)	Shipboard composite depth (mcd)	Revised composite depth (rmcd)	Composite depth, this study (Bmcd)	Ages		Sedimentation rates	
					Shackleton age model (Ma)	Isotope age model (Ma)	Shackleton ages (m/m.y.)	Isotope ages (m/m.y.)
4H–2, 2	32.02	35.32	35.34	35.14	1.1476	—	37.03	—
4H–2, 17	32.17	35.47	35.48	35.29	1.1517	—	37.03	—
4H–2, 32	32.32	35.62	35.63	35.44	1.1557	—	37.03	—
4H–2, 47	32.47	35.77	35.78	35.59	1.1598	—	37.03	—
4H–2, 63.5	32.635	35.94	35.93	35.76	1.1642	—	37.03	—
4H–2, 77	32.77	36.07	36.02	35.89	1.1679	—	37.03	—
4H–2, 88	32.88	36.18	36.10	36.00	1.1708	—	37.03	—
4H–2, 107	33.07	36.37	36.26	36.19	1.1760	—	37.03	—
4H–2, 122	33.22	36.52	36.39	36.34	1.1800	—	37.03	—
4H–2, 137	33.37	36.67	36.50	36.49	1.1841	—	37.03	—
4H–3, 2	33.52	36.82	36.59	36.64	1.1881	—	37.03	—
4H–3, 17	33.67	36.97	36.68	36.79	1.1922	—	37.03	—
4H–3, 32	33.82	37.12	36.78	36.94	1.1962	—	37.03	—
4H–3, 47	33.97	37.27	36.99	37.09	1.2003	—	37.03	—
4H–3, 61	34.11	37.41	37.42	37.23	1.2041	—	37.03	—
4H–3, 77	34.27	37.57	37.84	37.39	1.2074	—	48.10	—
4H–3, 92	34.42	37.72	37.97	37.54	1.2102	—	52.50	—
4H–3, 107	34.57	37.87	38.07	37.69	1.2131	—	52.50	—
4H–3, 122	34.72	38.02	38.19	37.84	1.2162	—	48.04	—
4H–3, 137	34.87	38.17	38.33	37.99	1.2199	—	41.07	—
4H–4, 2	35.02	38.32	38.48	38.14	1.2235	—	41.07	—
4H–4, 17	35.17	38.47	38.61	38.29	1.2272	—	41.07	—
4H–4, 30	35.30	38.60	38.72	38.42	1.2303	—	41.07	—
4H–4, 47	35.47	38.77	38.86	38.59	1.2345	—	41.07	—
4H–4, 61	35.61	38.91	38.96	38.73	1.2379	—	41.07	—
4H–4, 77	35.77	39.07	39.06	38.89	1.2418	—	41.07	—
4H–4, 92	35.92	39.22	39.15	39.04	1.2470	—	28.90	—
4H–4, 107	36.07	39.37	39.25	39.19	1.2529	—	25.17	—
4H–4, 122	36.22	39.52	39.37	39.34	1.2589	—	25.17	—
4H–4, 137	36.37	39.67	39.52	39.49	1.2648	—	25.17	—
4H–5, 2	36.52	39.82	39.73	39.64	1.2708	—	25.17	—
4H–5, 17	36.67	39.97	39.95	39.79	1.2742	—	44.22	—
4H–5, 30	36.80	40.10	40.17	39.92	1.2766	—	54.55	—
4H–5, 47	36.97	40.27	40.38	40.09	1.2797	—	54.55	—
4H–5, 61	37.11	40.41	40.48	40.23	1.2823	—	54.55	—
4H–5, 77	37.27	40.57	40.59	40.39	1.2875	—	30.78	—
4H–5, 92	37.42	40.72	40.68	40.54	1.2930	—	26.87	—
4H–5, 107	37.57	40.87	40.79	40.69	1.2986	—	26.88	—
4H–5, 122	37.72	41.02	40.95	40.84	1.3042	—	26.87	—
4H–5, 137	37.87	41.17	41.19	40.99	1.3097	—	27.55	—
4H–6, 2	38.02	41.32	41.41	41.14	1.3150	—	28.25	—
4H–6, 17	38.17	41.47	41.56	41.29	1.3203	—	28.25	—
4H–6, 29	38.29	41.59	41.66	41.41	1.3245	—	28.25	—
4H–6, 47	38.47	41.77	41.85	41.59	1.3285	—	45.63	—
4H–6, 64	38.64	41.94	42.05	41.76	1.3307	—	75.00	—
4H–6, 77	38.77	42.07	42.19	41.89	1.3325	—	75.00	—
4H–6, 92	38.92	42.22	42.30	42.04	1.3345	—	75.00	—
138-847D-								
4H–6, 107	39.07	42.37	42.39	42.19	1.3365	—	75.00	—
4H–6, 122	39.22	42.52	42.46	42.34	1.3403	—	38.65	—
4H–6, 137	39.37	42.67	42.55	42.49	1.3449	—	32.86	—
4H–7, 2	39.52	42.82	42.69	42.64	1.3495	—	32.86	—
4H–7, 17	39.67	42.97	42.99	42.79	1.3540	—	32.86	—
4H–7, 32	39.82	43.12	43.36	42.94	1.3586	—	32.86	—
4H–7, 47	39.97	43.27	43.46	43.09	1.3632	—	32.86	—
5H–3, 107	39.17	43.37	43.38	43.17	1.3656	—	32.86	—
5H–3, 122	39.32	43.52	43.53	43.32	1.3702	—	32.86	—
5H–3, 137	39.47	43.67	43.67	43.47	1.3747	—	32.86	—
5H–4, 2	39.62	43.82	43.82	43.62	1.3792	—	33.44	—
5H–4, 17	39.77	43.97	43.99	43.77	1.3826	—	44.52	—
5H–4, 32	39.92	44.12	44.14	43.92	1.3860	—	44.52	—
5H–4, 47	40.07	44.27	44.27	44.07	1.3893	—	44.52	—
5H–4, 62	40.22	44.42	44.41	44.22	1.3927	—	44.52	—
5H–4, 77	40.37	44.57	44.55	44.37	1.3961	—	44.52	—
5H–4, 92	40.52	44.72	44.72	44.52	1.3994	—	44.52	—
138-847C-								
5H–1, 47	40.47	44.97	44.84	44.62	1.4030	—	28.23	—
5H–1, 62	40.62	45.12	45.01	44.77	1.4089	—	25.16	—
5H–1, 77	40.77	45.27	45.15	44.92	1.4149	—	25.16	—
5H–1, 92	40.92	45.42	45.30	45.07	1.4209	—	25.16	—
5H–1, 107	41.07	45.57	45.48	45.22	1.4268	—	25.16	—
5H–1, 122	41.22	45.72	45.61	45.37	1.4325	—	26.46	—
5H–1, 137	41.37	45.87	45.75	45.52	1.4375	—	30.08	—
5H–2, 2	41.52	46.02	45.97	45.67	1.4425	—	30.08	—
5H–2, 17	41.67	46.17	46.15	45.82	1.4475	—	30.08	—
5H–2, 28	41.78	46.28	46.29	45.93	1.4511	—	30.08	—
5H–2, 47	41.97	46.47	46.51	46.12	1.4574	—	30.08	—
5H–2, 64	42.14	46.64	46.67	46.29	1.4631	—	30.08	—
5H–2, 77	42.27	46.77	46.76	46.42	1.4674	—	30.08	—
5H–2, 92	42.42	46.92	46.90	46.57	1.4724	—	30.08	—
5H–2, 107	42.57	47.07	47.08	46.72	1.4774	—	30.08	—
5H–2, 122	42.72	47.22	47.22	46.87	1.4824	—	30.08	—

Table 1 (continued).

Core, section, interval (cm)	ODP depth (mbsf)	Shipboard composite depth (mcd)	Revised composite depth (rmcd)	Composite depth, this study (Bmcd)	Ages		Sedimentation rates	
					Shackleton age model (Ma)	Isotope age model (Ma)	Shackleton ages (m/m.y.)	Isotope ages (m/m.y.)
5H-2, 137	42.87	47.37	47.36	47.02	1.4873	—	30.08	—
5H-3, 2	43.02	47.52	47.53	47.17	1.4923	—	30.08	—
5H-3, 17	43.17	47.67	47.67	47.32	1.4973	—	30.01	—
5H-3, 28	43.28	47.78	47.78	47.43	1.5010	—	30.00	—
5H-3, 47	43.47	47.97	47.99	47.62	1.5073	—	30.00	—
5H-3, 62	43.62	48.12	48.11	47.77	1.5123	—	30.00	—
5H-3, 77	43.77	48.27	48.26	47.92	1.5173	—	30.00	—
5H-3, 92	43.92	48.42	48.43	48.07	1.5223	—	30.00	—
5H-3, 107	44.07	48.57	48.57	48.22	1.5273	—	30.00	—
5H-3, 122	44.22	48.72	48.72	48.37	1.5321	—	31.54	—
5H-3, 137	44.37	48.87	48.89	48.52	1.5368	—	31.79	—
5H-4, 2	44.52	49.02	49.04	48.67	1.5415	—	31.79	—
5H-4, 17	44.67	49.17	49.17	48.82	1.5462	—	31.79	—
5H-4, 28	44.78	49.28	49.27	48.93	1.5497	—	31.79	—
5H-4, 47	44.97	49.47	49.46	49.12	1.5557	—	31.79	—
5H-4, 62	45.12	49.62	49.63	49.27	1.5604	—	31.79	—
5H-4, 77	45.27	49.77	49.77	49.42	1.5651	—	31.79	—
5H-4, 92	45.42	49.92	49.92	49.57	1.5703	—	28.85	—
5H-4, 107	45.57	50.07	50.07	49.72	1.5758	—	27.18	—
5H-4, 122	45.72	50.22	50.23	49.87	1.5813	—	27.18	—
5H-4, 137	45.87	50.37	50.40	50.02	1.5869	—	27.18	—
5H-5, 2	46.02	50.52	50.54	50.17	1.5924	—	27.18	—
5H-5, 17	46.17	50.67	50.67	50.32	1.5979	—	27.18	—
5H-5, 28	46.28	50.78	50.78	50.43	1.6020	—	27.18	—
5H-5, 47	46.47	50.97	50.97	50.62	1.6092	—	26.39	—
5H-5, 62	6.62	51.12	51.10	50.77	1.6151	—	25.38	—
5H-5, 77	46.77	51.27	51.27	50.92	1.6210	—	25.38	—
5H-5, 92	46.92	51.42	51.42	51.07	1.6269	—	25.38	—
5H-5, 107	47.07	51.57	51.57	51.22	1.6328	—	25.38	—
5H-5, 122	47.22	51.72	51.71	51.37	1.6387	—	25.38	—
5H-5, 137	47.37	51.87	51.83	51.52	1.6446	—	25.38	—
5H-6, 2	47.52	52.02	51.93	51.67	1.6505	—	25.38	—
5H-6, 17	47.67	52.17	52.02	51.82	1.6564	—	25.38	—
5H-6, 28	47.78	52.28	52.09	51.93	1.6608	—	25.38	—
5H-6, 47	47.97	52.47	52.24	52.12	1.6682	—	25.38	—
5H-6, 64	48.14	52.64	52.41	52.29	1.6749	—	25.38	—
5H-6, 77	48.27	52.77	52.73	52.42	1.6801	—	25.38	—
5H-6, 92	48.42	52.92	52.95	52.57	1.6860	—	25.38	—
5H-6, 107	48.57	53.07	53.03	52.72	1.6919	—	25.38	—
5H-6, 122	48.72	53.22	53.10	52.87	1.6972	—	28.16	—
5H-6, 137	48.87	53.37	53.21	53.02	1.6987	—	97.62	—
5H-7, 2	49.02	53.52	53.37	53.17	1.7003	—	97.62	—
5H-7, 17	49.17	53.67	53.55	53.32	1.7018	—	97.62	—
5H-7, 28	49.28	53.78	53.68	53.43	1.7029	—	97.62	—
5H-7, 47	49.47	53.97	54.00	53.62	1.7049	—	97.62	—
5H-7, 64	49.64	54.14	54.20	53.79	1.7066	—	97.62	—
138-847D-								
6H-3, 32	47.92	54.12	54.14	53.89	1.7077	—	97.62	—
6H-3, 47	48.07	54.27	54.28	54.04	1.7092	—	97.62	—
6H-3, 62	48.22	54.42	54.42	54.19	1.7107	—	97.62	—
6H-3, 77	48.37	54.57	54.56	54.34	1.7123	—	97.62	—
6H-3, 92	48.52	54.72	54.70	54.49	1.7138	—	97.62	—
6H-3, 107	48.67	54.87	54.86	54.64	1.7153	—	97.62	—
6H-3, 122	48.82	55.02	55.02	54.79	1.7169	—	97.62	—
6H-3, 137	48.97	55.17	55.20	54.94	1.7203	—	43.43	—
138-847C-								
6H-1, 17	49.67	55.37	55.42	54.95	1.7209	—	17.19	—
6H-1, 30	49.80	55.50	55.50	55.08	1.7285	—	17.19	—
6H-1, 47	49.97	55.67	55.67	55.25	1.7384	—	17.19	—
6H-1, 62	50.12	55.82	55.82	55.40	1.7471	—	17.19	—
6H-1, 77	50.27	55.97	55.97	55.55	1.7534	—	23.75	—
6H-1, 92	50.42	56.12	56.12	55.70	1.7585	—	29.34	—
6H-1, 107	50.57	56.27	56.27	55.85	1.7636	—	29.34	—
6H-1, 122	50.72	56.42	56.42	56.00	1.7687	—	29.34	—
6H-1, 137	50.87	56.57	56.57	56.15	1.7739	—	29.34	—
6H-2, 2	51.02	56.72	56.70	56.30	1.7790	—	29.34	—
6H-2, 17	51.17	56.87	56.86	56.45	1.7841	—	29.34	—
6H-2, 30	51.30	57.00	57.00	56.58	1.7885	—	29.34	—
6H-2, 47	51.47	57.17	57.17	56.75	1.7943	—	29.34	—
6H-2, 58	51.58	57.28	57.28	56.86	1.7981	—	29.34	—
6H-2, 77	51.77	57.47	57.47	57.05	1.8045	—	29.34	—
6H-2, 92	51.92	57.62	57.61	57.20	1.8096	—	29.34	—
6H-2, 107	52.07	57.77	57.77	57.35	1.8130	—	44.02	—
6H-2, 122	52.22	57.92	57.92	57.50	1.8158	—	53.81	—
6H-2, 137	52.37	58.07	58.07	57.65	1.8186	—	53.81	—
6H-3, 2	52.52	58.22	58.22	57.80	1.8214	—	53.81	—
6H-3, 17	52.67	58.37	58.37	57.95	1.8242	—	53.81	—
6H-3, 29	52.79	58.49	58.49	58.07	1.8264	—	53.81	—
6H-3, 47	52.97	58.67	58.67	58.25	1.8298	—	53.81	—
6H-3, 62	53.12	58.82	58.82	58.40	1.8325	—	54.46	—
6H-3, 77	53.27	58.97	58.98	58.55	1.8351	—	57.21	—
6H-3, 92	53.42	59.12	59.12	58.70	1.8378	—	57.21	—

Table 1 (continued).

Core, section, interval (cm)	ODP depth (mbsf)	Shipboard composite depth (mcd)	Revised composite depth (rmcd)	Composite depth, this study (Bmcd)	Ages		Sedimentation rates	
					Shackleton age model (Ma)	Isotope age model (Ma)	Shackleton ages (m/m.y.)	Isotope ages (m/m.y.)
6H–3, 107	53.57	59.27	59.27	58.85	1.8404	—	57.21	—
6H–3, 122	53.72	59.42	59.44	59.00	1.8430	—	57.21	—
6H–3, 137	53.87	59.57	59.57	59.15	1.8456	—	57.21	—
6H–4, 2	54.02	59.72	59.70	59.30	1.8483	—	57.21	—
6H–4, 17	54.17	59.87	59.86	59.45	1.8509	—	57.21	—
6H–4, 28	54.28	59.98	59.99	59.56	1.8528	—	57.21	—
6H–4, 47	54.47	60.17	60.16	59.75	1.8561	—	57.21	—
6H–4, 62	54.62	60.32	60.32	59.90	1.8587	—	57.21	—
6H–4, 77	54.77	60.47	60.47	60.05	1.8614	—	57.21	—
6H–4, 92	54.92	60.62	60.62	60.20	1.8640	—	57.21	—
6H–4, 107	55.07	60.77	60.77	60.35	1.8666	—	57.21	—
6H–4, 122	55.22	60.92	60.92	60.50	1.8692	—	57.21	—
6H–4, 137	55.37	61.07	61.07	60.65	1.8719	—	57.21	—
6H–5, 2	55.52	61.22	61.22	60.80	1.8745	—	57.21	—
6H–5, 17	55.67	61.37	61.37	60.95	1.8801	—	26.59	—
6H–5, 28	55.78	61.48	61.48	61.06	1.8848	—	23.45	—
6H–5, 47	55.97	61.67	61.67	61.25	1.8929	—	23.45	—
6H–5, 62	56.12	61.82	61.82	61.40	1.8993	—	23.45	—
6H–5, 77	56.27	61.97	61.97	61.55	1.9050	—	26.51	—
6H–5, 92	56.42	62.12	62.12	61.70	1.9086	—	41.40	—
6H–5, 107	56.57	62.27	62.27	61.85	1.9122	—	41.40	—
6H–5, 122	56.72	62.42	62.42	62.00	1.9158	—	41.40	—
6H–5, 137	56.87	62.57	62.57	62.15	1.9195	—	41.40	—
6H–6, 2	57.02	62.72	62.72	62.30	1.9231	—	41.40	—
6H–6, 17	57.17	62.87	62.87	62.45	1.9267	—	41.40	—
6H–6, 28	57.28	62.98	62.98	62.56	1.9294	—	41.40	—
6H–6, 47	57.47	63.17	63.17	62.75	1.9340	—	41.40	—
6H–6, 58	57.58	63.28	63.28	62.86	1.9366	—	41.40	—
6H–6, 77	57.77	63.47	63.47	63.05	1.9412	—	41.40	—
6H–6, 92	57.92	63.62	63.63	63.20	1.9448	—	41.40	—
6H–6, 107	58.07	63.77	63.76	63.35	1.9477	—	52.01	—
6H–6, 122	58.22	63.92	63.92	63.50	1.9495	—	84.55	—
6H–6, 137	58.37	64.07	64.08	63.65	1.9513	—	84.55	—
6H–7, 2	58.52	64.22	64.21	63.80	1.9530	—	84.55	—
6H–7, 17	58.67	64.37	64.37	63.95	1.9548	—	84.55	—
138-847D-								
7H–3, 17	57.27	64.47	64.45	64.05	1.9560	—	84.55	—
7H–3, 32	57.42	64.62	64.64	64.20	1.9578	—	84.55	—
7H–3, 47	57.57	64.77	64.83	64.35	1.9619	—	36.49	—
7H–3, 62	57.72	64.92	64.95	64.50	1.9663	—	33.56	—
7H–3, 77	57.87	65.07	65.07	64.65	1.9708	—	33.56	—
7H–3, 92	58.02	65.22	65.22	64.80	1.9753	—	33.56	—
7H–3, 107	58.17	65.37	65.37	64.95	1.9798	—	33.56	—
7H–3, 122	58.32	65.52	65.50	65.10	1.9842	—	33.56	—
7H–3, 137	58.47	65.67	65.66	65.25	1.9887	—	33.56	—
7H–4, 2	58.62	65.82	65.83	65.40	1.9932	—	33.56	—
7H–4, 17	58.77	65.97	65.98	65.55	1.9976	—	33.56	—
7H–4, 32	58.92	66.12	66.12	65.70	2.0021	—	33.56	—
7H–4, 47	59.07	66.27	66.27	65.85	2.0065	—	34.31	—
7H–4, 62	59.22	66.42	66.42	66.00	2.0108	—	34.50	—
7H–4, 77	59.37	66.57	66.57	66.15	2.0152	—	34.50	—
7H–4, 92	59.52	66.72	66.71	66.30	2.0195	—	34.50	—
138-847C-								
7H–1, 17	59.17	66.97	66.73	66.32	2.0201	—	34.50	—
7H–1, 30	59.30	67.10	66.86	66.45	2.0235	—	38.62	—
7H–1, 47	59.47	67.27	67.02	66.62	2.0261	—	64.21	—
7H–1, 62	59.62	67.42	67.16	66.77	2.0285	—	64.21	—
7H–1, 77	59.77	67.57	67.31	66.92	2.0308	—	64.21	—
7H–1, 92	59.92	67.72	67.48	67.07	2.0331	—	64.21	—
7H–1, 107	60.07	67.87	67.68	67.22	2.0355	—	64.21	—
7H–1, 122	60.22	68.02	67.87	67.37	2.0378	—	64.21	—
7H–1, 137	60.37	68.17	68.03	67.52	2.0401	—	64.21	—
7H–2, 2	60.52	68.32	68.18	67.67	2.0428	—	55.98	—
7H–2, 17	60.67	68.47	68.35	67.82	2.0469	—	37.00	—
7H–2, 30	60.80	68.60	68.51	67.95	2.0504	—	37.00	—
7H–2, 47	60.97	68.77	68.74	68.12	2.0555	—	33.12	—
7H–2, 64	61.14	68.94	68.95	68.29	2.0609	—	31.33	—
7H–2, 77	61.27	69.07	69.08	68.42	2.0651	—	31.33	—
7H–2, 92	61.42	69.22	69.22	68.57	2.0699	—	31.33	—
7H–2, 107	61.57	69.37	69.37	68.72	2.0747	—	31.33	—
7H–2, 122	61.72	69.52	69.52	68.87	2.0794	—	31.33	—
7H–2, 137	61.87	69.67	69.67	69.02	2.0842	—	31.33	—
7H–3, 2	62.02	69.82	69.83	69.17	2.0890	—	31.33	—
7H–3, 17	62.17	69.97	69.98	69.32	2.0938	—	31.33	—
7H–3, 30	62.30	70.10	70.10	69.45	2.0983	—	28.86	—
7H–3, 47	62.47	70.27	70.27	69.62	2.1058	—	22.86	—
7H–3, 62	62.62	70.42	70.42	69.77	2.1123	—	22.86	—
7H–3, 77	62.77	70.57	70.57	69.92	2.1188	—	23.17	—
7H–3, 92	62.92	70.72	70.72	70.07	2.1247	—	25.45	—
7H–3, 107	63.07	70.87	70.87	70.22	2.1303	—	26.71	—
7H–3, 122	63.22	71.02	71.02	70.37	2.1351	—	30.91	—
7H–3, 137	63.37	71.17	71.17	70.52	2.1400	—	30.91	—

Table 1 (continued).

Core, section, interval (cm)	ODP depth (mbsf)	Shipboard composite depth (mcd)	Revised composite depth (rmcd)	Composite depth, this study (Bmcd)	Ages		Sedimentation rates	
					Shackleton age model (Ma)	Isotope age model (Ma)	Shackleton ages (m/m.y.)	Isotope ages (m/m.y.)
7H–4, 2	63.52	71.32	71.32	70.67	2.1450	—	30.28	—
7H–4, 17	63.67	71.47	71.47	70.82	2.1499	—	30.28	—
7H–4, 30	63.80	71.60	71.60	70.95	2.1542	—	30.28	—
7H–4, 47	63.97	71.77	71.77	71.12	2.1598	—	30.28	—
7H–4, 62	64.12	71.92	71.92	71.27	2.1648	—	30.28	—
7H–4, 77	64.27	72.07	72.07	71.42	2.1697	—	30.28	—
7H–4, 92	64.42	72.22	72.22	71.57	2.1747	—	30.28	—
7H–4, 107	64.57	72.37	72.37	71.72	2.1796	—	30.28	—
7H–4, 122	64.72	72.52	72.52	71.87	2.1846	—	30.28	—
7H–4, 137	64.87	72.67	72.67	72.02	2.1895	—	30.28	—
7H–5, 2	65.02	72.82	72.82	72.17	2.1945	—	30.28	—
7H–5, 17	65.17	72.97	72.97	72.32	2.1994	—	30.28	—
7H–5, 30	65.30	73.10	73.10	72.45	2.2037	—	30.28	—
7H–5, 47	65.47	73.27	73.27	72.62	2.2093	—	30.28	—
7H–5, 62	65.62	73.42	73.42	72.77	2.2141	—	31.58	—
7H–5, 77	65.77	73.57	73.57	72.92	2.2187	—	32.27	—
7H–5, 92	65.92	73.72	73.72	73.07	2.2234	—	32.27	—
7H–5, 107	66.07	73.87	73.87	73.22	2.2280	—	32.27	—
7H–5, 122	66.22	74.02	74.02	73.37	2.2327	—	32.27	—
7H–5, 137	66.37	74.17	74.17	73.52	2.2362	—	42.64	—
7H–6, 2	66.52	74.32	74.32	73.67	2.2396	—	43.64	—
7H–6, 17	66.67	74.47	74.47	73.82	2.2431	—	43.64	—
7H–6, 30	66.80	74.60	74.60	73.95	2.2461	—	43.64	—
7H–6, 47	66.97	74.77	74.78	74.12	2.2500	—	43.64	—
7H–6, 64	67.14	74.94	74.94	74.29	2.2539	—	43.64	—
7H–6, 77	67.27	75.07	75.07	74.42	2.2585	—	27.75	—
7H–6, 92	67.42	75.22	75.21	74.57	2.2652	—	22.61	—
7H–6, 107	67.57	75.37	75.36	74.72	2.2718	—	22.61	—
7H–6, 122	67.72	75.52	75.52	74.87	2.2784	—	22.78	—
7H–6, 137	67.87	75.67	75.68	75.02	2.2843	—	25.56	—
7H–7, 2	68.02	75.82	75.83	75.17	2.2901	—	25.56	—
7H–7, 17	68.17	75.97	75.97	75.32	2.2960	—	25.56	—
7H–7, 30	68.30	76.10	76.08	75.45	2.3011	—	25.56	—
138-847D-								
8H–3, 122	67.82	76.12	76.13	75.55	2.3050	—	25.56	—
8H–3, 137	67.97	76.27	76.26	75.70	2.3100	—	30.23	—
8H–4, 2	68.12	76.42	76.40	75.85	2.3149	—	30.23	—
8H–4, 17	68.27	76.57	76.56	76.00	2.3199	—	30.23	—
8H–4, 32	68.42	76.72	76.73	76.15	2.3248	—	30.23	—
8H–4, 47	68.57	76.87	76.88	76.30	2.3298	—	30.23	—
8H–4, 62	68.72	77.02	77.02	76.45	2.3348	—	30.23	—
8H–4, 77	68.87	77.17	77.17	76.60	2.3397	—	30.23	—
8H–4, 92	69.02	77.32	77.32	76.75	2.3447	—	30.23	—
8H–4, 107	69.17	77.47	77.48	76.90	2.3493	—	32.58	—
8H–4, 122	69.32	77.62	77.62	77.05	2.3532	—	38.57	—
8H–4, 137	69.47	77.77	77.77	77.20	2.3571	—	38.57	—
8H–5, 2	69.62	77.92	77.91	77.35	2.3610	—	38.57	—
8H–5, 17	69.77	78.07	78.06	77.50	2.3649	—	38.57	—
8H–5, 32	69.92	78.22	78.22	77.65	2.3687	—	38.57	—
138-847C-								
8H–2, 2	70.02	78.22	78.26	77.75	2.3713	—	38.57	—
8H–2, 17	70.17	78.37	78.48	77.90	2.3752	—	38.57	—
8H–2, 32	70.32	78.52	78.61	78.05	2.3791	—	38.57	—
8H–2, 47	70.47	78.67	78.72	78.20	2.3830	—	38.57	—
8H–2, 62	70.62	78.82	78.81	78.35	2.3869	—	38.57	—
8H–2, 78	70.78	78.98	78.94	78.51	2.3916	—	34.18	—
8H–2, 92	70.92	79.12	79.07	78.65	2.3971	—	25.47	—
8H–2, 107	71.07	79.27	79.22	78.80	2.4030	—	25.47	—
8H–2, 122	71.22	79.42	79.37	78.95	2.4088	—	25.47	—
8H–2, 137	71.37	79.57	79.51	79.10	2.4147	—	25.47	—
8H–3, 2	71.52	79.72	79.66	79.25	2.4206	—	25.47	—
8H–3, 17	71.67	79.87	79.79	79.40	2.4244	—	39.36	—
8H–3, 32	71.82	80.02	79.89	79.55	2.4276	—	47.19	—
8H–3, 47	71.97	80.17	79.99	79.70	2.4308	—	47.19	—
8H–3, 62	72.12	80.32	80.13	79.85	2.4340	—	47.19	—
8H–3, 78	72.28	80.48	80.35	80.01	2.4374	—	47.19	—
8H–3, 92	72.42	80.62	80.56	80.15	2.4403	—	47.98	—
8H–3, 107	72.57	80.77	80.71	80.30	2.4434	—	48.21	—
8H–3, 122	72.72	80.92	80.83	80.45	2.4465	—	48.21	—
8H–3, 137	72.87	81.07	80.98	80.60	2.4496	—	48.21	—
8H–4, 2	73.02	81.22	81.19	80.75	2.4527	—	48.21	—
8H–4, 17	73.17	81.37	81.38	80.90	2.4558	—	48.21	—
8H–4, 32	73.32	81.52	81.52	81.05	2.4590	—	48.21	—
8H–4, 47	73.47	81.67	81.65	81.20	2.4621	—	48.21	—
8H–4, 62	73.62	81.82	81.81	81.35	2.4652	—	48.21	—
8H–4, 78	73.78	81.98	81.99	81.51	2.4685	—	48.21	—
8H–4, 92	73.92	82.12	82.13	81.65	2.4714	—	48.21	—
8H–4, 107	74.07	82.27	82.27	81.80	2.4745	—	48.21	—
8H–4, 122	74.22	82.42	82.42	81.95	2.4781	—	41.57	—
8H–4, 137	74.37	82.57	82.58	82.10	2.4837	—	26.82	—
8H–5, 2	74.52	82.72	82.73	82.25	2.4893	—	26.82	—
8H–5, 17	74.67	82.87	82.87	82.40	2.4949	—	26.82	—

Table 1 (continued).

Core, section, interval (cm)	ODP depth (mbsf)	Shipboard composite depth (mcd)	Revised composite depth (rmcd)	Composite depth, this study (Bmcd)	Ages		Sedimentation rates	
					Shackleton age model (Ma)	Isotope age model (Ma)	Shackleton ages (m/m.y.)	Isotope ages (m/m.y.)
8H-5, 32	74.82	83.02	83.01	82.55	2.5005	—	26.82	—
8H-5, 47	74.97	83.17	83.17	82.70	2.5061	—	26.82	—
8H-5, 62	75.12	83.32	83.33	82.85	2.5117	—	26.82	—
8H-5, 78	75.28	83.48	83.49	83.01	2.5176	—	26.82	—
8H-5, 92	75.42	83.62	83.61	83.15	2.5223	—	29.81	—
8H-5, 107	75.57	83.77	83.75	83.30	2.5264	—	37.31	—
8H-5, 122	75.72	83.92	83.91	83.45	2.5304	—	37.31	—
8H-5, 137	75.87	84.07	84.08	83.60	2.5344	—	37.31	—
8H-6, 2	76.02	84.22	84.22	83.75	2.5384	—	37.31	—
8H-6, 17	76.17	84.37	84.35	83.90	2.5424	—	37.31	—
8H-6, 32	76.32	84.52	84.47	84.05	2.5465	—	37.31	—
8H-6, 47	76.47	84.67	84.60	84.20	2.5531	—	22.65	—
8H-6, 62	76.62	84.82	84.72	84.35	2.5601	—	21.36	—
8H-6, 78	76.78	84.98	84.83	84.51	2.5676	—	21.36	—
8H-6, 92	76.92	85.12	84.92	84.65	2.5713	—	37.79	—
138-847D-								
9H-3, 32	76.42	85.12	85.10	84.85	2.5755	—	47.83	—
9H-3, 47	76.57	85.27	85.26	85.00	2.5786	—	47.83	—
9H-3, 62	76.72	85.42	85.42	85.15	2.5818	—	47.83	—
9H-3, 77	76.87	85.57	85.57	85.30	2.5849	—	47.83	—
9H-3, 92	77.02	85.72	85.73	85.45	2.5880	—	47.83	—
9H-3, 107	77.17	85.87	85.87	85.60	2.5912	—	47.83	—
9H-3, 122	77.32	86.02	86.02	85.75	2.5948	—	40.72	—
9H-3, 137	77.47	86.17	86.17	85.90	2.5987	—	38.64	—
9H-4, 2	77.62	86.32	86.32	86.05	2.6026	—	38.64	—
9H-4, 17	77.77	86.47	86.47	86.20	2.6065	—	38.64	—
9H-4, 32	77.92	86.62	86.63	86.35	2.6104	—	38.64	—
9H-4, 47	78.07	86.77	86.78	86.50	2.6145	—	36.73	—
9H-4, 62	78.22	86.92	86.92	86.65	2.6214	—	21.74	—
9H-4, 77	78.37	87.07	87.07	86.80	2.6283	—	21.74	—
9H-4, 92	78.52	87.22	87.21	86.95	2.6352	—	21.74	—
9H-4, 107	78.67	87.37	87.36	87.10	2.6404	—	28.40	—
9H-4, 122	78.82	87.52	87.51	87.25	2.6451	—	31.96	—
9H-4, 137	78.97	87.67	87.66	87.40	2.6498	—	31.96	—
9H-5, 2	79.12	87.82	87.82	87.55	2.6545	—	31.96	—
9H-5, 17	79.27	87.97	87.97	87.70	2.6592	—	31.96	—
138-847C-								
9H-1, 32	78.32	88.22	88.12	87.87	2.6645	—	31.96	—
9H-1, 47	78.47	88.37	88.21	88.02	2.6692	—	31.96	—
9H-1, 62	78.62	88.52	88.37	88.17	2.6739	—	31.96	—
9H-1, 77	78.77	88.67	88.61	88.32	2.6786	—	31.96	—
9H-1, 92	78.92	88.82	88.85	88.47	2.6834	—	31.58	—
9H-1, 107	79.07	88.97	89.02	88.62	2.6889	—	27.08	—
9H-1, 122	79.22	89.12	89.14	88.77	2.6944	—	27.08	—
9H-1, 137	79.37	89.27	89.27	88.92	2.7000	—	27.08	—
9H-2, 2	79.52	89.42	89.42	89.07	2.7055	—	27.08	—
9H-2, 17	79.67	89.57	89.61	89.22	2.7133	—	19.32	—
9H-2, 32	79.82	89.72	89.79	89.37	2.7219	—	17.50	—
9H-2, 47	79.97	89.87	89.91	89.52	2.7295	—	19.64	—
9H-2, 62	80.12	90.02	90.00	89.67	2.7325	—	50.60	—
9H-2, 77	80.27	90.17	90.10	89.82	2.7354	—	50.60	—
9H-2, 92	80.42	90.32	90.27	89.97	2.7384	—	50.60	—
9H-2, 107	80.57	90.47	90.47	90.12	2.7414	—	50.60	—
9H-2, 122	80.72	90.62	90.62	90.27	2.7443	—	50.60	—
9H-2, 137	80.87	90.77	90.77	90.42	2.7473	—	50.60	—
9H-3, 2	81.02	90.92	90.92	90.57	2.7502	—	50.60	—
9H-3, 17	81.17	91.07	91.07	90.72	2.7532	—	50.60	—
9H-3, 32	81.32	91.22	91.22	90.87	2.7607	—	19.97	—
9H-3, 47	81.47	91.37	91.37	91.02	2.7699	—	16.36	—
9H-3, 62	81.62	91.52	91.52	91.17	2.7776	—	19.55	—
9H-3, 77	81.77	91.67	91.67	91.32	2.7823	—	32.00	—
9H-3, 92	81.92	91.82	91.82	91.47	2.7865	—	34.92	—
9H-3, 107	82.07	91.97	91.97	91.62	2.7893	—	55.00	—
9H-3, 122	82.22	92.12	92.12	91.77	2.7920	—	55.00	—
9H-3, 137	82.37	92.27	92.27	91.92	2.7947	—	55.00	—
9H-4, 2	82.52	92.42	92.42	92.07	2.7975	—	55.00	—
9H-4, 17	82.67	92.57	92.57	92.22	2.8010	—	42.31	—
9H-4, 32	82.82	92.72	92.72	92.37	2.8048	—	40.00	—
9H-4, 47	82.97	92.87	92.87	92.52	2.8085	—	40.00	—
9H-4, 62	83.12	93.02	93.02	92.67	2.8123	—	40.00	—
9H-4, 77	83.27	93.17	93.17	92.82	2.8160	—	40.00	—
9H-4, 92	83.42	93.32	93.32	92.97	2.8198	—	40.00	—
9H-4, 107	83.57	93.47	93.47	93.12	2.8235	—	40.00	—
9H-4, 122	83.72	93.62	93.61	93.27	2.8273	—	40.00	—
9H-4, 137	83.87	93.77	93.77	93.42	2.8310	—	40.00	—
9H-5, 2	84.02	93.92	93.92	93.57	2.8348	—	40.00	—
9H-5, 17	84.17	94.07	94.07	93.72	2.8414	—	22.63	—
9H-5, 32	84.32	94.22	94.22	93.87	2.8482	—	21.95	—
9H-5, 47	84.47	94.37	94.37	94.02	2.8550	—	21.95	—
9H-5, 62	84.62	94.52	94.52	94.17	2.8619	—	21.95	—
9H-5, 77	84.77	94.67	94.67	94.32	2.8687	—	21.95	—
9H-5, 92	84.92	94.82	94.82	94.47	2.8755	—	21.95	—

Table 1 (continued).

Core, section, interval (cm)	ODP depth (mbsf)	Shipboard composite depth (mcd)	Revised composite depth (rmcd)	Composite depth, this study (Bmcd)	Ages		Sedimentation rates	
					Shackleton age model (Ma)	Isotope age model (Ma)	Shackleton ages (m/m.y.)	Isotope ages (m/m.y.)
9H-5, 107	85.07	94.97	94.97	94.62	2.8828	—	20.79	—
9H-5, 122	85.22	95.12	95.12	94.77	2.8900	—	20.71	—
9H-5, 137	85.37	95.27	95.27	94.92	2.8972	—	20.71	—
9H-6, 2	85.52	95.42	95.42	95.07	2.9042	—	21.44	—
9H-6, 17	85.67	95.57	95.57	95.22	2.9078	—	41.82	—
9H-6, 32	85.82	95.72	95.72	95.37	2.9114	—	41.82	—
9H-6, 47	85.97	95.87	95.87	95.52	2.9150	—	41.82	—
9H-6, 62	86.12	96.02	96.02	95.67	2.9186	—	41.82	—
9H-6, 77	86.27	96.17	96.17	95.82	2.9222	—	41.82	—
9H-6, 92	86.42	96.32	96.32	95.97	2.9258	—	41.82	—
9H-6, 107	86.57	96.47	96.48	96.12	2.9283	—	59.91	—
9H-6, 122	86.72	96.62	96.63	96.27	2.9307	—	61.82	—
9H-6, 137	86.87	96.77	96.74	96.42	2.9331	—	61.82	—
9H-7, 2	87.02	96.92	96.85	96.57	2.9355	—	61.82	—
9H-7, 17	87.17	97.07	97.05	96.72	2.9407	—	29.14	—
9H-7, 32	87.32	97.22	97.25	96.87	2.9496	—	16.87	—
9H-7, 48	87.48	97.38	97.35	97.03	2.9558	—	25.75	—
9H-7, 62	87.62	97.52	97.45	97.17	2.9612	—	25.75	—
9H-7, 77	87.77	97.67	97.67	97.32	2.9671	—	25.75	—

[a]The section depth is the midpoint of a 4-cm sample.

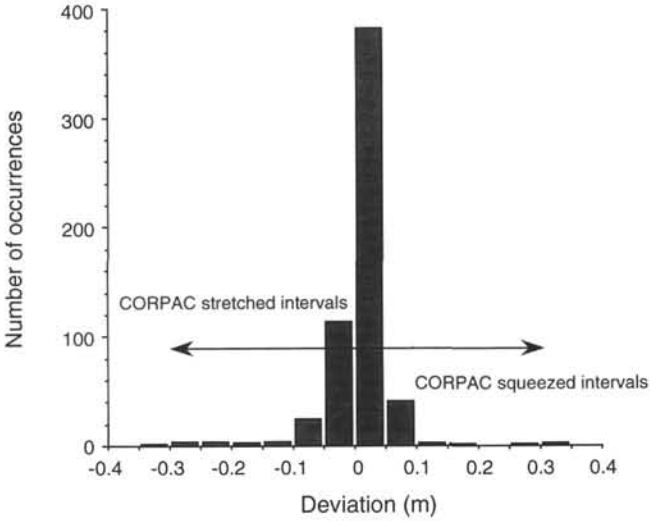

Figure 3. Histogram of the extent to which sample intervals have been stretched (negative values) or squeezed (positive values) when constructing revised composite depths (rmcd) for Hole 847C using the method of Hagelberg et al. (this volume). Of the 579 samples having a spacing near 15 cm, 98 were stretched or squeezed by more than 5 cm.

dried overnight at 100°C and then placed in a desiccator to cool for at least 1 hr.

Calcium carbonate content was measured on a gasometric apparatus similar to that described by Jones and Kaiteris (1983). The Brown University system uses a differential pressure gauge in place of a vacuum gauge, and carbonate reactions are measured at atmospheric pressure. The calcium carbonate was digested in 3 mL of 43% phosphoric acid (a 1:1 mixture of 85% phosphoric acid and deionized water). Replicate analyses of both standards and samples routinely give an analytical precision of better than 0.5% by weight. To ensure that our analyses are consistent with the shipboard data, we measured the calcite content on 22 samples from Site 847 that had been analyzed aboard the *JOIDES Resolution* using the coulometric procedure (Shipboard Scientific Party, 1992). No systematic offsets are apparent (Fig. 5), and the small differences are within the analytical errors of the two techniques.

Opal content was measured in the samples following the technique of Mortlock and Froelich (1989), except that buffered 0.5 M acetic acid, rather than hydrochloric acid, was used to remove the carbonate material. A hot (85°C) 2M Na_2CO_3 leach was used to extract the biogenic opal. Samples were placed in a water bath for 6 hr and stirred at 1- to 2-hr intervals. Measurements of dissolved silica were performed using a Spectronics 601 spectrophotometer; the precision based on standards and replicates was better than 1% by weight. Silicon concentrations were converted to opal using a factor of 2.5, which applies to samples having a mixture of diatom and radiolarian skeletal material (Mortlock and Froelich, 1989). Residuals after the opal leach of selected samples were examined microscopically to ensure that complete or near-complete digestion of biogenic opal was obtained using a 2M Na_2CO_3 extract solution. Some samples had relatively well-preserved radiolarian parts in the residuals. Additional experiments were performed to ensure that these undigested tests represented only a small portion of the total opal in the sample. Results of these experiments are reported in the Appendix. We conclude from these experiments that our procedure extracted most (>95%) of the biogenic opal contained in these Site 847 samples.

Dry Bulk Density

Dry bulk density (DBD) data needed to calculate MARs were derived from the shipboard GRAPE wet-bulk-density (WBD) measurements. A total of 105 discrete DBD values were obtained by shipboard scientists within Cores 1H through 9H of Hole 847B (Shipboard Scientific Party, 1992). These data are compared to the associated GRAPE values for each sample (Fig. 6). To obtain values for each sample depth, the GRAPE data, having a sample spacing of ~2 cm, were first smoothed with a nine-point Gaussian filter (T. Hagelberg, pers. comm., 1993) and then sampled at the mcd corresponding to the shipboard DBD measurements. This smoothing was necessary to reduce the high-frequency variability before interpolation to discrete sample depths. The linear regression between the GRAPE data and the discrete samples [DBD = –1.695 + 1.538 * GRAPE; $r = 0.94$] was used to estimate the DBD for each sample in this study. The smoothed GRAPE records from Holes 847B, 847C, and 847D were sampled at the depths (mcd) corresponding to samples used in this study. These data are listed in Table 2.

RESULTS AND DISCUSSION

Site 847 is located west of the Galapagos Islands beneath highly productive surface waters associated with the equatorial divergence (Fig. 1). The sediments are largely a mixture of biogenic carbonate and opal, with lesser amounts of detrital material transported to the site by

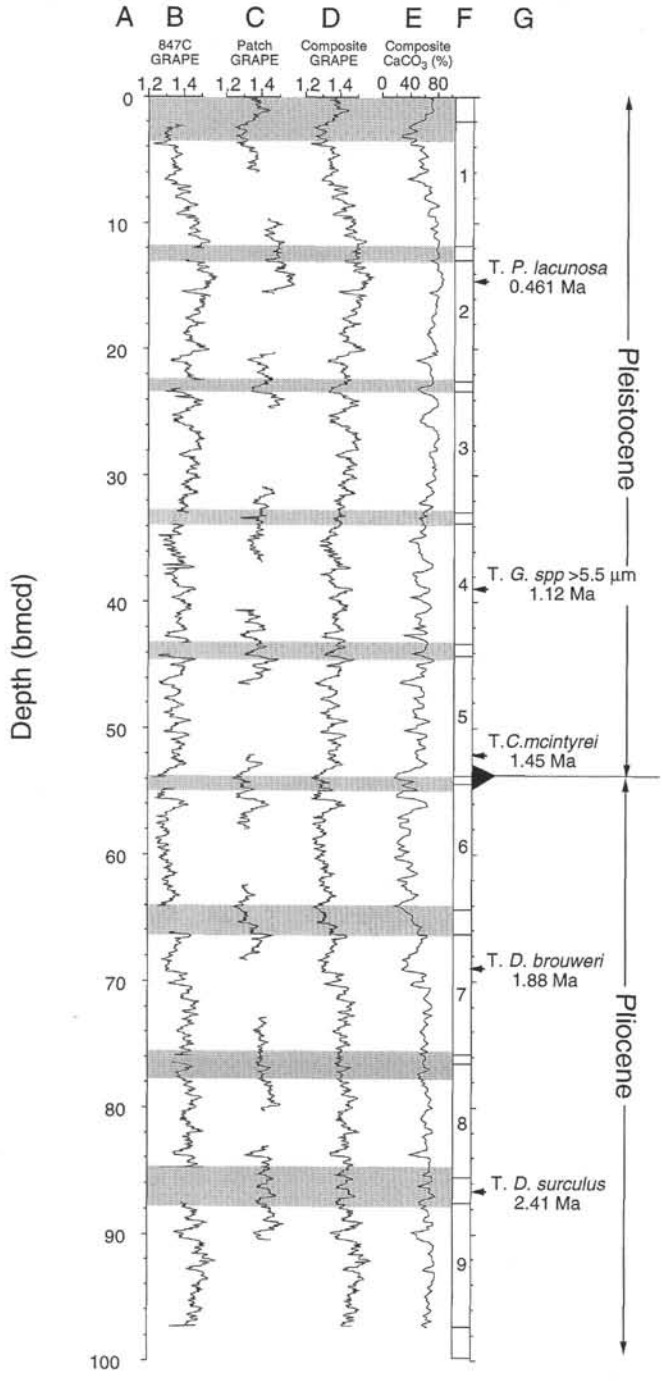

Figure 4. Composite depth reconstruction for the top nine cores in Site 847 using Hole 847C as the primary data and splicing in data from Holes 847B and 847D to account for sediment missing or disturbed at core breaks (shaded areas). **A.** Depth below the seafloor in composite depth of this study (Bmcd). **B.** GRAPE data sampled at ~2-cm intervals from Hole 847C and smoothed using a nine-point Gaussian filter. **C.** GRAPE data from Holes 847B and 847D for the intervals spanning and adjacent to the core breaks in Hole 847C. The first patch is from Hole 847B and all other patch data are from Hole 847D. **D.** Composite GRAPE data for Site 847 following the scheme listed in Table 3. **E.** %$CaCO_3$ data for the composite at Site 847. Sample spacing is ~15 cm. Note that much of the structure in the GRAPE data is resolved in the more coarsely sampled carbonate data. **F.** Core numbers corresponding to Hole 847C. **G.** Selected nannofossil datums used as control points for the shipboard sedimentation rate model for Site 847 (Shipboard Scientific Party, 1992). The location of the Pleistocene/Pliocene boundary was based on the nannofossil data reported for Site 847 (Shipboard Scientific Party, 1992).

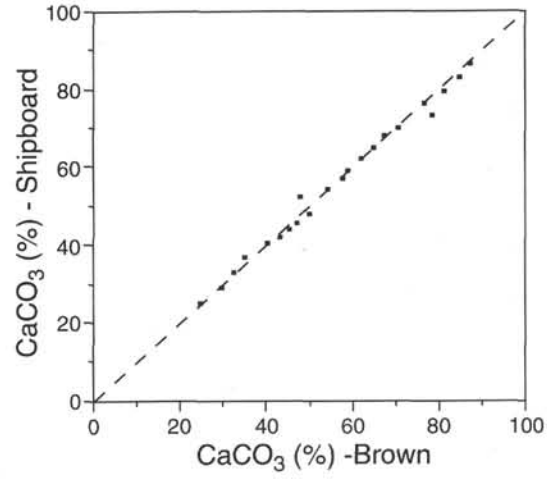

Figure 5. Scatter plot of calcium carbonate concentrations for 22 samples using the shipboard coulometric procedure (Shipboard Scientific Party, 1992) and gasometric technique. The 1:1 correspondence line is shown (dashed).

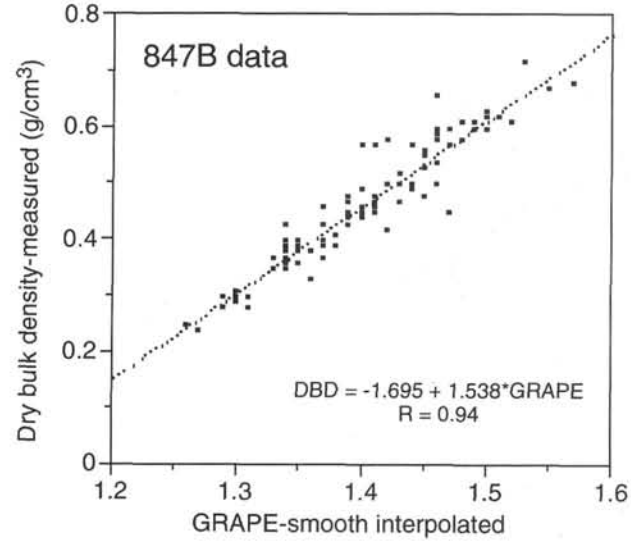

Figure 6. Scatter plot of discrete dry density values measured in Hole 847B samples in Cores 1H to 9H vs. the corresponding GRAPE density samples. The GRAPE data were smoothed using a nine-point Gaussian filter and were sampled at depths corresponding to the discrete dry-bulk-density (DBD) samples. The linear regression model based on these data and shown in the figure was used to calculate dry-bulk-density values for samples in this study.

means of winds (Fig. 7). At a water depth of 3334 m, the site is near the top of the regional sediment lysocline (Berger et al., 1976), and the carbonate sediment component is relatively well preserved. Opal and carbonate concentrations have a high negative correlation (Fig. 8A, $r = -0.94$); these two components mirror one another downcore (Fig. 7B). Because of the large contrast in the density and differential packing of carbonate and opal sediment components, the GRAPE WBD records exhibit a pattern that matches the relative changes in the proportions of carbonate and opal (Fig. 7A). A comparison of the opal and carbonate concentrations in the Site 847 samples to corresponding values of GRAPE density reveals a curvilinear relationship, with greater scatter in the high-opal, low-carbonate range (Figs. 8B–8C). We tentatively attribute this larger scatter to the relative increase in a third component, detrital material, within some of the low-carbonate intervals.

Mayer (1991) used the high correlation between GRAPE and calcium carbonate concentrations to derive an empirical relationship for

Table 2. Data for Site 847 samples.

Core, section, interval (cm)	ODP depth (mbsf)	Opal (%)	Analyses (#)	$CaCO_3$	Analyses (#)	GRAPE (smoothed and interpolated)	Estimated $CaCO_3$	Dry bulk density (g/cm3)	Weight >150 µm (%)	Whole foraminifers (%)	Radiolarians > 150 µm (%)
138-847B-											
1H-1, 2	0.02	19.37	1	66.05	2	1.340	46.44	0.366	5.46	54.75	37.35
1H-1, 19	0.19	16.62	1	72.83	2	1.355	50.18	0.389	5.87	57.66	19.39
1H-1, 30	0.30	18.76	1	70.12	2	1.392	58.78	0.446	10.52	76.22	18.59
1H-1, 47	0.47	15.46	1	71.41	2	1.393	58.99	0.447	12.53	74.52	16.56
1H-1, 59	0.59	15.95	1	69.60	2	1.367	53.05	0.407	9.31	57.65	25.00
1H-1, 77	0.77	15.36	1	70.56	2	1.386	57.43	0.437	9.30	55.10	26.32
1H-1, 92	0.92	17.57	1	70.79	2	1.379	55.84	0.426	9.99	48.08	29.91
1H-1, 107	1.07	18.05	1	73.19	2	1.437	67.99	0.515	10.32	68.31	20.33
1H-1, 123	1.23	18.40	1	69.98	2	1.404	61.34	0.464	7.27	58.84	27.77
1H-1, 137	1.37	20.73	1	60.75	2	1.387	57.63	0.438	6.74	71.51	25.16
1H-2, 2	1.52	26.30	1	61.06	1	1.365	52.55	0.404	5.88	66.89	26.92
1H-2, 24	1.74	28.14	1	61.58	1	1.353	49.63	0.386	9.79	80.58	10.34
1H-2, 37	1.87	32.92	1	58.14	1	1.353	49.63	0.386	5.78	78.76	16.16
1H-2, 52	2.02	33.22	1	50.30	1	1.321	41.41	0.337	8.40	79.57	20.59
1H-2, 67	2.17	31.45	1	44.33	1	1.317	40.32	0.331	2.66	70.29	36.79
1H-2, 80	2.30	32.70	1	42.07	1	1.273	27.79	0.263	2.73	72.63	47.34
1H-2, 92	2.42	33.66	1	37.62	1	1.246	19.45	0.221	2.41	52.15	69.06
1H-2, 107	2.57	32.97	1	43.99	1	1.277	28.97	0.269	4.56	60.23	51.14
1H-2, 123	2.73	30.46	1	49.97	1	1.319	40.84	0.334	5.34	54.61	51.08
1H-2, 137	2.87	31.61	1	41.79	1	1.303	36.45	0.309	5.10	71.82	46.99
1H-3, 2	3.02	36.09	1	29.01	2	1.295	34.19	0.297	2.34	66.84	50.64
1H-3, 17	3.17	37.42	1	28.14	2	1.278	29.24	0.271	1.97	51.78	73.12
1H-3, 30	3.30	30.14	1	45.50	1	1.290	32.74	0.289	3.33	49.92	62.73
1H-3, 47	3.47	28.61	1	49.12	1	1.323	41.89	0.340	4.35	62.13	50.28
138-847C-											
1H-1, 122	3.22	31.16	1	48.57	1	1.319	40.81	0.334	6.66	69.13	57.00
1H-1, 137	3.37	36.45	1	40.94	2	1.296	34.44	0.298	4.34	66.49	60.06
1H-2, 2	3.52	37.58	1	40.16	2	1.244	18.75	0.218	3.34	46.88	55.39
1H-2, 17	3.67	26.32	1	59.77	1	1.351	49.06	0.383	4.85	55.52	60.45
1H-2, 32	3.82	27.79	1	56.83	1	1.356	50.29	0.391	7.25	52.21	67.82
1H-2, 47	3.97	27.68	1	53.44	1	1.348	48.31	0.378	6.59	67.84	47.51
1H-2, 65	4.15	23.61	1	59.86	1	1.354	49.79	0.387	5.89	—	—
1H-2, 77	4.27	24.75	1	61.74	1	1.380	55.95	0.427	5.19	74.88	54.51
1H-2, 92	4.42	22.45	1	65.52	1	1.376	55.02	0.421	5.17	—	—
1H-2, 107	4.57	24.71	1	59.02	1	1.359	50.99	0.395	4.75	—	—
1H-2, 122	4.72	31.80	1	52.23	1	1.333	44.46	0.355	5.43	—	—
1H-2, 137	4.87	29.93	1	54.48	1	1.348	48.27	0.378	3.64	—	—
1H-3, 2	5.02	25.62	1	59.28	1	1.350	48.77	0.381	5.47	—	—
1H-3, 17	5.17	27.13	1	56.87	1	1.340	46.24	0.366	2.99	—	—
1H-3, 32	5.32	29.91	1	53.90	1	1.365	52.41	0.404	2.88	—	—
1H-3, 47	5.47	20.00	1	65.86	1	1.377	55.22	0.423	2.99	—	—
1H-3, 62	5.62	21.48	1	64.74	1	1.374	54.52	0.418	3.50	—	—
1H-3, 77	5.77	25.18	1	55.30	1	1.347	47.99	0.377	3.34	—	—
1H-3, 92	5.92	29.57	1	49.85	1	1.352	49.23	0.384	2.41	—	—
1H-3, 107	6.07	29.52	1	48.56	1	1.318	40.44	0.332	1.87	—	—
1H-3, 122	6.22	37.62	1	36.46	2	1.297	34.62	0.300	2.45	—	—
1H-3, 137	6.37	28.65	1	50.61	1	1.319	40.69	0.334	2.48	—	—
1H-4, 2	6.52	23.07	1	60.36	1	1.352	49.21	0.384	4.29	—	—
1H-4, 17	6.67	25.30	1	59.75	1	1.338	45.68	0.363	2.80	—	—
1H-4, 32	6.82	20.58	1	69.75	1	1.417	63.88	0.484	2.63	—	—
1H-4, 47	6.97	20.11	1	67.98	1	1.397	59.66	0.454	3.95	—	—
1H-4, 62	7.12	20.03	1	66.51	1	1.379	55.63	0.426	3.34	—	—
1H-4, 77	7.27	15.68	1	71.32	2	1.435	67.43	0.512	1.65	—	—
1H-4, 92	7.42	20.38	1	64.74	1	1.390	58.10	0.443	2.02	—	—
1H-4, 107	7.57	26.20	1	60.81	1	1.364	52.10	0.403	1.85	—	—
1H-4, 122	7.72	27.70	1	60.02	2	1.357	50.40	0.392	2.77	—	—
1H-4, 137	7.87	28.35	1	63.02	1	1.399	60.06	0.457	6.80	—	—
1H-5, 2	8.02	22.01	1	71.66	1	1.422	64.86	0.492	3.64	—	—
1H-5, 17	8.17	10.46	1	75.93	1	1.434	67.21	0.511	4.29	—	—
1H-5, 32	8.32	9.51	1	81.62	2	1.477	74.89	0.577	5.07	—	—
1H-5, 47	8.47	13.30	1	74.77	1	1.428	66.04	0.501	5.61	—	—
1H-5, 62	8.62	16.56	1	68.24	1	1.402	60.69	0.461	4.34	—	—
1H-5, 77	8.77	16.34	1	66.50	1	1.417	63.82	0.484	4.05	—	—
1H-5, 92	8.92	18.21	1	65.17	1	1.372	53.95	0.415	2.47	—	—
1H-5, 107	9.07	20.84	1	64.50	2	1.374	54.41	0.418	2.12	—	—
1H-5, 122	9.22	14.35	1	76.75	1	1.467	73.20	0.561	2.47	—	—
1H-5, 137	9.37	12.64	1	75.80	1	1.433	66.99	0.509	3.10	—	—
1H-6, 2	9.52	11.89	1	75.89	1	1.477	74.87	0.577	2.53	—	—
1H-6, 17	9.67	9.88	1	80.24	1	1.484	76.00	0.587	1.72	—	—
1H-6, 32	9.82	11.18	1	78.68	1	1.483	75.83	0.586	2.10	—	—
1H-6, 47	9.97	13.20	1	76.27	1	1.456	71.25	0.544	2.74	—	—
1H-6, 62	10.12	17.86	1	69.41	2	1.440	68.31	0.520	3.67	—	—
1H-6, 77	10.27	13.56	1	74.95	1	1.477	74.85	0.577	2.79	—	—
1H-6, 92	10.42	12.73	1	78.43	2	1.486	76.30	0.591	4.48	—	—
1H-6, 107	10.57	13.78	1	74.44	1	1.445	69.24	0.527	9.93	—	—
1H-6, 122	10.72	16.54	1	73.00	1	1.436	67.53	0.514	9.35	—	—
1H-6, 137	10.87	13.22	1	74.43	1	1.478	75.00	0.578	4.27	—	—
1H-7, 2	11.02	8.68	1	81.50	1	1.493	77.38	0.601	2.09	—	—
1H-7, 17	11.17	8.34	1	82.26	1	1.549	84.96	0.687	3.37	—	—
1H-7, 32	11.32	9.32	1	81.12	1	1.527	82.23	0.654	2.45	—	—

Table 2 (continued).

Core, section, interval (cm)	ODP depth (mbsf)	Opal (%)	Analyses (#)	$CaCO_3$	Analyses (#)	GRAPE (smoothed and interpolated)	Estimated $CaCO_3$	Dry bulk density (g/cm3)	Weight >150 µm (%)	Whole foraminifers (%)	Radiolarians > 150 µm (%)
1H-7, 47	11.47	9.29	1	80.80	1	1.502	78.73	0.615	2.83	—	—
138-847D-											
2H-3, 62	10.22	10.00	1	80.48	1	1.506	79.31	0.621	3.57	—	—
2H-3, 77	10.37	9.58	1	79.91	1	1.499	78.28	0.611	2.66	—	—
2H-3, 92	10.52	9.61	1	77.56	1	1.500	78.42	0.612	3.31	—	—
2H-3, 107	10.67	11.70	1	79.00	1	1.492	77.20	0.600	1.54	—	—
2H-3, 122	10.82	11.44	1	80.78	2	1.509	79.73	0.626	2.81	—	—
2H-3, 137	10.97	9.28	1	80.76	1	1.489	76.73	0.595	1.42	—	—
2H-4, 2	11.12	9.89	1	81.23	1	1.503	78.86	0.617	2.19	—	—
2H-4, 17	11.27	11.32	1	78.54	1	1.489	76.72	0.595	2.69	—	—
138-847C-											
2H-4, 32	11.42	15.12	1	70.27	1	1.426	65.52	0.498	2.31	—	—
2H-1, 17	11.67	12.49	1	76.74	2	1.435	67.28	0.512	3.53	76.77	50.65
2H-1, 30	11.82	9.52	1	80.72	1	1.502	78.70	0.615	2.80	64.89	65.76
2H-1, 47	11.97	10.62	1	79.53	1	1.481	75.43	0.583	6.29	72.60	55.21
2H-1, 62	12.12	9.51	1	80.66	1	1.541	83.96	0.675	5.44	57.95	35.64
2H-1, 77	12.27	11.54	1	79.04	1	1.483	75.75	0.586	6.93	59.91	19.00
2H-1, 92	12.42	9.11	1	83.47	1	1.504	78.98	0.618	4.07	73.34	17.20
2H-1, 107	12.57	7.18	1	86.52	1	1.542	84.08	0.677	4.25	75.27	17.73
2H-1, 122	12.72	8.73	1	84.41	2	1.544	84.32	0.680	3.67	75.77	15.56
2H-1, 137	12.87	6.35	1	85.79	1	1.582	88.41	0.738	3.99	84.89	9.35
2H-2, 2	13.02	5.76	1	88.56	1	1.574	87.63	0.726	4.42	76.29	8.53
2H-2, 17	13.17	6.85	1	85.49	1	1.546	84.55	0.683	4.02	75.46	15.77
2H-2, 30	13.30	7.60	1	86.34	1	1.548	84.79	0.686	3.85	77.25	12.84
2H-2, 47	13.47	8.08	1	85.45	1	1.541	83.94	0.675	3.98	79.24	11.08
2H-2, 64	13.64	6.81	1	83.01	1	1.541	83.94	0.675	5.46	75.30	15.89
2H-2, 77	13.77	7.90	1	81.98	1	1.527	82.16	0.654	4.40	76.74	7.72
2H-2, 92	13.92	11.43	1	78.77	1	1.460	71.84	0.551	3.24	85.08	11.49
2H-2, 107	14.07	19.30	1	67.77	2	1.411	62.39	0.475	3.03	61.82	42.60
2H-2, 122	14.22	11.88	1	76.63	1	1.489	76.66	0.595	2.96	46.45	33.62
2H-2, 137	14.37	10.31	1	80.73	1	1.528	82.28	0.655	5.49	51.78	27.32
2H-3, 2	14.52	11.92	1	79.73	1	1.513	80.23	0.632	2.36	53.76	36.84
2H-3, 17	14.67	12.55	1	77.89	1	1.498	78.04	0.609	3.84	56.89	32.63
2H-3, 30	14.82	12.06	1	78.95	1	1.499	78.19	0.611	4.82	60.16	26.26
2H-3, 47	14.97	12.28	1	76.68	2	1.511	79.94	0.629	3.81	61.40	39.60
2H-3, 62	15.12	12.39	1	78.68	1	1.509	79.65	0.626	3.46	68.62	24.50
2H-3, 77	15.27	11.71	1	76.09	1	1.503	78.77	0.617	5.68	74.87	17.97
2H-3, 92	15.42	12.26	1	76.47	1	1.473	74.04	0.571	6.92	85.67	11.01
2H-3, 107	15.57	11.66	1	77.06	1	1.474	74.20	0.572	5.02	81.62	13.51
2H-3, 122	15.72	11.45	1	77.69	1	1.492	77.10	0.600	4.46	79.47	14.77
2H-3, 137	15.87	11.75	1	73.15	1	1.474	74.19	0.572	3.81	76.87	21.35
2H-4, 2	16.02	16.00	1	70.86	1	1.444	68.88	0.526	4.25	85.00	18.01
2H-4, 17	16.17	16.17	1	70.65	1	1.414	62.96	0.480	2.99	81.23	32.21
2 H-4, 32	16.32	14.94	1	70.64	1	1.443	68.68	0.524	2.86	73.24	39.07
2H -4, 47	16.47	14.86	1	74.30	1	1.453	70.52	0.540	3.27	—	—
2H-4, 62	16.62	12.18	1	75.71	1	1.490	76.77	0.597	4.05	—	—
2H-4, 77	16.77	11.70	1	73.36	1	1.475	74.34	0.574	4.35	—	—
2H-4, 92	16.92	16.55	1	68.74	1	1.433	66.75	0.509	2.07	—	—
2H-4, 107	17.07	15.80	1	66.39	2	1.420	64.16	0.489	3.16	—	—
2H-4, 122	17.22	16.14	1	70.17	2	1.427	65.57	0.500	7.40	—	—
2H-4, 137	17.37	21.86	1	64.63	1	1.399	59.74	0.457	3.84	—	—
2H-5, 2	17.52	20.39	1	66.44	1	1.426	65.36	0.498	5.49	—	—
2H-5, 17	17.67	15.17	1	69.61	1	1.448	69.58	0.532	8.31	—	—
2H-5, 30	17.82	17.16	1	71.30	1	1.438	67.69	0.517	9.74	—	—
2H-5, 47	17.97	15.07	1	72.50	1	1.415	63.11	0.481	5.41	—	—
2H-5, 62	18.12	14.81	1	74.54	1	1.459	71.56	0.549	8.42	—	—
2H-5, 77	18.27	12.29	1	77.08	1	1.479	74.97	0.580	7.25	—	—
2H-5, 92	18.42	11.33	1	78.07	1	1.515	80.44	0.635	6.58	—	—
2H-5, 107	18.57	12.28	1	76.95	2	1.523	81.53	0.647	4.54	—	—
2H-5, 122	18.72	12.22	1	80.75	2	1.521	81.26	0.644	5.79	—	—
2H-5, 137	18.87	19.20	1	72.08	2	1.451	70.10	0.537	3.35	—	—
2H-6, 2	19.02	14.20	1	78.42	2	1.447	69.36	0.531	2.67	—	—
2H-6, 17	19.17	18.39	1	66.33	1	1.410	62.04	0.474	1.93	—	—
2H-6, 30	19.32	22.76	1	60.84	1	1.384	56.35	0.434	2.69	—	—
2H-6, 47	19.47	31.64	1	50.13	2	1.339	45.44	0.364	2.08	—	—
2H-6, 64	19.62	20.96	1	65.95	1	1.371	53.33	0.414	1.48	—	—
2H-6, 77	19.77	19.90	1	67.39	1	1.406	61.18	0.467	4.85	—	—
2H-6, 92	19.92	21.70	1	69.16	1	1.437	67.45	0.515	3.25	—	—
2H-6, 107	20.07	21.41	1	70.83	1	1.436	67.25	0.514	4.71	69.28	33.12
2H-6, 122	20.22	21.77	1	69.59	1	1.426	65.28	0.498	5.26	72.33	25.15
2H-6, 137	20.37	21.47	1	68.57	1	1.408	61.58	0.471	4.08	75.52	33.06
2H-7, 2	20.52	20.21	1	69.33	1	1.424	64.88	0.495	1.94	83.87	25.39
2H-7, 17	20.67	20.74	1	71.40	1	1.431	66.26	0.506	2.65	76.31	40.89
2H-7, 30	20.82	17.03	1	73.78	1	1.424	64.87	0.495	4.64	70.87	20.87
138-847D-											
3H-3, 62	19.72	17.58	1	72.72	1	1.445	68.93	0.527	5.31	68.43	25.83
3H-3, 77	19.87	15.18	1	73.27	1	1.437	67.41	0.515	4.35	75.12	27.92
3H-3, 92	20.02	13.92	1	73.50	1	1.428	65.65	0.501	3.57	75.40	43.03
3H-3, 107	20.17	15.41	1	69.85	1	1.404	60.70	0.464	3.49	80.94	42.61
3H-3, 122	20.32	26.55	2	56.70	2	1.373	53.73	0.417	2.52	80.48	59.57
3H-3, 137	20.47	30.32	2	51.44	2	1.359	50.38	0.395	2.67	76.92	54.55

Table 2 (continued).

Core, section, interval (cm)	ODP depth (mbsf)	Opal (%)	Analyses (#)	$CaCO_3$	Analyses (#)	GRAPE (smoothed and interpolated)	Estimated $CaCO_3$	Dry bulk density (g/cm3)	Weight >150 µm (%)	Whole foraminifers (%)	Radiolarians > 150 µm (%)
138-847C-											
3H-1, 17	21.17	26.11	1	56.42	2	1.385	56.50	0.435	2.87	78.38	64.16
3H-1, 32	21.32	22.53	1	61.02	1	1.395	58.73	0.451	3.69	72.67	68.07
3H-1, 47	21.47	15.24	1	73.38	1	1.412	62.37	0.477	2.36	42.66	73.69
3H-1, 62	21.62	15.52	1	74.47	1	1.435	67.00	0.512	2.94	54.50	37.21
3H-1, 77	21.77	13.60	2	78.90	1	1.457	71.09	0.546	2.68	68.72	23.77
3H-1, 92	21.92	11.26	2	79.44	1	1.498	77.87	0.609	4.28	64.22	29.58
3H-1, 107	22.07	12.74	2	79.78	1	1.469	73.18	0.564	4.71	67.07	30.04
3H-1, 122	22.22	9.42	1	81.13	1	1.491	76.78	0.598	6.47	68.49	19.54
3H-1, 137	22.37	12.63	1	79.92	1	1.458	71.26	0.547	6.96	65.22	14.86
3H-2, 2	22.52	19.04	1	72.93	1	1.450	69.80	0.535	5.37	63.81	38.26
3H-2, 17	22.67	21.70	1	71.37	1	1.422	64.39	0.492	5.16	66.79	29.98
3H-2, 30	22.82	20.31	1	68.73	1	1.416	63.16	0.483	5.18	58.18	40.41
3H-2, 47	22.97	25.74	1	61.46	1	1.380	55.30	0.427	5.20	—	—
3H-2, 65	23.12	27.69	1	57.83	1	1.353	48.83	0.386	6.93	49.73	65.41
3H-2, 77	23.27	28.54	2	59.34	1	1.386	56.66	0.437	5.39	—	—
3H-2, 92	23.42	26.62	2	54.33	2	1.345	46.81	0.374	8.34	—	—
3H-2, 107	23.57	28.60	2	55.96	1	1.367	52.23	0.407	5.16	44.22	75.22
3H-2, 122	23.72	26.12	1	62.79	1	1.387	56.87	0.438	5.69	—	—
3H-2, 137	23.87	25.69	1	63.55	1	1.399	59.53	0.457	7.62	—	—
3H-3, 2	24.02	14.42	1	74.87	1	1.451	69.95	0.537	11.82	—	—
3H-3, 17	24.17	15.95	1	74.25	1	1.432	66.34	0.507	6.68	—	—
3H-3, 32	24.32	12.31	1	78.45	1	1.447	69.20	0.531	5.23	—	—
3H-3, 47	24.47	12.88	1	78.23	1	1.498	77.82	0.609	6.26	—	—
3H-3, 62	24.62	10.46	1	81.37	1	1.486	75.94	0.591	5.61	—	—
3H-3, 76	24.76	10.75	1	79.81	1	1.495	77.35	0.604	5.23	—	—
3H-3 , 92	24.92	10.90	1	81.74	1	1.492	76.88	0.600	5.14	—	—
3H-3, 107	25.07	16.20	1	78.03	1	1.484	75.61	0.587	7.80	—	—
3H-3, 122	25.22	15.82	1	76.33	1	1.472	73.62	0.569	6.19	—	—
3H-3, 137	25.37	20.20	3	74.32	1	1.490	76.56	0.597	5.08	—	—
3H-4, 2	25.52	18.41	3	74.16	1	1.482	75.27	0.584	4.13	—	—
3H-4, 17	25.67	11.39	1	79.08	1	1.490	76.55	0.597	4.83	—	—
3H-4, 32	25.82	12.11	1	78.98	1	1.492	76.86	0.600	4.86	—	—
3H-4, 47	25.97	19.35	1	68.58	1	1.431	66.10	0.506	3.87	—	—
3H-4, 62	26.12	19.91	1	68.43	1	1.411	62.03	0.475	3.28	—	—
3H-4, 76	26.26	17.00	1	68.41	1	1.387	56.79	0.438	4.86	—	—
3H-4, 92	26.42	16.62	1	72.99	1	1.448	69.33	0.532	2.09	—	—
3H-4, 107	26.57	15.89	1	74.89	1	1.441	68.02	0.521	2.97	—	—
3H-4, 122	26.72	15.64	1	73.50	1	1.459	71.33	0.549	3.89	—	—
3H-4, 137	26.87	11.91	1	77.02	1	1.475	74.09	0.574	3.76	—	—
3H-5, 2	27.02	13.01	1	76.34	1	1.494	77.15	0.603	6.83	—	—
3H-5, 17	27.17	18.35	1	71.98	2	1.440	67.81	0.520	3.14	—	—
3H-5, 32	27.32	13.44	1	79.22	2	1.464	72.19	0.557	6.21	—	—
3H-5, 47	27.47	13.47	1	75.30	1	1.429	65.66	0.503	8.66	—	—
3H-5, 62	27.62	15.58	1	73.43	1	1.428	65.46	0.501	4.28	—	—
3H-5, 76	27.76	18.55	1	74.17	1	1.455	70.58	0.543	5.44	—	—
3H-5, 92	27.92	17.70	1	76.83	1	1.467	72.70	0.561	5.37	—	—
3H-5, 107	28.07	13.18	1	78.09	1	1.485	75.70	0.589	8.08	—	—
3H-5, 122	28.22	18.26	1	74.68	1	1.448	69.29	0.532	5.69	—	—
3H-5, 137	28.37	21.22	1	67.66	1	1.414	62.59	0.480	3.90	—	—
3H-6, 2	28.52	25.39	1	63.16	2	1.420	63.82	0.489	4.05	—	—
3H-6, 17	28.67	22.30	1	67.67	1	1.406	60.89	0.467	4.12	—	—
3H-6, 30	28.82	19.18	1	72.50	1	1.430	65.82	0.504	7.43	—	—
3H-6, 47	28.97	18.93	1	71.62	1	1.445	68.71	0.527	6.79	—	—
3H-6, 65	29.12	16.17	1	75.81	1	1.476	74.20	0.575	5.38	—	—
3H-6, 77	29.27	18.11	1	73.45	1	1.484	75.52	0.587	5.80	—	—
3H-6, 92	29.42	23.77	1	68.03	1	1.424	64.61	0.495	5.29	—	—
3H-6, 107	29.57	27.99	2	63.08	1	1.417	63.18	0.484	4.01	—	—
3H-6, 122	29.72	24.88	1	64.08	1	1.403	60.22	0.463	6.01	—	—
3H-6, 137	29.87	30.43	1	57.44	1	1.380	55.08	0.427	3.23	—	—
3H-7, 2	30.02	36.73	2	53.55	2	1.399	59.34	0.457	3.36	—	—
3H-7, 17	30.17	22.38	1	67.81	1	1.404	60.42	0.464	6.25	—	—
3H-7, 30	30.30	15.93	1	73.19	2	1.425	64.79	0.497	6.87	—	—
3H-7, 47	30.47	23.07	1	67.56	1	1.395	58.45	0.451	8.46	—	—
3H-7, 62	30.62	27.03	1	61.62	1	1.396	58.67	0.452	6.07	—	—
138-847D-											
4H-3, 47	29.07	28.10	3	60.12	1	1.403	60.19	0.463	—	—	—
4H-3, 62	29.22	29.87	3	58.62	1	1.404	60.40	0.464	—	—	—
4H-3, 77	29.37	25.56	3	64.98	1	1.415	62.72	0.481	—	—	—
4H-3, 92	29.52	22.66	3	53.06	1	1.370	52.70	0.412	—	—	—
4H-3, 107	29.67	24.63	3	57.93	1	1.389	57.09	0.441	—	—	—
4H-3, 122	29.82	28.81	3	58.77	1	1.403	60.17	0.463	—	—	—
4H-3, 137	29.97	29.01	3	59.55	1	1.408	61.24	0.471	—	—	—
4H-1, 32	30.82	28.00	1	62.93	1	1.393	57.97	0.447	5.03	—	—
4H-1, 47	30.97	27.24	1	62.83	1	1.369	52.43	0.411	6.46	—	—
4H-1, 61	31.11	30.99	2	58.87	1	1.348	47.28	0.378	5.26	—	—
4H-1, 77	31.27	26.62	1	54.22	2	1.341	45.49	0.367	5.30	—	—
4H-1, 92	31.42	23.61	1	58.98	1	1.372	53.13	0.415	4.63	—	—
4H-1, 107	31.57	24.28	1	63.53	2	1.381	55.23	0.429	5.36	—	—
4H-1, 122	31.72	29.14	1	57.09	1	1.365	51.45	0.404	4.74	—	—
4H-1, 137	31.87	37.01	3	45.74	2	1.339	44.95	0.364	3.68	—	—
138-847C-											
4H-2, 2	32.02	31.44	3	39.59	1	1.293	32.36	0.294	—	—	—

Table 2 (continued).

Core, section, interval (cm)	ODP depth (mbsf)	Opal (%)	Analyses (#)	$CaCO_3$	Analyses (#)	GRAPE (smoothed and interpolated)	Estimated $CaCO_3$	Dry bulk density (g/cm3)	Weight >150 µm (%)	Whole foraminifers (%)	Radiolarians > 150 µm (%)
4H-2, 17	32.17	32.62	1	49.86	1	1.331	42.85	0.352	—	—	—
4H-2, 32	32.32	31.05	1	53.79	1	1.330	42.58	0.351	—	—	—
4H-2, 47	32.47	30.48	1	52.30	1	1.312	37.71	0.323	—	—	—
4H-2, 63.5	32.64	27.49	1	53.61	1	1.357	49.47	0.392	—	—	—
4H-2, 77	32.77	26.42	1	56.24	1	1.311	37.42	0.321	—	—	—
4H-2, 88	32.88	26.61	1	52.84	1	1.336	44.14	0.360	—	—	—
4H-2, 107	33.07	26.74	1	58.05	1	1.383	55.64	0.432	—	—	—
4H-2, 122	33.22	28.49	1	56.50	1	1.348	47.20	0.378	—	—	—
4H-2, 137	33.37	29.01	1	59.22	1	1.408	61.16	0.471	—	—	—
4H-3, 2	33.52	26.20	1	62.68	1	1.371	52.83	0.414	—	—	—
4H-3, 17	33.67	18.03	1	67.80	1	1.401	59.64	0.460	—	—	—
4H-3, 32	33.82	13.17	1	72.90	1	1.420	63.65	0.489	—	—	—
4H-3, 47	33.97	14.73	1	72.90	1	1.440	67.61	0.520	—	—	—
4H-3, 61	34.11	13.14	1	72.48	1	1.453	70.04	0.540	—	—	—
4H-3, 77	34.27	15.75	1	67.50	1	1.333	43.30	0.355	—	—	—
4H-3, 92	34.42	22.48	1	58.83	1	1.354	48.67	0.387	—	—	—
4H-3, 107	34.57	31.91	1	45.12	1	1.343	45.89	0.371	—	—	—
4H-3, 122	34.72	32.84	1	46.37	1	1.304	35.39	0.311	—	—	—
4H-3, 137	34.87	32.58	1	51.13	1	1.351	47.90	0.383	—	—	—
4H-4, 2	35.02	31.43	1	48.92	1	1.353	48.40	0.386	—	—	—
4H-4, 17	35.17	36.17	1	48.30	1	1.338	44.58	0.363	—	—	—
4H-4, 30	35.30	35.40	1	51.93	1	1.355	48.89	0.389	—	—	—
4H-4, 47	35.47	32.25	1	50.12	1	1.362	50.60	0.400	—	—	—
4H-4, 61	35.61	27.81	1	57.09	1	1.369	52.28	0.411	—	—	—
4H-4, 77	35.77	16.89	1	69.28	1	1.424	64.41	0.495	—	—	—
4H-4, 92	35.92	15.64	1	68.51	1	1.472	73.35	0.569	—	—	—
4H-4, 107	36.07	17.69	1	67.00	1	1.426	64.80	0.498	—	—	—
4H-4, 122	36.22	23.47	1	58.19	1	1.396	58.47	0.452	—	—	—
4H-4, 137	36.37	24.67	1	56.82	1	1.390	57.13	0.443	—	—	—
4H-5, 2	36.52	35.98	2	41.84	1	1.352	48.10	0.384	—	—	—
4H-5, 17	36.67	26.03	1	57.82	1	1.367	51.77	0.407	—	—	—
4H-5, 30	36.80	27.06	1	59.24	1	1.408	61.06	0.471	—	—	—
4H-5, 47	36.97	22.48	1	67.93	1	1.412	61.90	0.477	—	—	—
4H-5, 61	37.11	18.40	1	69.79	1	1.442	67.91	0.523	—	—	—
4H-5, 77	37.27	15.87	1	70.65	1	1.442	67.90	0.523	—	—	—
4H-5, 92	37.42	19.98	1	68.08	1	1.426	64.77	0.498	—	—	—
4H-5, 107	37.57	20.70	3	64.03	1	1.406	60.61	0.467	—	—	—
4H-5, 122	37.72	27.68	1	56.08	1	1.384	55.72	0.434	—	—	—
4H-5, 137	37.87	31.77	1	50.52	1	1.382	55.26	0.431	—	—	—
4H-6, 2	38.02	35.51	1	48.51	1	1.365	51.24	0.404	—	—	—
4H-6, 17	38.17	30.94	1	57.03	1	1.390	57.07	0.443	—	—	—
4H-6, 29	38.29	31.14	1	56.80	1	1.375	53.62	0.420	—	—	—
4H-6, 47	38.47	30.75	3	54.58	1	1.367	51.71	0.407	—	—	—
4H-6, 64	38.64	34.12	2	53.20	1	1.380	54.77	0.427	—	—	—
4H-6, 77	38.77	23.23	2	63.61	1	1.393	57.73	0.447	—	—	—
4H-6, 92	38.92	34.08	2	45.85	1	1.397	58.61	0.454	—	—	—
4H-6, 107	39.07	22.86	1	59.44	1	1.418	63.09	0.486	—	—	—
4H-6, 122	39.22	17.80	1	65.38	1	1.378	54.29	0.424	—	—	—
4H-6, 137	39.37	19.87	1	61.31	1	1.313	37.73	0.324	—	—	—
4H-7, 2	39.52	44.41	2	32.20	1	1.320	39.64	0.335	—	—	—
4H-7, 17	39.67	32.77	1	50.72	1	1.324	40.72	0.341	—	—	—
4H-7, 32	39.82	21.91	1	59.22	1	1.412	61.82	0.477	—	—	—
4H-7, 47	39.97	21.14	1	66.13	1	1.430	65.49	0.504	—	—	—
138-847D-											
5H-3, 107	39.17	18.69	3	66.20	1	1.400	59.23	0.458	—	—	—
5H-3, 122	39.32	21.00	3	64.49	1	1.388	56.56	0.440	—	—	—
5H-3, 137	39.47	23.83	3	63.94	1	1.402	59.66	0.461	—	—	—
5H-4, 2	39.62	25.86	3	62.68	1	1.417	62.84	0.484	—	—	—
5H-4, 17	39.77	22.75	3	60.95	1	1.375	53.54	0.420	—	—	—
5H-4, 32	39.92	24.41	1	58.49	1	1.348	46.94	0.378	—	—	—
5H-4, 47	40.07	35.95	1	43.72	2	1.321	39.86	0.337	—	—	—
5H-4, 62	40.22	26.39	1	57.52	1	1.341	45.14	0.367	—	—	—
5H-4, 77	40.37	21.64	1	66.40	1	1.410	61.35	0.474	—	—	—
5H-4, 92	40.52	16.94	1	74.55	2	1.489	76.03	0.595	—	—	—
138-847C-											
5H-1, 47	40.47	10.55	1	74.20	1	1.461	71.29	0.552	—	—	—
5H-1, 62	40.62	19.24	1	67.18	1	1.407	60.70	0.469	—	—	—
5H-1, 77	40.77	29.17	1	50.80	1	1.368	51.84	0.409	—	—	—
5H-1, 92	40.92	25.85	1	51.42	1	1.344	45.88	0.372	—	—	—
5H-1, 107	41.07	21.87	1	64.09	1	1.409	61.11	0.472	—	—	—
5H-1, 122	41.22	19.59	2	64.68	1	1.412	61.74	0.477	—	—	—
5H-1, 137	41.37	26.75	1	58.11	1	1.400	59.16	0.458	—	—	—
5H-2, 2	41.52	27.83	1	57.10	1	1.393	57.61	0.447	—	—	—
5H-2, 17	41.67	21.17	1	62.59	1	1.398	58.71	0.455	—	—	—
5H-2, 28	41.78	23.93	1	54.14	1	1.360	49.86	0.397	—	—	—
5H-2, 47	41.97	31.23	1	43.55	1	1.318	38.96	0.332	—	—	—
5H-2, 64	42.14	46.69	1	30.34	1	1.295	32.49	0.297	—	—	—
5H-2, 77	42.27	49.40	1	26.97	1	1.285	29.57	0.281	—	—	—
5H-2, 92	42.42	34.81	1	44.45	1	1.291	31.32	0.291	—	—	—
5H-2, 107	42.57	19.56	3	57.79	1	1.348	46.84	0.378	—	—	—
5H-2, 122	42.72	23.59	1	56.58	1	1.348	46.84	0.378	—	—	—
5H-2, 137	42.87	23.52	1	59.05	1	1.387	56.21	0.438	—	—	—
5H-3, 2	43.02	19.61	1	62.49	2	1.381	54.83	0.429	—	—	—

Table 2 (continued).

Core, section, interval (cm)	ODP depth (mbsf)	Opal (%)	Analyses (#)	$CaCO_3$	Analyses (#)	GRAPE (smoothed and interpolated)	Estimated $CaCO_3$	Dry bulk density (g/cm3)	Weight >150 µm (%)	Whole foraminifers (%)	Radiolarians > 150 µm (%)
5H-3, 17	43.17	20.28	1	60.86	1	1.373	52.95	0.417	—	—	—
5H-3, 28	43.28	22.64	1	59.74	1	1.362	50.30	0.400	—	—	—
5H-3, 47	43.47	30.50	1	47.50	1	1.308	36.14	0.317	—	—	—
5H-3, 62	43.62	26.86	1	53.19	1	1.325	40.80	0.343	—	—	—
5H-3, 77	43.77	26.32	1	52.62	1	1.351	47.56	0.383	—	—	—
5H-3, 92	43.92	22.54	1	59.86	1	1.372	52.69	0.415	—	—	—
5H-3, 107	44.07	19.96	1	61.34	1	1.403	59.73	0.463	—	—	—
5H-3, 122	44.22	21.61	1	59.83	1	1.371	52.44	0.414	—	—	—
5H-3, 137	44.37	27.73	1	46.34	1	1.333	42.90	0.355	—	—	—
5H-4, 2	44.52	30.56	1	45.93	1	1.338	44.21	0.363	—	—	—
5H-4, 17	44.67	26.76	1	47.69	1	1.297	32.97	0.300	—	—	—
5H-4, 28	44.78	22.61	1	51.04	1	1.331	42.36	0.352	—	—	—
5H-4, 47	44.97	25.57	1	47.38	1	1.329	41.82	0.349	—	—	—
5H-4, 62	45.12	16.99	1	61.84	1	1.388	56.37	0.440	—	—	—
5H-4, 77	45.27	14.61	2	70.19	1	1.438	66.89	0.517	—	—	—
5H-4, 92	45.42	18.35	1	62.06	1	1.409	60.98	0.472	—	—	—
5H-4, 107	45.57	26.49	1	51.03	1	1.374	53.11	0.418	—	—	—
5H-4, 122	45.72	24.99	1	51.05	1	1.358	49.24	0.394	—	—	—
5H-4, 137	45.87	23.37	1	50.15	2	1.336	43.64	0.360	—	—	—
5H-5, 2	46.02	31.28	1	33.07	1	1.337	43.89	0.361	—	—	—
5H-5, 17	46.17	28.34	1	45.06	1	1.295	32.34	0.297	—	—	—
5H-5, 28	46.28	18.68	1	63.63	1	1.404	59.88	0.464	—	—	—
5H-5, 47	46.47	18.82	1	65.49	1	1.436	66.47	0.514	—	—	—
5H-5, 62	46.62	20.77	1	58.62	1	1.399	58.78	0.457	—	—	—
5H-5, 77	46.77	24.20	1	51.77	1	1.352	47.71	0.384	—	—	—
5H-5, 92	46.92	19.44	1	56.88	1	1.372	52.59	0.415	—	—	—
5H-5, 107	47.07	21.09	1	53.93	1	1.356	48.70	0.391	—	—	—
5H-5, 122	47.22	19.16	1	61.86	1	1.409	60.93	0.472	—	—	—
5H-5, 137	47.37	18.34	1	63.62	1	1.381	54.69	0.429	—	—	—
5H-6, 2	47.52	24.12	1	55.32	1	1.387	56.07	0.438	—	—	—
5H-6, 17	47.67	28.43	1	49.40	1	1.339	44.35	0.364	—	—	—
5H-6, 28	47.78	27.52	1	49.12	1	1.344	45.64	0.372	—	—	—
5H-6, 47	47.97	23.41	1	52.70	1	1.380	54.44	0.427	—	—	—
5H-6, 64	48.14	23.36	1	50.40	1	1.351	47.41	0.383	—	—	—
5H-6, 77	48.27	23.27	2	53.50	1	1.340	44.59	0.366	—	—	—
5H-6, 92	48.42	19.18	1	57.62	1	1.361	49.89	0.398	—	—	—
5H-6, 107	48.57	17.50	1	65.34	1	1.375	53.25	0.420	—	—	—
5H-6, 122	48.72	18.14	1	61.32	1	1.419	62.99	0.487	—	—	—
5H-6, 137	48.87	22.93	1	56.26	1	1.365	50.85	0.404	—	—	—
5H-7, 2	49.02	28.95	1	46.47	1	1.364	50.60	0.403	—	—	—
5H-7, 17	49.17	31.47	1	41.28	1	1.311	36.76	0.321	—	—	—
5H-7, 28	49.28	34.66	1	37.09	1	1.320	39.24	0.335	—	—	—
5H-7, 47	49.47	38.06	1	23.91	1	1.299	33.36	0.303	—	—	—
5H-7, 64	49.64	39.65	1	22.54	1	1.261	21.99	0.244	—	—	—
138-847D-											
6H-3, 32	47.92	36.99	2	19.28	2	1.285	29.28	0.281	—	—	—
6H-3, 47	48.07	32.01	1	25.54	2	1.277	26.88	0.269	—	—	—
6H-3, 62	48.22	27.53	1	47.83	1	1.309	36.18	0.318	—	—	—
6H-3, 77	48.37	31.78	1	39.92	1	1.310	36.45	0.320	—	—	—
6H-3, 92	48.52	37.43	1	30.12	1	1.292	31.31	0.292	—	—	—
6H-3, 107	48.67	32.81	1	36.76	1	1.302	34.18	0.308	—	—	—
6H-3, 122	48.82	26.34	1	50.04	1	1.349	46.82	0.380	—	—	—
6H-3, 137	48.97	26.36	1	52.26	1	1.345	45.80	0.374	—	—	—
138-847C-											
6H-1, 17	49.67	35.42	1	31.38	1	1.287	29.82	0.284	1.92	79.48	—
6H-1, 30	49.80	39.42	1	30.83	1	1.283	28.63	0.278	1.97	81.53	—
6H-1, 47	49.97	40.88	1	22.63	1	1.262	22.23	0.246	2.52	82.94	—
6H-1, 62	50.12	35.43	1	22.75	2	1.278	27.12	0.271	1.71	59.69	—
6H-1, 77	50.27	23.63	1	45.53	1	1.249	18.12	0.226	4.18	41.16	—
6H-1, 92	50.42	20.43	1	60.70	1	1.375	53.15	0.420	4.86	44.25	—
6H-1, 107	50.57	19.32	1	64.29	1	1.409	60.80	0.472	3.31	39.94	—
6H-1, 122	50.72	15.35	1	66.03	1	1.381	54.55	0.429	6.37	39.11	—
6H-1, 137	50.87	17.63	1	66.93	1	1.414	61.85	0.480	5.58	53.20	—
6H-2, 2	51.02	26.01	1	55.85	1	1.383	55.00	0.432	6.13	66.07	—
6H-2, 17	51.17	32.23	1	44.37	1	1.355	48.27	0.389	4.21	65.38	—
6H-2, 30	51.30	32.20	1	44.63	1	1.333	42.61	0.355	3.12	68.73	—
6H-2, 47	51.47	36.08	1	38.06	1	1.302	34.09	0.308	2.74	65.37	—
6H-2, 58	51.58	39.11	1	31.95	1	1.310	36.35	0.320	2.61	55.05	—
6H-2, 77	51.77	41.22	1	24.51	1	1.266	23.40	0.252	2.57	66.67	—
6H-2, 92	51.92	30.83	1	39.57	1	1.310	36.34	0.320	2.29	36.54	—
6H-2, 107	52.07	31.32	1	40.46	1	1.317	38.27	0.331	4.12	31.65	—
6H-2, 122	52.22	38.08	1	27.66	1	1.269	24.30	0.257	5.37	66.94	—
6H-2, 137	52.37	38.78	1	28.55	1	1.293	31.47	0.294	2.54	46.05	—
6H-3, 2	52.52	39.92	1	27.43	1	1.289	30.29	0.288	7.01	47.93	—
6H-3, 17	52.67	35.81	1	38.01	1	1.285	29.11	0.281	4.54	56.65	—
6H-3, 29	52.79	32.07	1	43.71	1	1.311	36.58	0.321	4.00	66.75	—
6H-3, 47	52.97	36.25	1	41.76	1	1.327	40.95	0.346	6.85	60.61	—
6H-3, 62	53.12	32.81	1	41.51	1	1.323	39.87	0.340	5.00	55.54	—
6H-3, 77	53.27	42.08	1	34.11	1	1.306	35.16	0.314	5.20	47.57	—
6H-3, 92	53.42	42.56	1	29.50	1	1.261	21.78	0.244	4.67	—	—
6H-3, 107	53.57	40.13	3	26.85	1	1.271	24.86	0.260	2.72	—	—
6H-3, 122	53.72	45.85	1	23.02	1	1.264	22.70	0.249	2.39	—	—
6H-3, 137	53.87	45.94	1	24.82	1	1.261	21.76	0.244	3.96	—	—

Table 2 (continued).

Core, section, interval (cm)	ODP depth (mbsf)	Opal (%)	Analyses (#)	$CaCO_3$	Analyses (#)	GRAPE (smoothed and interpolated)	Estimated $CaCO_3$	Dry bulk density (g/cm3)	Weight >150 µm (%)	Whole foraminifers (%)	Radiolarians > 150 µm (%)
6H-4, 2	54.02	44.88	1	33.81	1	1.321	39.29	0.337	3.57	56.54	—
6H-4, 17	54.17	49.37	1	27.96	1	1.300	33.42	0.304	3.63	71.79	—
6H-4, 28	54.28	48.38	1	25.48	1	1.282	28.15	0.277	2.08	39.88	—
6H-4, 47	54.47	35.87	2	41.33	1	1.318	38.46	0.332	4.52	64.44	—
6H-4, 62	54.62	46.38	1	32.28	1	1.295	31.96	0.297	3.18	—	—
6H-4, 77	54.77	44.60	1	32.21	2	1.311	36.51	0.321	2.97	—	—
6H-4, 92	54.92	48.89	1	19.23	1	1.296	32.24	0.298	2.59	—	—
6H-4, 107	55.07	50.45	1	22.70	1	1.285	29.01	0.281	1.71	—	—
6H-4, 122	55.22	46.46	1	34.74	1	1.311	36.49	0.321	3.20	—	—
6H-4, 137	55.37	35.01	1	45.78	1	1.308	35.64	0.317	3.84	—	—
6H-5, 2	55.52	28.71	1	44.56	1	1.339	44.04	0.364	3.82	—	—
6H-5, 17	55.67	33.83	1	41.16	1	1.313	37.03	0.324	3.18	—	—
6H-5, 28	55.78	39.24	1	36.95	1	1.311	36.47	0.321	4.09	—	—
6H-5, 47	55.97	33.48	1	43.66	1	1.331	41.91	0.352	2.64	—	—
6H-5, 62	56.12	29.16	1	49.85	1	1.323	39.76	0.340	3.52	—	—
6H-5, 77	56.27	25.79	1	52.34	1	1.352	47.34	0.384	3.63	—	—
6H-5, 92	56.42	31.00	1	43.45	1	1.347	46.07	0.377	3.07	—	—
6H-5, 107	56.57	41.42	1	32.19	1	1.310	36.16	0.320	2.96	—	—
6H-5, 122	56.72	47.87	1	23.66	1	1.290	30.42	0.289	2.04	—	—
6H-5, 137	56.87	38.54	1	37.83	1	1.322	39.46	0.338	2.37	—	—
6H-6, 2	57.02	37.72	1	37.50	1	1.317	38.09	0.331	2.22	—	—
6H-6, 17	57.17	36.30	1	30.17	2	1.304	34.45	0.311	2.76	—	—
6H-6, 28	57.28	35.18	1	37.55	1	1.346	45.78	0.375	2.14	—	—
6H-6, 47	57.47	36.62	1	36.09	1	1.316	37.79	0.329	2.16	—	—
6H-6, 58	57.58	27.30	1	45.08	1	1.332	42.12	0.354	2.51	—	—
6H-6, 77	57.77	33.31	1	43.92	1	1.348	46.28	0.378	2.99	—	—
6H-6, 92	57.92	23.20	1	55.05	1	1.369	51.48	0.411	3.18	—	—
6H-6, 107	58.07	29.55	1	48.06	1	1.349	46.52	0.380	3.12	—	—
6H-6, 122	58.22	31.11	1	46.77	1	1.343	44.98	0.371	1.88	—	—
6H-6, 137	58.37	41.29	1	36.18	1	1.342	44.71	0.369	1.90	—	—
6H-7, 2	58.52	36.92	1	30.60	1	1.316	37.75	0.329	1.80	—	—
6H-7, 17	58.67	47.41	2	27.11	1	1.310	36.08	0.320	1.69	—	—
138-847D-											
7H-3, 17	57.27	50.42	1	19.59	2	1.276	26.17	0.268	—	—	—
7H-3, 32	57.42	44.53	1	30.20	1	1.278	26.77	0.271	—	—	—
7H-3, 47	57.57	41.19	1	33.92	1	1.291	30.62	0.291	—	—	—
7H-3, 62	57.72	38.93	1	36.92	1	1.297	32.36	0.300	—	—	—
7H-3, 77	57.87	39.53	1	40.00	1	1.316	37.72	0.329	—	—	—
7H-3, 92	58.02	34.90	1	45.41	1	1.315	37.44	0.328	—	—	—
7H-3, 107	58.17	33.81	2	47.28	1	1.330	41.51	0.351	—	—	—
7H-3, 122	58.32	36.82	2	44.40	1	1.318	38.26	0.332	—	—	—
7H-3, 137	58.47	34.87	1	45.76	1	1.313	36.87	0.324	—	—	—
7H-4, 2	58.62	31.87	1	48.09	1	1.302	33.76	0.308	—	—	—
7H-4, 17	58.77	27.63	1	50.51	1	1.355	47.96	0.389	—	—	—
7H-4, 32	58.92	21.95	1	59.55	1	1.391	56.54	0.444	—	—	—
7H-4, 47	59.07	27.41	1	55.82	1	1.359	48.95	0.395	—	—	—
7H-4, 62	59.22	22.56	1	56.16	1	1.356	48.19	0.391	—	—	—
7H-4, 77	59.37	23.88	2	52.37	1	1.367	50.90	0.407	—	—	—
7H-4, 92	59.52	24.13	1	53.52	1	1.400	58.53	0.458	—	—	—
138-847C-											
7H-1, 17	59.17	20.12	1	66.52	1	1.401	58.75	0.460	—	—	—
7H-1, 30	59.30	18.98	1	66.88	1	1.448	68.35	0.532	—	—	—
7H-1, 47	59.47	23.72	1	58.37	1	1.409	60.48	0.472	—	—	—
7H-1, 62	59.62	25.88	1	59.20	1	1.388	55.82	0.440	—	—	—
7H-1, 77	59.77	26.72	1	58.67	1	1.373	52.31	0.417	—	—	—
7H-1, 92	59.92	27.76	1	55.79	1	1.391	56.49	0.444	—	—	—
7H-1, 107	60.07	30.84	1	55.32	1	1.358	48.64	0.394	—	—	—
7H-1, 122	60.22	31.02	1	51.94	1	1.355	47.89	0.389	—	—	—
7H-1, 137	60.37	30.61	1	53.63	1	1.360	49.13	0.397	—	—	—
7H-2, 2	60.52	32.08	1	52.13	1	1.372	52.04	0.415	—	—	—
7H-2, 17	60.67	36.48	1	46.89	1	1.337	43.26	0.361	—	—	—
7H-2, 30	60.80	40.45	1	40.27	1	1.327	40.59	0.346	—	—	—
7H-2, 47	60.97	37.26	1	42.31	1	1.328	40.86	0.347	—	—	—
7H-2, 64	61.14	40.04	1	31.97	1	1.289	29.87	0.288	—	—	—
7H-2, 77	61.27	36.13	1	38.64	1	1.318	38.13	0.332	—	—	—
7H-2, 92	61.42	35.45	1	38.33	1	1.319	38.40	0.334	—	—	—
7H-2, 107	61.57	34.76	1	39.45	1	1.327	40.57	0.346	—	—	—
7H-2, 122	61.72	37.39	1	36.69	1	1.305	34.48	0.312	—	—	—
7H-2, 137	61.87	36.83	1	30.88	1	1.313	36.72	0.324	—	—	—
7H-3, 2	62.02	34.31	1	35.30	1	1.312	36.43	0.323	—	—	—
7H-3, 17	62.17	17.06	1	62.61	1	1.365	50.30	0.404	—	—	—
7H-3, 30	62.30	15.95	1	65.91	1	1.428	64.36	0.501	—	—	—
7H-3, 47	62.47	18.32	1	58.58	1	1.383	54.57	0.432	—	—	—
7H-3, 62	62.62	20.43	1	60.47	1	1.396	57.53	0.452	—	—	—
7H-3, 77	62.77	19.92	1	62.59	1	1.409	60.38	0.472	—	—	—
7H-3, 92	62.92	22.85	1	48.01	1	1.352	47.04	0.384	—	—	—
7H-3, 107	63.07	25.78	1	43.91	1	1.329	41.05	0.349	—	—	—
7H-3, 122	63.22	25.62	1	50.68	1	1.398	57.96	0.455	—	—	—
7H-3, 137	63.37	13.30	1	71.89	1	1.460	70.46	0.551	—	—	—
7H-4, 2	63.52	13.30	1	70.77	1	1.457	69.91	0.546	—	—	—
7H-4, 17	63.67	14.15	1	70.40	1	1.440	66.70	0.520	—	—	—
7H-4, 30	63.80	15.11	1	68.92	1	1.441	66.89	0.521	—	—	—
7H-4, 47	63.97	18.30	1	65.63	1	1.400	58.38	0.458	—	—	—

Table 2 (continued).

Core, section, interval (cm)	ODP depth (mbsf)	Opal (%)	Analyses (#)	$CaCO_3$	Analyses (#)	GRAPE (smoothed and interpolated)	Estimated $CaCO_3$	Dry bulk density (g/cm3)	Weight >150 µm (%)	Whole foraminifers (%)	Radiolarians > 150 µm (%)
7H-4, 62	64.12	17.63	1	62.55	1	1.407	59.91	0.469	—	—	—
7H-4, 77	64.27	17.52	1	64.45	1	1.403	59.03	0.463	—	—	—
7H-4, 92	64.42	15.93	1	68.77	1	1.451	68.78	0.537	—	—	—
7H-4, 107	64.57	14.95	1	71.46	1	1.482	74.26	0.584	—	—	—
7H-4, 122	64.72	13.26	1	74.88	1	1.472	72.56	0.569	—	—	—
7H-4, 137	64.87	11.95	1	73.70	1	1.450	68.58	0.535	—	—	—
7H-5, 2	65.02	13.84	1	71.80	1	1.475	73.07	0.574	—	—	—
7H-5, 17	65.17	19.47	1	63.83	1	1.442	67.05	0.523	—	—	—
7H-5, 30	65.30	19.44	1	61.21	1	1.414	61.37	0.480	—	—	—
7H-5, 47	65.47	13.82	1	74.13	1	1.464	71.13	0.557	—	—	—
7H-5, 62	65.62	15.79	1	69.18	1	1.451	68.75	0.537	—	—	—
7H-5, 77	65.77	17.71	1	63.59	1	1.429	64.46	0.503	—	—	—
7H-5, 92	65.92	19.08	1	63.73	1	1.423	63.23	0.494	—	—	—
7H-5, 107	66.07	17.68	1	65.55	1	1.442	67.02	0.523	—	—	—
7H-5, 122	66.22	13.73	1	68.52	1	1.458	70.03	0.547	—	—	—
7H-5, 137	66.37	16.14	1	61.89	1	1.432	65.05	0.507	—	—	—
7H-6, 2	66.52	19.71	1	63.40	1	1.405	59.40	0.466	—	—	—
7H-6, 17	66.67	21.28	1	58.99	1	1.402	58.74	0.461	—	—	—
7H-6, 30	66.80	22.32	1	56.91	1	1.375	52.56	0.420	—	—	—
7H-6, 47	66.97	20.72	1	61.59	1	1.413	61.11	0.478	—	—	—
7H-6, 64	67.14	18.88	1	63.45	1	1.433	65.23	0.509	—	—	—
7H-6, 77	67.27	17.28	1	64.61	1	1.439	66.41	0.518	—	—	—
7H-6, 92	67.42	17.85	1	62.44	1	1.411	60.67	0.475	—	—	—
7H-6, 107	67.57	17.35	1	64.28	1	1.410	60.45	0.474	—	—	—
7H-6, 122	67.72	14.56	1	68.74	1	1.442	66.98	0.523	—	—	—
7H-6, 137	67.87	15.55	1	65.03	1	1.467	71.61	0.561	—	—	—
7H-7, 2	68.02	19.71	1	61.59	1	1.416	61.72	0.483	—	—	—
7H-7, 17	68.17	20.67	1	58.15	1	1.385	54.86	0.435	—	—	—
7H-7, 30	68.30	17.92	1	64.85	1	1.420	62.55	0.489	—	—	—
138-847D-											
8H-3, 122	67.82	17.32	1	67.37	1	1.416	61.71	0.483	—	—	—
8H-3, 137	67.97	26.92	1	57.28	1	1.400	58.25	0.458	—	—	—
8H-4, 2	68.12	22.23	1	63.02	1	1.404	59.12	0.464	—	—	—
8H-4, 17	68.27	22.49	1	64.21	1	1.425	63.57	0.497	—	—	—
8H-4, 32	68.42	23.61	1	64.43	1	1.419	62.32	0.487	—	—	—
8H-4, 47	68.57	24.32	1	61.34	1	1.401	58.45	0.460	—	—	—
8H-4, 62	68.72	22.33	1	60.98	1	1.390	55.97	0.443	—	—	—
8H-4, 77	68.87	20.32	1	62.08	1	1.397	57.55	0.454	—	—	—
8H-4, 92	69.02	21.01	1	63.12	1	1.425	63.54	0.497	—	—	—
8H-4, 107	69.17	16.62	1	70.33	1	1.456	69.57	0.544	—	—	—
8H-4, 122	69.32	18.06	1	69.70	1	1.439	66.34	0.518	—	—	—
8H-4, 137	69.47	25.98	1	58.27	1	1.396	57.31	0.452	—	—	—
8H-5, 2	69.62	25.88	1	53.94	1	1.419	62.29	0.487	—	—	—
8H-5, 17	69.77	26.71	1	57.68	1	1.412	60.80	0.477	—	—	—
8H-5, 32	69.92	24.25	1	54.68	1	1.416	61.65	0.483	—	—	—
138-847C-											
8H-2, 2	70.02	25.67	1	62.18	1	1.394	56.84	0.449	—	—	—
8H-2, 17	70.17	24.05	1	59.54	1	1.407	59.72	0.469	—	—	—
8H-2, 32	70.32	22.59	1	64.36	1	1.458	69.92	0.547	—	—	—
8H-2, 47	70.47	24.98	1	60.11	1	1.425	63.51	0.497	—	—	—
8H-2, 62	70.62	22.24	1	66.67	1	1.423	63.09	0.494	—	—	—
8H-2, 78	70.78	18.94	1	68.05	1	1.451	68.61	0.537	—	—	—
8H-2, 92	70.92	20.18	1	67.49	1	1.458	69.90	0.547	—	—	—
8H-2, 107	71.07	21.72	1	64.76	1	1.442	66.88	0.523	—	—	—
8H-2, 122	71.22	22.30	1	66.77	1	1.421	62.66	0.491	—	—	—
8H-2, 137	71.37	19.86	1	68.42	1	1.457	69.71	0.546	—	—	—
8H-3, 2	71.52	17.14	1	72.85	1	1.509	78.37	0.626	—	—	—
8H-3, 17	71.67	18.72	1	72.37	1	1.486	74.75	0.591	—	—	—
8H-3, 32	71.82	20.94	1	71.43	1	1.459	70.06	0.549	—	—	—
8H-3, 47	71.97	19.95	1	69.25	1	1.457	69.69	0.546	—	—	—
8H-3, 62	72.12	18.61	1	70.07	1	1.465	71.14	0.558	—	—	—
8H-3, 78	72.28	14.59	1	75.32	1	1.478	73.40	0.578	—	—	—
8H-3, 92	72.42	22.63	1	68.15	1	1.445	67.42	0.527	—	—	—
8H-3, 107	72.57	23.90	1	64.97	1	1.436	65.66	0.514	—	—	—
8H-3, 122	72.72	24.39	1	64.00	1	1.422	62.82	0.492	—	—	—
8H-3, 137	72.87	26.48	1	61.12	1	1.405	59.20	0.466	—	—	—
8H-4, 2	73.02	27.25	1	60.32	1	1.413	60.92	0.478	—	—	—
8H-4, 17	73.17	26.49	1	59.37	1	1.411	60.49	0.475	—	—	—
8H-4, 32	73.32	21.26	1	62.54	1	1.400	58.09	0.458	—	—	—
8H-4, 47	73.47	18.43	1	66.76	1	1.443	67.01	0.524	—	—	—
8H-4, 62	73.62	21.65	1	65.02	1	1.446	67.58	0.529	—	—	—
8H-4, 78	73.78	19.50	1	64.04	1	1.435	65.43	0.512	—	—	—
8H-4, 92	73.92	15.82	1	71.81	1	1.469	71.80	0.564	—	—	—
8H-4, 107	74.07	14.16	1	74.11	1	1.502	77.25	0.615	—	—	—
8H-4, 122	74.22	14.25	1	75.72	1	1.512	78.76	0.631	—	—	—
8H-4, 137	74.37	18.90	1	66.47	1	1.438	66.01	0.517	—	—	—
8H-5, 2	74.52	21.73	1	61.77	1	1.443	66.98	0.524	—	—	—
8H-5, 17	74.67	20.67	1	64.79	1	1.414	61.09	0.480	—	—	—
8H-5, 32	74.82	19.99	1	66.40	1	1.445	67.36	0.527	—	—	—
8H-5, 47	74.97	21.82	1	64.94	1	1.447	67.74	0.531	—	—	—
8H-5, 62	75.12	18.41	1	66.85	1	1.455	69.24	0.543	—	—	—
8H-5, 78	75.28	18.48	1	67.24	1	1.444	67.16	0.526	—	—	—
8H-5, 92	75.42	16.00	1	68.34	1	1.437	65.79	0.515	—	—	—

Table 2 (continued).

Core, section, interval (cm)	ODP depth (mbsf)	Opal (%)	Analyses (#)	$CaCO_3$	Analyses (#)	GRAPE (smoothed and interpolated)	Estimated $CaCO_3$	Dry bulk density (g/cm3)	Weight >150 µm (%)	Whole foraminifers (%)	Radiolarians > 150 µm (%)
8H-5, 107	75.57	18.10	1	67.86	1	1.434	65.19	0.511	—	—	—
8H-5, 122	75.72	24.06	1	58.17	1	1.394	56.67	0.449	—	—	—
8H-5, 137	75.87	29.67	3	49.85	1	1.353	46.84	0.386	—	—	—
8H-6, 2	76.02	35.46	1	41.41	1	1.359	48.34	0.395	—	—	—
8H-6, 17	76.17	15.81	1	69.45	1	1.443	66.94	0.524	—	—	—
8H-6, 32	76.32	13.01	1	72.63	1	1.474	72.62	0.572	—	—	—
8H-6, 47	76.47	14.15	1	71.77	1	1.450	68.27	0.535	—	—	—
8H-6, 62	76.62	14.96	1	69.53	1	1.435	65.36	0.512	—	—	—
8H-6, 78	76.78	14.99	1	71.32	1	1.481	73.80	0.583	—	—	—
8H-6, 92	76.92	15.45	1	71.62	1	1.458	69.75	0.547	—	—	—
138-847D-											
9H-3, 32	76.42	14.86	1	68.39	1	1.449	68.07	0.534	—	—	—
9H-3, 47	76.57	15.34	1	71.27	1	1.423	62.91	0.494	—	—	—
9H-3, 62	76.72	19.72	1	66.59	1	1.416	61.44	0.483	—	—	—
9H-3, 77	76.87	22.59	1	61.90	1	1.385	54.56	0.435	—	—	—
9H-3, 92	77.02	16.05	1	73.94	1	1.443	66.90	0.524	—	—	—
9H-3, 107	77.17	12.48	1	74.56	1	1.473	72.41	0.571	—	—	—
9H-3, 122	77.32	13.85	1	75.72	1	1.444	67.09	0.526	—	—	—
9H-3, 137	77.47	17.49	1	69.19	1	1.448	67.85	0.532	—	—	—
9H-4, 2	77.62	22.28	1	61.85	1	1.440	66.30	0.520	—	—	—
9H-4, 17	77.77	30.25	1	54.64	1	1.394	56.59	0.449	—	—	—
9H-4, 32	77.92	18.48	1	71.00	1	1.398	57.49	0.455	—	—	—
9H-4, 47	78.07	14.79	1	71.78	1	1.458	69.71	0.547	—	—	—
9H-4, 62	78.22	15.69	1	68.72	1	1.459	69.89	0.549	—	—	—
9H-4, 77	78.37	15.26	1	74.40	1	1.457	69.52	0.546	—	—	—
9H-4, 92	78.52	12.02	1	78.99	1	1.490	75.24	0.597	—	—	—
9H-4, 107	78.67	12.07	1	71.87	1	1.460	70.06	0.551	—	—	—
9H-4, 122	78.82	19.04	1	60.84	1	1.407	59.45	0.469	—	—	—
9H-4, 137	78.97	25.76	1	57.40	1	1.385	54.49	0.435	—	—	—
9H-5, 2	79.12	24.84	1	58.01	1	1.402	58.34	0.461	—	—	—
138-847C-											
9H-5, 17	79.27	18.91	2	66.75	1	1.444	67.04	0.526	—	—	—
9H-1, 32	78.32	24.25	1	59.75	1	1.407	59.43	0.469	—	—	—
9H-1, 47	78.47	15.40	1	66.61	1	1.448	67.79	0.532	—	—	—
9H-1, 62	78.62	14.03	1	70.30	1	1.486	74.56	0.591	—	—	—
9H-1, 77	78.77	13.90	1	69.57	1	1.473	72.35	0.571	—	—	—
9H-1, 92	78.92	14.16	1	71.20	1	1.468	71.46	0.563	—	—	—
9H-1, 107	79.07	17.17	1	65.83	1	1.459	69.84	0.549	—	—	—
9H-1, 122	79.22	20.35	1	62.95	1	1.431	64.44	0.506	—	—	—
9H-1, 137	79.37	17.26	1	63.71	1	1.442	66.61	0.523	—	—	—
9H-2, 2	79.52	12.86	1	76.21	1	1.522	80.07	0.646	—	—	—
9H-2, 17	79.67	11.98	1	76.42	1	1.513	78.76	0.632	—	—	—
9H-2, 32	79.82	14.62	1	67.30	1	1.473	72.32	0.571	—	—	—
9H-2, 47	79.97	17.56	1	70.93	1	1.477	73.01	0.577	—	—	—
9H-2, 62	80.12	23.66	1	62.78	1	1.437	65.61	0.515	—	—	—
9H-2, 77	80.27	37.48	2	46.00	1	1.362	48.89	0.400	—	—	—
9H-2, 92	80.42	31.31	1	52.54	1	1.400	57.82	0.458	—	—	—
9H-2, 107	80.57	33.38	1	54.02	1	1.392	56.01	0.446	—	—	—
9H-2, 122	80.72	33.61	1	54.22	1	1.396	56.92	0.452	—	—	—
9H-2, 137	80.87	26.55	1	61.12	1	1.445	67.16	0.527	—	—	—
9H-3, 2	81.02	15.65	1	71.50	1	1.489	75.00	0.595	—	—	—
9H-3, 17	81.17	13.53	1	74.45	1	1.510	78.28	0.627	—	—	—
9H-3, 32	81.32	11.62	1	77.71	1	1.526	80.59	0.652	—	—	—
9H-3, 47	81.47	11.99	1	76.35	1	1.505	77.52	0.620	—	—	—
9H-3, 62	81.62	11.16	1	77.05	1	1.489	74.98	0.595	—	—	—
9H-3, 77	81.77	12.58	1	74.18	1	1.500	76.74	0.612	—	—	—
9H-3, 92	81.92	13.67	1	70.17	1	1.487	74.65	0.592	—	—	—
9H-3, 107	82.07	9.92	1	74.19	2	1.531	81.27	0.660	—	—	—
9H-3, 122	82.22	10.82	1	75.07	1	1.526	80.58	0.652	—	—	—
9H-3, 137	82.37	8.68	1	75.33	1	1.520	79.73	0.643	—	—	—
9H-4, 2	82.52	8.47	1	76.94	1	1.580	87.13	0.735	—	—	—
9H-4, 17	82.67	8.20	1	77.57	1	1.508	77.95	0.624	—	—	—
9H-4, 32	82.82	9.13	1	78.18	1	1.537	82.06	0.669	—	—	—
9H-4, 47	82.97	11.57	1	73.01	1	1.515	78.99	0.635	—	—	—
9H-4, 62	83.12	16.16	1	65.62	1	1.450	68.05	0.535	—	—	—
9H-4, 77	83.27	17.82	1	62.36	1	1.432	64.53	0.507	—	—	—
9H-4, 92	83.42	9.85	1	76.19	1	1.496	76.07	0.606	—	—	—
9H-4, 107	83.57	9.45	1	78.41	1	1.527	80.69	0.654	—	—	—
9H-4, 122	83.72	9.08	1	79.17	1	1.526	80.55	0.652	—	—	—
9H-4, 137	83.87	10.20	1	78.06	1	1.531	81.23	0.660	—	—	—
9H-5, 2	84.02	10.37	1	77.16	1	1.548	83.45	0.686	—	—	—
9H-5, 17	84.17	10.60	1	74.24	1	1.509	78.07	0.626	—	—	—
9H-5, 32	84.32	11.96	2	76.37	1	1.504	77.31	0.618	—	—	—
9H-5, 47	84.47	13.34	1	73.13	1	1.503	77.15	0.617	—	—	—
9H-5, 62	84.62	16.02	1	69.24	1	1.459	69.70	0.549	—	—	—
9H-5, 77	84.77	15.40	1	72.04	1	1.502	76.99	0.615	—	—	—
9H-5, 92	84.92	12.22	1	75.59	1	1.521	79.82	0.644	—	—	—
9H-5, 107	85.07	13.19	1	71.61	1	1.500	76.67	0.612	—	—	—
9H-5, 122	85.22	15.11	1	68.83	1	1.460	69.87	0.551	—	—	—
9H-5, 137	85.37	17.59	1	64.86	1	1.462	70.23	0.554	—	—	—
9H-6, 2	85.52	17.25	1	68.79	1	1.474	72.36	0.572	—	—	—

Table 2 (continued).

Core, section, interval (cm)	ODP depth (mbsf)	Opal (%)	Analyses (#)	$CaCO_3$	Analyses (#)	GRAPE (smoothed and interpolated)	Estimated $CaCO_3$	Dry bulk density (g/cm3)	Weight >150 µm (%)	Whole foraminifers (%)	Radiolarians > 150 µm (%)
9H-6, 17	85.67	17.09	1	66.19	1	1.479	73.22	0.580	—	—	—
9H-6, 32	85.82	15.71	1	70.82	1	1.460	69.85	0.551	—	—	—
9H-6, 47	85.97	15.58	1	71.30	1	1.467	71.11	0.561	—	—	—
9H-6, 62	86.12	17.75	1	68.59	1	1.449	67.79	0.534	—	—	—
9H-6, 77	86.27	17.09	1	68.89	1	1.476	72.69	0.575	—	—	—
9H-6, 92	86.42	13.12	1	74.58	1	1.514	78.77	0.634	—	—	—
9H-6, 107	86.57	13.52	1	73.28	1	1.509	78.02	0.626	—	—	—
9H-6, 122	86.72	17.14	1	69.94	1	1.477	72.85	0.577	—	—	—
9H-6, 137	86.87	20.90	1	63.20	1	1.436	65.23	0.514	—	—	—
9H-7, 2	87.02	18.30	1	68.79	1	1.480	73.36	0.581	—	—	—
9H-7, 17	87.17	17.69	1	67.01	1	1.459	69.63	0.549	—	—	—
9H-7, 32	87.32	15.78	1	74.09	1	1.487	74.52	0.592	—	—	—
9H-7, 48	87.48	16.72	1	64.71	1	1.432	64.41	0.507	—	—	—
9H-7, 62	87.62	17.44	1	61.51	1	1.425	62.98	0.497	—	—	—
9H-7, 77	87.77	15.26	1	68.05	1	1.450	67.93	0.535	—	—	—

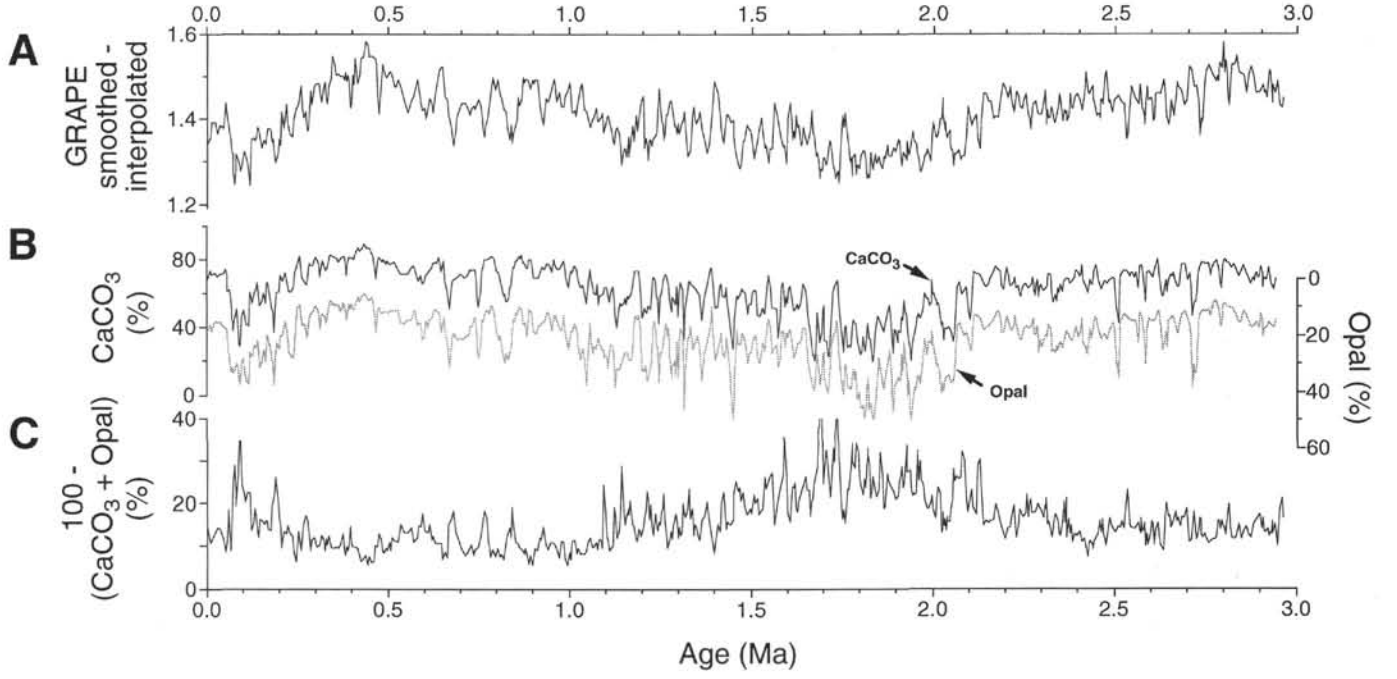

Figure 7. **A.** Time series for the past 3 m.y. of GRAPE density data smoothed with a nine-point Gaussian filter and sampled at depths corresponding to samples used in this study. **B.** %$CaCO_3$ and %opal. **C.** %Lithogenic estimated from [100 – ($CaCO_3$ + opal)]. Note that the opal scale has been inverted. The ages were derived from the GRAPE-based age model of Shackleton et al. (this volume).

estimating calcium carbonate concentrations from the GRAPE density values in nearby piston cores and DSDP sites. This empirical relationship was applied to Leg 138 sites in the study of spatial and temporal variability of carbonate by Hagelberg et al. (this volume). Here, we apply the empirical relationship of Mayer (1991) to the smoothed GRAPE data to estimate carbonate concentrations for the samples analyzed in this study (Table 2). The smoothed data were used because the raw GRAPE data have substantial high-frequency variability, which induces a greater scatter in the estimated $CaCO_3$ concentrations. The estimated carbonate stratigraphy matches the pattern of measured carbonate rather well ($r = 0.93$; Figs. 9A–9B), and the mean of the absolute value of the difference of the measured and estimated values is 4.5%. Some large differences do occur, especially on rapid transitions. The GRAPE data were interpolated to obtain values corresponding to samples used in this study, and this interpolation may contribute to the offsets. GRAPE density and carbonate data had a different sample spacing, and linear interpolation between the adjacent ~2-cm-spaced GRAPE measurements was performed to obtain values for comparing with the carbonate measurements. In addition, GRAPE measurements were performed on cores before they were split, whereas sampling for the chemical measurements was performed after they had been split. Depth offsets resulting from core curation may also be responsible for these large differences.

The differences of the estimated and measured carbonate values were compared to the opal and calcium carbonate concentration data to determine whether the differences can be attributed to either of these components. The estimate of carbonate from GRAPE data assumes that much of the variability results from changes in the relative proportions and packing characteristics of carbonate and opal (Herbert and Mayer, 1991). Should carbonate or opal components at Site 847 have different characteristics from those sites to the west, where the empirical relationships were developed and first applied, the offsets might correlate with either carbonate or opal concentrations. However, no correlation can be seen between the residuals and either carbonate or opal concentrations (Figs. 9C–9D).

Because of its relatively close proximity to South America, Site 847 is likely to have more terrigenous influx than sites to the west. The influx of substantial amounts of this third component is likely to induce errors in the predictions. We used [100 – ($CaCO_3$ + opal)] as a measure of the detrital influx (Fig. 7C). The magnitude of the terrigenous values estimated from this method is twice that of estimates based on a sequential leach (S. Hovan, pers. comm., 1992). As

Table 3. Composite depth reconstruction for Site 847.

Patch no.	Core, section, interval (cm)	ODP depth (mbsf)	Interval length (m)	Shipboard composite (mcd)	Composite this study (Bmcd)
1	138-847B-1H-1, 0 to 138-847B-1H-3, 47	0.00–3.47	3.47	0.00–3.47	0.00–3.47
	138-847C-1H-1, 122 to 138-847C-1H-7, 47	3.22–11.47	8.25	3.62–11.87	3.50–11.75
2	138-847D-2H-3, 62 to 138-847D-2H-4, 32	10.22–11.42	1.20	12.02–13.22	11.76–12.96
	138-847C-2H-1, 17 to 138-847C-2H-7, 30	11.67–20.80	9.13	13.35–22.48	13.08–22.21
3	138-847D-3H-3, 62 to 138-847D-3H-3, 137	19.72–20.47	0.75	22.72–23.47	22.38–23.13
	138-847C-3H-1, 17 to 138-847C-3H-7, 62	21.17–30.62	9.45	23.57–33.02	23.31–32.76
4	138-847D-4H-3, 47 to 138-847D-4H-3, 137	29.07–29.97	0.90	33.07–33.97	32.86–33.76
	138-847C-4H-1, 32 to 138-847C-4H-7, 47	30.82–39.97	9.15	34.12–43.27	33.94–43.09
5	138-847D-5H-3, 107 to 138-847D-5H-4, 92	39.17–40.52	1.35	43.37–44.72	43.17–44.52
	138-847C-5H-1, 47 to 138-847C-5H-7, 64	40.47–49.64	9.17	44.97–54.14	44.62–53.79
6	138-847D-6H-3, 32 to 138-847D-6H-3, 137	47.92–48.97	1.05	54.12–55.17	53.89–54.94
	138-847C-6H-1, 17 to 138-847C-6H-7, 17	49.67–58.67	9.00	55.37–64.37	54.95—63.95
7	138-847D-7H-3, 17 to 138-847D-7H-4, 92	57.27–59.52	2.25	64.47–66.72	64.05–66.30
	138-847C-7H-1, 17 to 138-847C-7H-7, 30	59.17–68.30	9.13	66.97–76.10	66.32—75.45
8	138-847D-8H-3, 122 to 138-847D-8H-5, 32	67.82–69.92	2.10	76.12–78.22	75.55–77.65
	138-847C-8H-2, 2 to 138-847C-8H-6, 92	70.02–76.92	6.90	78.22–85.12	77.75–84.65
9	138-847D-9H-3, 32 to 138-847D-9H-5, 17	76.42–79.27	2.85	85.12–87.97	84.85–87.70
	138-847C-9H-1, 32 to 138-847C-9H-7, 77	78.32–87.77	9.45	88.22–97.67	87.87–97.32

Table 4. GRAPE-based age model from Shackleton et al. (this volume).

Composite depth (rmcd)	Composite depth (Bmcd)	Age (Ma)	Composite depth (rmcd)	Composite depth (Bmcd)	Age (Ma)
0.000	0.000	0.000	55.870	55.450	1.750
1.110	1.110	0.056	57.650	57.240	1.811
2.730	2.730	0.082	58.790	58.370	1.832
3.470	3.470	0.103	61.250	60.830	1.875
4.110	4.060	0.126	61.930	61.510	1.904
7.650	7.530	0.218	63.710	63.290	1.947
8.830	8.600	0.262	64.670	64.220	1.958
9.790	9.515	0.290	66.150	65.730	2.003
10.290	10.000	0.311	66.830	66.420	2.023
11.130	10.700	0.333	68.150	67.640	2.042
11.810	11.520	0.354	68.590	68.010	2.052
12.230	12.000	0.372	70.070	69.420	2.097
13.770	13.510	0.408	70.550	69.900	2.118
15.190	14.920	0.462	70.830	70.180	2.129
16.050	15.780	0.484	71.170	70.520	2.140
17.450	17.175	0.528	73.330	72.670	2.211
18.230	17.960	0.577	74.030	73.380	2.233
20.330	20.060	0.648	74.990	74.340	2.255
21.470	21.130	0.692	75.510	74.860	2.278
21.710	21.330	0.712	76.130	75.550	2.305
22.690	22.350	0.749	77.430	76.850	2.348
24.290	24.075	0.787	78.910	78.470	2.390
25.150	24.890	0.824	79.690	79.285	2.422
28.150	27.890	0.908	80.390	80.040	2.438
29.610	29.350	0.978	82.390	81.920	2.477
30.430	30.170	1.000	83.570	83.100	2.521
31.530	31.270	1.050	84.490	84.070	2.547
32.670	32.340	1.072	84.850	84.540	2.569
37.510	37.265	1.205	85.910	85.640	2.592
38.150	37.790	1.215	86.770	86.490	2.614
39.090	38.940	1.243	87.250	86.990	2.637
39.770	39.670	1.272	88.830	88.460	2.683
40.510	40.270	1.283	89.470	89.110	2.707
41.070	40.915	1.307	89.890	89.495	2.729
41.730	41.480	1.327	91.110	90.760	2.754
42.410	42.230	1.337	91.470	91.120	2.776
43.810	43.610	1.379	91.790	91.440	2.786
44.750	44.545	1.400	92.450	92.100	2.798
45.570	45.325	1.431	93.930	93.580	2.835
47.550	47.190	1.493	94.830	94.480	2.876
48.590	48.240	1.528	95.410	95.060	2.904
49.830	49.480	1.567	96.330	95.980	2.926
50.890	50.540	1.606	96.970	96.660	2.937
53.090	52.850	1.697	97.230	96.855	2.949
55.150	54.900	1.718	97.750	97.370	2.969

shown in the Appendix, a strong base (NaOH) used in the sequential leach might remove silica from the clays, thus causing one to underestimate the terrigenous portion of the sediments. In addition, incomplete digestion of radiolarians and the accumulation of other sedimentary components, such as oxyhydroxides, salts, and organics, might contribute to some of this difference. These added influxes are likely to shift the concentrations to lower values, but the pattern of change probably would remain the same. A comparison of our esti-

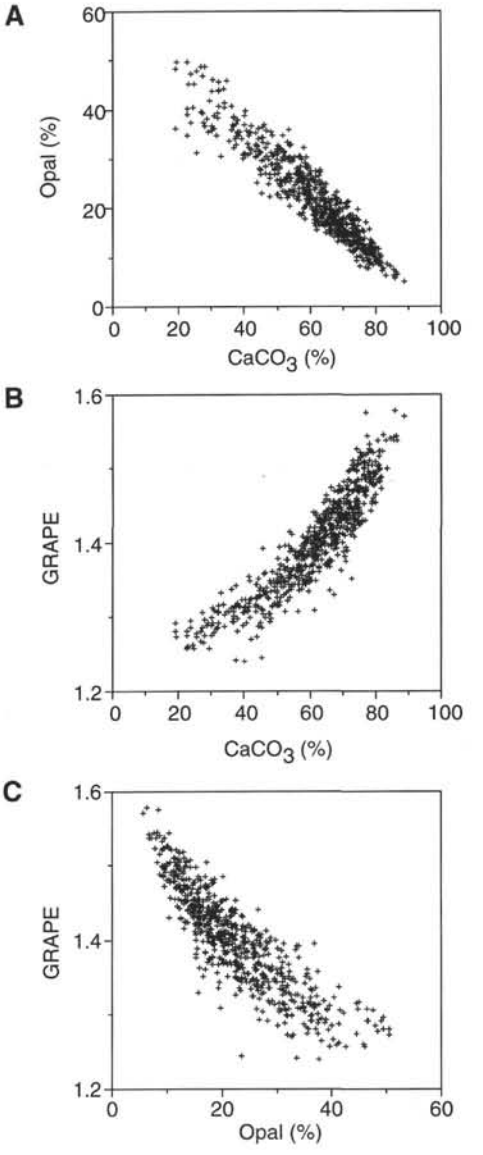

Figure 8. Scatter plots of (**A**) %$CaCO_3$ and %opal, (**B**) %$CaCO_3$ and GRAPE, and (**C**) %opal and GRAPE data given in Table 2. The opal and carbonate data are highly correlated ($r = -0.94$). A comparison of GRAPE data to the chemical data reveals a curvilinear relationship, with a large scatter in the high opal range.

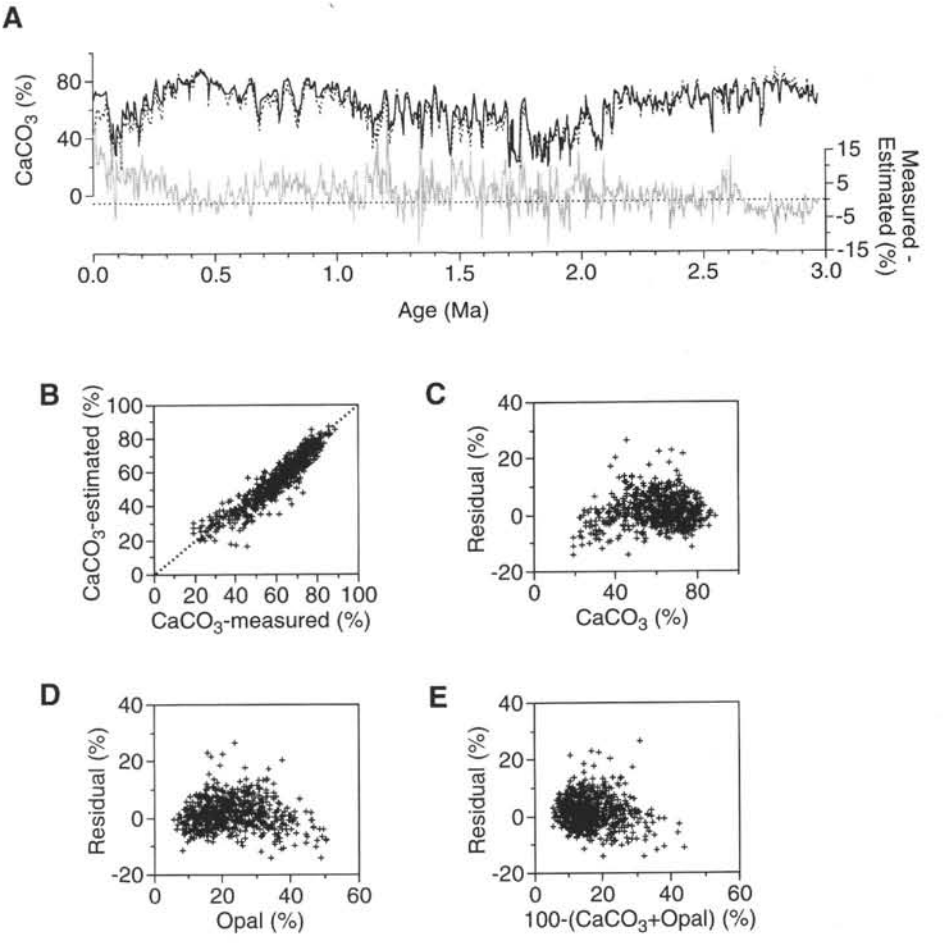

Figure 9. **A.** Time series of measured %$CaCO_3$ and values estimated from GRAPE density data using the equations of Mayer (1991) for Cores 1H to 9H from Site 847. Also shown is a time series of the difference between measured and estimated values. The largest differences occur on the transitions between high and low values of %$CaCO_3$. **B.** Scatter plot of measured vs. estimated %$CaCO_3$ values. The 1:1 line is shown. **C–E.** Scatter plots of difference between the measured and estimated %$CaCO_3$ vs. %$CaCO_3$, %opal, and %lithogenic as estimated from [100 – ($CaCO_3$ + opal)].

mate of the detrital component to the residuals of the carbonate predictions also reveals no correlation (Fig. 9E), and the differences exhibit a random scatter, which may reflect the limits of estimating carbonate from GRAPE data.

Biogenic Sedimentation (0–1 Ma)

The cyclic changes in carbonate and opal sedimentation in the equatorial Pacific Ocean have been the subject of numerous studies since they were first reported by Arrhenius (1952). During the late Pleistocene, the cycles in central equatorial Pacific locations closely followed the waxing and waning of the ice sheets, implying a response of the equatorial Pacific Ocean to global climatic forcing (Broecker, 1971; Luz and Shackleton, 1975; Pisias and Rea, 1988; Farrell and Prell, 1989). The cyclic changes at Site 847 exhibit some similarities, but also some distinct differences, compared with deeper sites farther to the west. The carbonate concentration changes do exhibit a general pattern of carbonate-rich intervals during glacial periods and carbonate-poor sediments associated with interglacial periods (Fig. 10). However, the amplitude of the signal is less pronounced at Site 847 compared with that at the central equatorial Pacific sites studied by Farrell and Prell (1989). This is to be expected because Site 847 is at or near the top of the sediment lysocline for this area (Berger et al., 1976) and carbonate dissolution, which is a major controlling factor on the amplitude of the central Pacific cycles, should have played a smaller role in altering the carbonate influx to Site 847. The low-carbonate interval during the last major interglacial period (0.08–0.12 Ma) is relatively more pronounced in Site 847 sediments than in sediments from central equatorial Pacific sites. This same event was observed in DSDP Site 572 (Farrell and Prell, 1991), also located near the top of the sediment lysocline for this region (Berger et al., 1976). Dilution by noncarbonate material such as opal may have played a role in the structure of the concentration record. By examining the data in terms of MARs, the effect of dilution should be ameliorated.

The structure in the time series of the MARs is a function of the sedimentation rates and, therefore, the age model used. In Figure 10, we show the time series and spectral characteristics $\delta^{18}O$ of *G. sacculifer*, GRAPE, %$CaCO_3$, and $CaCO_3$ MAR records for the past 1 m.y. using the isotope and GRAPE-based age models. The GRAPE-based chronology assumes that the concentration changes in the equatorial Pacific exhibit the same periodic nature as the Northern Hemisphere insolation changes (Shackleton et al., this volume). The close match between the time series and spectral characteristics of concentration data and oxygen isotopes using the two independent age models implies that the assumption concerning the periodic nature of the concentration changes is generally valid, especially in the low-frequency range (Fig. 10). However, temporal offsets are apparent which will

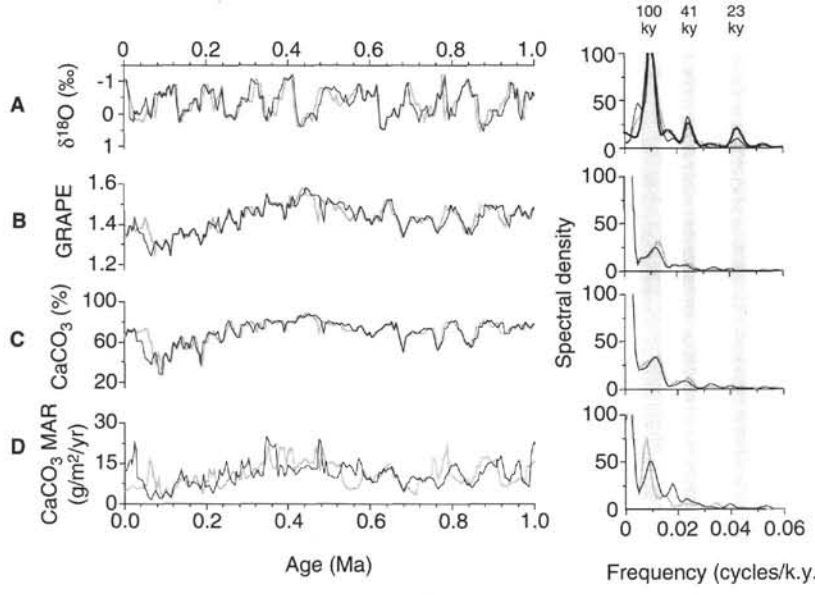

Figure 10. Time series and spectra for (**A**) $\delta^{18}O$ of *G. sacculifer,* (**B**) GRAPE-smoothed and interpolated, (**C**) $\%CaCO_3$, and (**D**) $CaCO_3$ MAR for the interval from 0 to 1 Ma. The ages are based on the *G. sacculifer* age model of Farrell et al. (this volume) (solid line) and the GRAPE-based, orbitally tuned model of Shackleton et al. (this volume) (thick dotted line). The spectra, plotted as spectral density vs. frequency, were calculated using $\Delta t = 4$ k.y., 90 lags, and a bandwidth of 0.004. The dashed line in Figure 10A is the spectra of the SPECMAP stacked isotope time series for the past 0.63 m.y.; 70 lags were used for this analysis. The shaded bands in each spectra depict the 100-, 41-, and 23-k.y. bands associated with variations in the Earth's orbital parameters.

have an impact on the phase estimates between the Site 847 time series using the GRAPE-based age models and records of global climate change (e.g., Imbrie et al., 1992). In addition, these temporal offsets will result in differences in MARs that rely on sedimentation rates derived from these age models (Fig. 10D). The $CaCO_3$ MAR time series based on the two chronologies are substantially different in the higher frequencies, but the same general trends in the data are apparent in both records (Fig. 10D). The $CaCO_3$ MAR time series using the oxygen isotope-based chronology is strikingly similar to that in the GRAPE and $\%CaCO_3$ records. For the past 1 m.y., the records exhibit a significant near-100 k.y. periodicity as well as an increase in $CaCO_3$ MAR between 0.3 and 0.6 Ma. The last interglacial period (0.08–0.12 Ma) was characterized by low $CaCO_3$ MAR, followed by a substantial increase to high values during the last glacial episode. We examined foraminifer preservation data and the relative influx of siliceous material to identify the cause of these large changes.

The accumulation of $CaCO_3$ should reflect the balance between processes of production and dissolution. The data on the percentage of whole planktonic foraminifers, relative to fragments, provide a relative index of the extent to which dissolution of carbonate has altered the record (Thunell, 1976). The values spanning the last interglacial period range from 47% to 72%, but show no distinct correlation of high fragmentation during low accumulation (Fig. 11B). In fact, the relative low $CaCO_3$ MARs near 0.07 and 0.09 Ma are associated with a foraminifer assemblage having the same preservation state as during the carbonate-rich glacial period (see also McKenna et al, this volume). During this interglacial time interval, the proportion of radiolarians, which reflects the siliceous component of the sediments, relative to foraminifers in the >150-μm fraction is larger than in the following glacial, although the overall accumulation of opal is not greater (Fig. 11C). Taken together, these data imply that the changes are related to the carbonate component and not the opal, and that carbonate production and not dissolution is responsible for the changes in $CaCO_3$ MAR. The production of carbonate was lower during the last interglacial, resulting in a relative increase in the siliceous component of the plankton.

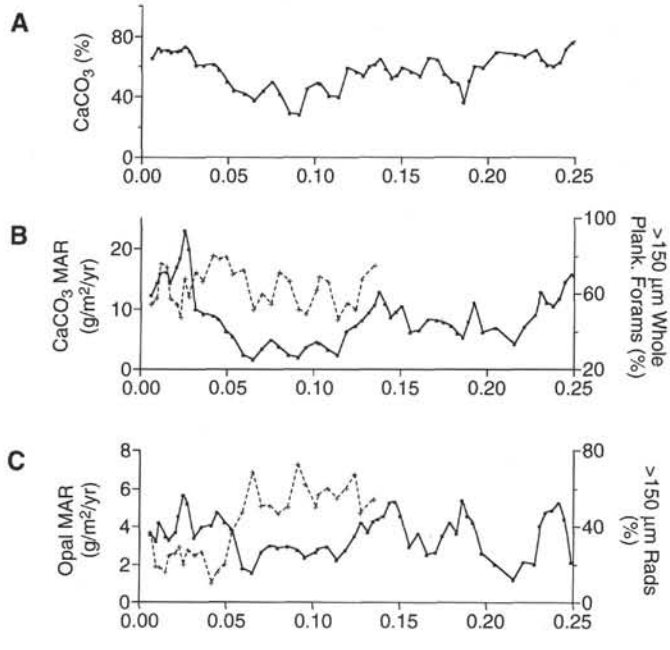

Figure 11. Time series for the past 0.5 m.y. of Site 847 carbonate and opal data. **A.** $\%CaCO_3$. **B.** $CaCO_3$ MAR (solid line) and percentage of whole planktonic foraminifers > 150 μm (dashed line). **C.** Opal MAR (solid line) and percentage of radiolarians > 150 μm relative to foraminifers (dashed line). The ages are based on the oxygen isotope chronostratigraphy.

Biogenic Sedimentation (0–3 Ma)

Time series of carbonate concentration and $CaCO_3$ and opal MAR for the past 3 m.y. are shown in Figure 12. The pattern of $\%CaCO_3$ for Site 847 is similar to that observed at DSDP Site 572, almost 20° to the west (Farrell and Prell, 1991). For this analysis, we used the age

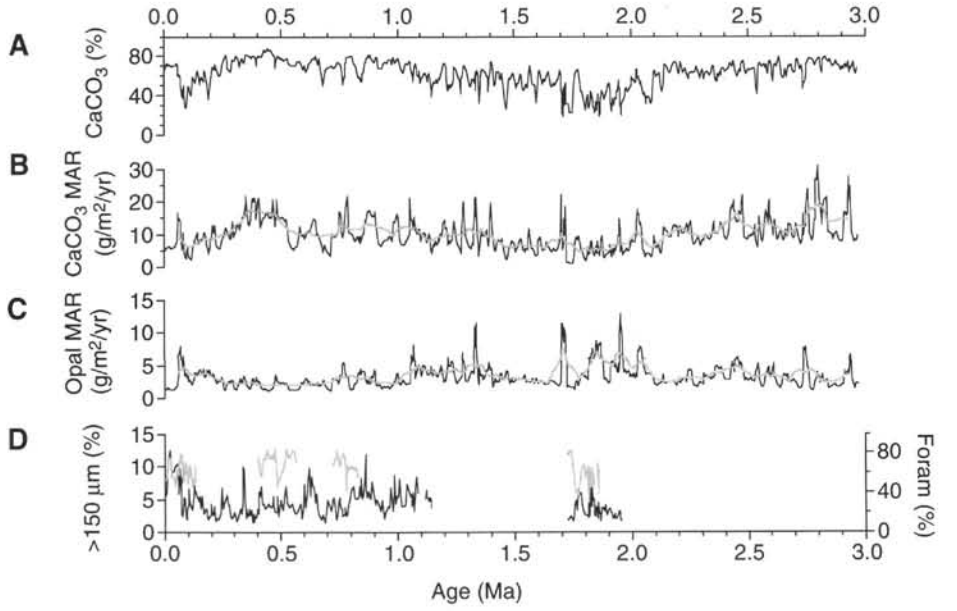

Figure 12. Time series of (**A**) %$CaCO_3$, (**B**) $CaCO_3$ MAR, (**C**) opal MAR, and (**D**) weight > 150 µm (solid) and %foraminifers (thick dotted) for Site 847 spanning the past 3 m.y. The GRAPE-based age model from Shackleton et al. (this volume) was used to provide the chronostratigraphic framework for these time series. The thick dotted lines in Figures 12B and 12C are 20-point running means that capture the major trends in the data.

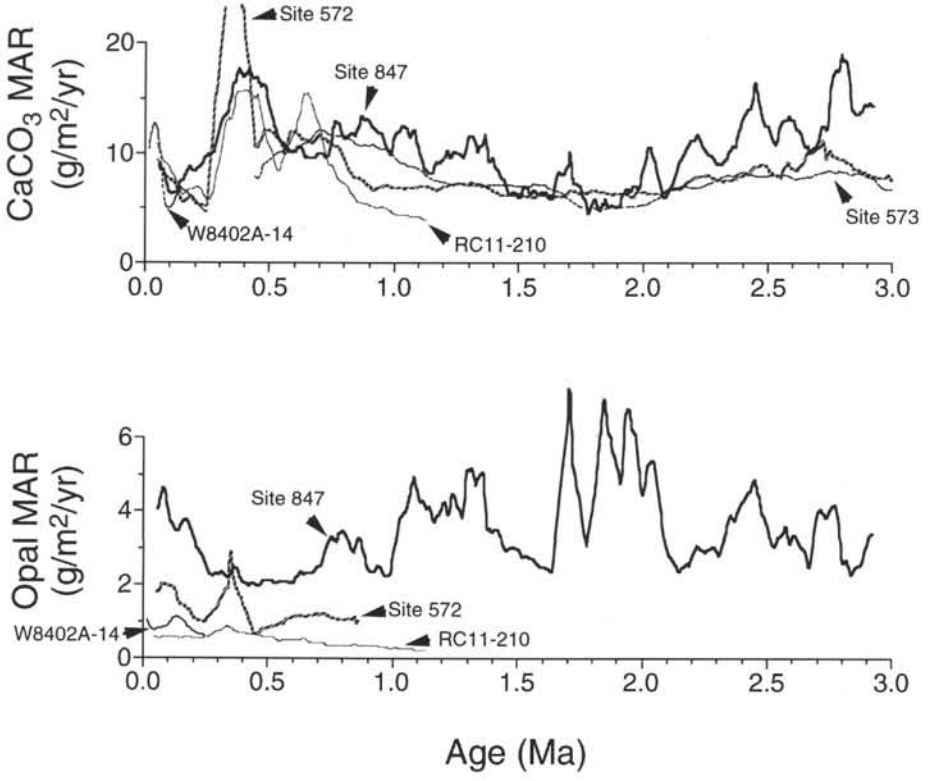

Figure 13. Time series of $CaCO_3$ and opal MARs for sites forming a transect along the equator from 140° to 95°W. The plots are 20-point running means of the data for each site to capture the major trends over the past 3 m.y. DSDP Site 573 (thin broken line), Core RC11-210 (thin dotted line), and Core W8402A-14 (thin dashed line) are all located near 140°W; DSDP Site 572 (thick dotted line) is in the middle near 114°W; and ODP Site 847 (thick solid line) is in the east near 95°W (see text for details).

model based on tuning the GRAPE data to the summer insolation changes. Therefore, as shown in the previous section, the timing of the higher frequency MAR maxima and minima are suspect, but the long-term trends generally are valid. A 20-point moving average is used to depict the trends in the MAR data for the past 3 m.y. (Fig. 12). High rates of $CaCO_3$ MAR near 2.8 Ma are followed by a distinct minima near 1.8 Ma. $CaCO_3$ MAR increases to a maxima near 0.4 Ma, followed by a significant decrease in production during the last interglacial period. We used preliminary preservation data to evaluate the relative influence of dissolution on the alteration of the record of carbonate production. In carbonate-rich sediments, where dissolution causes fragmentation of foraminifer tests into smaller particles, coarse fraction data (>150-μm wt%) have been used as an index of dissolution (Peterson and Prell, 1985). The coarse fraction data from Site 847 (Fig. 12) do not exhibit a correspondence with either the high-frequency or broad trends in the $CaCO_3$ MAR time series. We concluded that either the coarse fraction is not a reliable index of dissolution for the Site 847 samples or that production is responsible for the structure of the $CaCO_3$ MAR time series. Additional dissolution indexes, such as whole planktonic foraminifers (%), help to resolve this question. The preliminary data from this index show little correspondence with either the >150 μm (%) or MAR data (Fig. 12). Percentages of whole planktonic foraminifers have a similar range and magnitude within intervals of high and low $CaCO_3$ MAR. Intervals within the low accumulation events of the last interglacial and near 1.8 Ma have relatively high whole-to-fragment proportions, which implies that the minimum in accumulation is related to production rather than dissolution. However, Farrell and Prell (1991) suggested dissolution as the cause of these events at sites farther to the west. Although the data from Site 847 suggest that production controls the long-term changes in carbonate accumulation, additional work using more reliable dissolution indexes will be needed to decipher the cause of these events. Intervals of opal accumulation maxima at times of low $CaCO_3$ MAR (i.e., 1.7–2.0 Ma and 1.1–1.3 Ma) imply that production was dominated by siliceous organisms during these periods, especially because only a small proportion (~10%) of the opal rain is presently preserved at these sites (Dymond and Lyle, 1985; Archer et al., 1993).

Equatorial Transect

A recent compilation of surface primary productivity from the equatorial Pacific Ocean shows a two- to threefold increase in primary production along the equatorial Pacific transect from 140° to 95°W (Berger, 1989). Such a gradient should be reflected in the biogenic components of the underlying sediments. Lyle (1992) showed that the composition of surface sediments in the eastern Pacific does reflect the complex surface productivity gradients in this region near the coast of Central and South America. To evaluate the long-term changes in carbonate and opal productivity along the equator, we selected three sites along an equatorial transect from 140° to 95°W (Fig. 1). Site 847 provides the eastern anchor of the transect. A combination of data from Cores W8402A-14 (0°57′N, 138°57′W, 4287 m water depth), RC11-210 (1°49′N, 140°03′W, 4420 m water depth), and DSDP Site 573 (0°30′N, 133°19′W, 4301 m water depth) are used to quantify the biogenic sedimentation at the western location. The Core RC11-210 data are from Rea et al. (1991), the Core W8402A-14 data are from Lyle et al. (1988), and the DSDP Site 573 carbonate data are from Farrell and Prell (1991). DSDP Site 572 (1°26′N, 113°51′W, 3903 m water depth), midway between these sites, completes the transect with carbonate data from Farrell and Prell (1991) and opal data generated as part of this study. All age models were adjusted to be consistent with the orbitally tuned, GRAPE-based chronostratigraphy of Shackleton et al. (this volume). To capture the major trends in the carbonate and opal accumulation rate data for comparisons made in this study, we used a 20-point running mean of each time series (Fig. 13).

The west-to-east gradient in carbonate accumulation is small, especially between 1.5 and 2.0 Ma and during the past 0.5 m.y. One possibility is that dissolution of carbonate at the eastern sites has altered any preexisting gradient in the flux to the seafloor. Whole planktonic foraminifer (%) data was used to evaluate the dissolution gradient along the transect. Data for the past 0.5 m.y. show that the carbonate assemblage is better preserved in the eastern Site 847 compared with those in the deeper Sites W8402A-14 and DSDP 572 located farther west (Fig. 14); thus, dissolution cannot account for the small gradient. In fact, these data imply that the initial flux of carbonate before dissolution probably was greater in the central Pacific sites compared with that in the eastern sites. Although the surface gradient in production is not reflected by calcareous plankton, our preliminary data from the opal component show that opal accumulation does exhibit a strong west-to-east gradient during the past 1 m.y. (Fig. 13). Opal accumulation at Site 847 in the east is as much as four to five times the rate of the western Sites W8402A-14 and RC11-210. This factor is greater than the modern productivity gradient. Should opal production track the primary production, the longitudinal opal gradient would highlight the nonlinear relationship between production and preservation of opal in marine sediments, as noted by Broecker and Peng (1982).

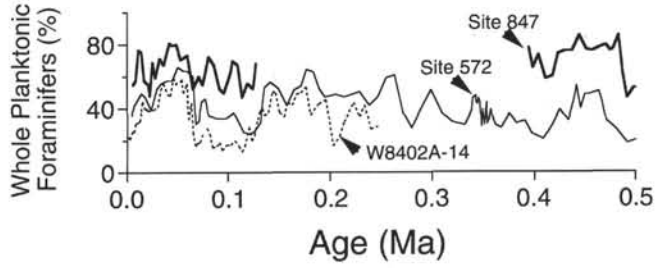

Figure 14. Time series of whole planktonic foraminifers (%) relative to fragments for the >150-μm fraction of Site W8402A-14 (dashed line, ~139°W, 4287 m water depth; Murray, unpubl. data), DSDP Site 572 (thin solid line, ~114°W, 3903 m water depth; Min-Te Chen, unpubl. data), and Site 847 (thick solid line, ~95°W, 3334 m water depth; this study).

CONCLUSIONS

Sedimentation during the past 3 m.y. at Site 847, beneath the high productivity region of the equatorial divergence, reflects long-term variations in the production of carbonate- and opal-secreting microplankton in this region. The cyclic changes in carbonate and opal components and their respective packing characteristics cause the density changes observed in the GRAPE WBD records generated by the Leg 138 shipboard scientists. Estimates of $CaCO_3$ (%) from the GRAPE data provide reliable values, with a mean difference of 4.5%. This difference appears to be random and probably reflects limitation of the GRAPE-based estimates.

A comparison of times series of the $\delta^{18}O$ of *G. sacculifer*, GRAPE, $\%CaCO_3$, and $CaCO_3$ MAR for the last 1 m.y. using age models based on oxygen isotope stratigraphy and tuning the GRAPE cycles to summer insolation at 65°N reveals that long-term changes are the same with the different models but that high-frequency orbital changes are different. This is especially true for the $CaCO_3$ MAR time series, where glacial to interglacial changes are age-model dependent.

An evaluation of distinct low-carbonate events during the last interglacial period and near 1.8 Ma suggests that production, not dissolution, is responsible for these changes. The relative increase in opal accumulation within these intervals implies that flux of material to the seafloor was attributed largely to siliceous microplankton, rather than calcareous organisms.

The long-term changes in carbonate and opal accumulation along a transect from the central to eastern equatorial Pacific during the past 3 m.y. show little gradient in carbonate accumulation, even though the carbonate component is better preserved in the eastern site. However,

a steep gradient in opal accumulation that is greater than the modern productivity changes across the region can be seen. These data highlight the nonlinear relationship between opal production and accumulation, where high rain rates have enhanced preservation.

ACKNOWLEDGMENTS

This project could not have been completed without the help of the world-class Brown sailors (Mike Zani, Site 847 carbonate and opal; Brian Doyle and Guy Adema, Site 572 opal) who spent numerous hours in the laboratory before the winds picked up. Mel Waldorf helped with sample grinding and Site 847 carbonate analyses before moving on to his pollen studies. We are grateful to Carmen Cors, April Martin, Jenna Cook, and Jane Donnelly for their help in preparation and counts of the faunal samples. Thanks to Min-Te Chen for providing unpublished fragmentation data for Site 572, Terri Hagelberg for providing revised composite depths for the Site 847 GRAPE data, and Nick Shackleton for distributing his orbitally tuned GRAPE-based age model. Technical support for this project was obtained by grants from JOI/USSAC (TAMRF-20528) and NSF/ATM (ATM-8812589).

REFERENCES*

Archer, D., Lyle, M., Rodgers, K., and Froelich, P., 1993. What controls opal preservation in tropical deep-sea sediments? *Paleoceanography,* 8:7–21.

Archer, D.E., 1991a. Equatorial Pacific calcite preservation cycles: production or dissolution? *Paleoceanography,* 6:561–571.

————, 1991b. Modeling the calcite lysocline. *J. Geophys. Res.,* 96:17037–17050.

Arrhenius, G., 1952. Sediment cores from the East Pacific. *In* Pettersson, H. (Ed.), *Rep. Swed. Deep-Sea Exped. 1947–48,* 5:1–227.

Berger, W.H., 1989. Global maps of ocean productivity. *In* Berger, W.H., Smetacek, V.S., and Wefer, G. (Eds.), *Productivity of the Oceans: Present and Past:* New York (Wiley), 429–455.

Berger, W.H., Adelseck, C.G, and Mayer, L., 1976. Distribution of carbonate in surface sediments of the Pacific Ocean. *J. Geophys. Res.,* 81:2617–2627.

Broecker, W.S., 1971. Calcite accumulation rates and glacial to interglacial changes in oceanic mixing. *In* Turekian, K.K. (Ed.), *The Late Cenozoic Glacial Ages:* New Haven, CT (Yale Univ. Press), 239–265.

Broecker, W.S., and Peng, T.-H., 1982. *Tracers in the Sea:* Palisades, NY (Lamont-Doherty Geological Observatory).

Chavez, F.P., and Barber, R.T., 1987. An estimate of new production in the equatorial Pacific. *Deep-Sea Res. Part A,* 34:1229–1243.

Clemens, S., Prell, W., Murray, D., Shimmield, G.B., and Weedon, G., 1991. Forcing mechanisms of the Indian Ocean monsoon. *Nature,* 353:720–725.

Dymond, J., and Lyle, M., 1985. Flux comparisons between sediments and sediment traps in the eastern tropical Pacific: implications for atmospheric CO_2 variations during the Pleistocene. *Limnol. Oceanogr.,* 30:699–712.

Farrell, J.W., 1991. Late Neogene palaeoceanography of the central equatorial Pacific: evidence from carbonate preservation and stable isotopes [Ph.D. thesis]. Brown Univ., Providence, RI.

Farrell, J.W., and Janecek, T.R., 1991. Late Neogene paleoceanography and paleoclimatology of the northeast Indian Ocean (Site 758). *In* Weissel, J., Peirce, J., Taylor, E., Alt, J., et al., *Proc. ODP, Sci. Results,* 121: College Station, TX (Ocean Drilling Program), 297–358.

Farrell, J.W., and Prell, W.L., 1989. Climatic change and $CaCO_3$ preservation: an 800,000 year bathymetric reconstruction from the central equatorial Pacific Ocean. *Paleoceanography,* 4:447–466.

————, 1991. Pacific $CaCO_3$ preservation and $\delta^{18}O$ since 4 Ma: paleoceanic and paleoclimatic implications. *Paleoceanography,* 6:485–498.

Hagelberg, T., Shackleton, N., Pisias, N., and Shipboard Scientific Party, 1992. Development of composite depth sections for Sites 844 through 854. *In* Mayer, L., Pisias, N., Janecek, T., et al., *Proc. ODP, Init. Repts.,* 138 (Pt. 1): College Station, TX (Ocean Drilling Program), 79–85.

Herbert, T.D., and Mayer, L.A., 1991. Long climatic time series from sediment physical property measurements. *J. Sediment. Petrol.,* 61:1089–1108.

Imbrie, J., Boyle, E.A., Clemens, S.C., Duffy, A., Howard, W.R., Kukla, G., Kutzbach, J., Martinson, D.G., McIntyre, A., Mix, A.C., Molfino, B., Morley, J.J., Peterson, L.C., Pisias, N.G., Prell, W.L., Raymo, M.E., Shackleton, N.J., and Toggweiler, J.R., 1992. On the structure and origin of major glaciation cycles, 1. Linear responses to Milankovitch forcing. *Paleoceanography,* 7:701–738.

Jones, G.A., and Kaiteris, P., 1983. A vacuum-gasometric technique for rapid and precise analysis of calcium carbonate in sediments and soils. *J. Sediment. Petrol.,* 53:655–660.

Keigwin, L., 1982. Isotopic paleoceanography of the Caribbean and East Pacific: role of Panama Uplift in late Neogene time. *Science,* 217:350–353.

Leinen, M., Cwienk, D., Heath, G.R., Biscaye, P.E., Kolla, V., Thiede, J., and Dauphin, J.P., 1986. Distribution of biogenic silica and quartz in recent deep-sea sediments. *Geology,* 14:199–203.

Luz, B., and Shackleton, N.J., 1975. $CaCO_3$ solution in the tropical East Pacific during the past 130,000 years. *In* Sliter, W.V., Bé, A.W., and Berger, W.H. (Eds.), *Dissolution of Deep-Sea Carbonates.* Spec. Publ. Cushman Found. Foraminiferal Res., 13:142–150.

Lyle, M., 1992. Composition maps of surface sediments of the eastern tropical Pacific Ocean. *In* Mayer, L., Pisias, N., Janecek, T., et al., *Proc. ODP, Init. Repts.,* 138 (Pt. 1): College Station, TX (Ocean Drilling Program), 101–115.

Lyle, M., Murray, D.W., Finney, B.P., Dymond, J., Robbins, J.M., and Brooksforce, K., 1988. The record of Late Pleistocene biogenic sedimentation in the eastern tropical Pacific Ocean. *Paleoceanography,* 3:39–59.

Mayer, L., Pisias, N., Janecek, T., et al., 1992. *Proc. ODP, Init. Repts.,* 138 (Pts. 1 and 2): College Station, TX (Ocean Drilling Program).

Mayer, L.A., 1991. Extraction of high-resolution carbonate data for paleoclimate reconstruction. *Nature,* 352:148–150.

Mortlock, R.A., and Froelich, P.N., 1989. A simple method for the rapid determination of biogenic opal in pelagic marine sediments. *Deep-Sea Res. Part A,* 36:1415–1426.

Murray, D.W., and Prell, W.L., 1991. Pliocene to Pleistocene variations in calcium carbonate, organic carbon, and opal on the Owen Ridge, northern Arabian Sea. *In* Prell, W.L., Niitsuma, N., et al., *Proc. ODP, Sci. Results,* 117: College Station, TX (Ocean Drilling Program), 343–363.

Murray, R.W., and Leinen, M., 1993. Chemical transport to the seafloor of the equatorial Pacific Ocean across a latitudinal transect at 135°W: tracking sedimentary major, trace, and rare earth element fluxes at the Equator and the Intertropical Convergence Zone. *Geochim. Cosmochim. Acta.,* 57:4141–4163.

Peterson, L.C., and Prell, W.L., 1985. Carbonate dissolution in Recent sediments of the eastern equatorial Indian Ocean: preservation patterns and carbonate loss above the lysocline. *Mar. Geol.,* 64:259–290.

Pisias, N.G., and Rea, D.K., 1988. Late Pleistocene paleoclimatology of the central Equatorial Pacific: sea surface response to the southeast trade winds. *Paleoceanography,* 3:21–37.

Rea, D.K., Pisias, N.G., and Newberry, T., 1991. Late Pleistocene paleoclimatology of the central Equatorial Pacific: flux patterns of biogenic sediments. *Paleoceanography,* 6:227–244.

Robinson, S.G., 1990. Applications for whole-core magnetic susceptibility measurements of deep-sea sediments: Leg 115 results. *In* Duncan, R.A., Backman, J., Peterson, L.C., et al., *Proc. ODP, Sci. Results,* 115: College Station, TX (Ocean Drilling Program), 737–771.

Ruddiman, W.F., Raymo, M.E., Martinson, D.G., Clement, B.M., and Backman, J., 1989. Pleistocene evolution: Northern Hemisphere ice sheets and North Atlantic Ocean. *Paleoceanography,* 4:353–412.

Shackleton, N.J., and Shipboard Scientific Party, 1992. Sedimentation rates: toward a GRAPE density stratigraphy for Leg 138 carbonate sections. *In* Mayer, L., Pisias, N., Janecek, T., et al., *Proc. ODP, Init. Repts.,* 138 (Pt. 1): College Station, TX (Ocean Drilling Program), 87–91.

Shipboard Scientific Party, 1992. Site 847. *In* Mayer, L., Pisias, N., Janecek, T., et al., *Proc. ODP, Init. Repts.,* 138 (Pt. 1): College Station, TX (Ocean Drilling Program), 335–393.

Takahashi, K., and Honjo, S., 1983. Radiolarian skeletons: size, weight, sinking speed, and residence time in tropical pelagic oceans. *Deep-Sea Res. Part A,* 30:543–568.

Thunell, R.C., 1976. Optimum indices of calcium carbonate dissolution in deep-sea sediments. *Geology,* 4:525–528.

* Abbreviations for names of organizations and publication titles in ODP reference lists follow the style given in *Chemical Abstracts Service Source Index* (published by American Chemical Society).

Date of initial receipt: 9 June 1993
Date of acceptance: 17 May 1994
Ms 138SR-122

APPENDIX
Tests of the Opal Leach on Selected Site 847 Samples

In this study, we used a 2 M Na_2CO_3 leach of a ground material to quantify the biogenic opal portion of the sample. This leach was made on a dried sample after removal of the carbonate and organic fractions. S. Hovan (U. of Michigan) used a sequential leach to quantify the lithogenic portion of Leg 138 samples. His values were significantly lower than our estimates based on [100 – ($CaCO_3$ + opal)], and he suggested that incomplete digestion of opal with our method was part of the discrepancy. Examination of the residual material after a 6-hr leach in an 85°C hot water bath revealed that some samples contained relatively undigested radiolarian parts. To quantify this additional opal material not digested by the primary leach and possibly to resolve the discrepancy noted by Hovan, additional digestions were made using a stronger base (2 N NaOH) for 5 hr and then 8 hr more to ensure complete digestion of the opal. The results are presented in the Appendix Table and Appendix Figure.

The duplicate treatments of the standard opal leach were performed on 9 samples of high to low carbonate and opal concentrations (18 total in the test analysis). The test samples were taken from the remaining one-third of the 5-cm^3 samples of bulk sediment and were not ground to be consistent with the treatment of samples by Hovan. After 6 hr in the hot water bath, the eight treated samples were centrifuged, 15 mL of the supernatant was removed for analysis, and then most of the remaining portion of the supernatant was removed without disturbing the solid material on the bottom of the centrifuge tube. These residuals of the leach were rinsed 3 times with hot distilled and deionized water (DDW). After the final rinse, one of the duplicates of each sample was sieved at 38 µm to separate the coarse biogenic from fine silt and clay materials. This provided a <38 µm, a >38 µm, and a total portion for each sample (Appendix Table). The unsieved sample was analyzed and compared to the combination of the <38 and >38 µm portions to ensure that none of the sample had been lost during the sieving process. All residuals were dried to remove remaining rinse water. Then 17.5 mL of 2 N NaOH was added, and the centrifuge tubes were placed in a hot water bath for 5 hr, with stirring at hourly intervals. The tubes then were centrifuged and 15 mL of the supernatant was removed for analysis. The leach residuals of the split and unsplit portions of the first four samples in Appendix Table were rinsed three times with hot DDW. Again, the residuals of these four samples were dried and treated with 17.5 mL of 2 N NaOH. The tubes were placed in a hot water bath for 8 hr, centrifuged, and 15 mL was removed for analysis. The residuals in all 12 tubes were examined under a microscope; no parts of the siliceous organisms were observed.

In all samples, more than 75% of the total silica leached was removed by the first treatment (Appendix Table and Appendix Figure). Of the additional silica removed with subsequent leaches, most came from the <38-µm fraction. This suggests that radiolarian parts did not contribute to much additional opal. The highest silica values in supernatants using the NaOH leach are from the <38-µm portion of low-carbonate samples (Appendix Table). We suggest that this silica was leached from clays and was not of biogenic origin. Therefore, although additional silica was leached from all samples, the source of most of this silica probably is the clays, not the biogenic opal. As far as opal from undigested radiolarians is concerned, the contribution is likely to be small. A total of 0.51% Si was leached from the >3-µm fraction of Sample 138-847C-1H-3, 92 cm. The original weight of the sample was 42.92 mg, and this amount of silicon represents ~0.55 mg of opal (2.5 × 0.219 mg Si-opal = 0.548 mg of opal). Takahashi and Honjo (1983) estimated that a typical radiolarian from Quaternary sediments weighed 0.136 µg. Thus, a total of 4000 radiolarians might account for the silica removed in the 13-hr NaOH leach of Sample 138-847C-1H-3, 92 cm. Visually, this is a large number, but it constitutes only about 4% of the total opal in the sample. However, this could be part of the difference between the terrigenous amount estimated from [100 – (CaCO3 + opal)] and the sequential leach of Hovan (this volume).

Appendix Table
Opal Extraction Tests

Core, section, interval (cm)	Weight (mg)	Si[a] (%)	Mean Si (%)	Split[b]	Si[c] (%)	Mean Si (%)	Split	Si[d] (%)	Mean Si (%)	Si[e] (%)	Si[f] (%)	$CaCO_3$[g] (%)
138-847C-1H-3, 92	48.97	11.41	11.41	Total	1.28	1.26	Total	0.30	0.31	12.98	11.83	49.85
					1.24			0.31				
	42.92	11.97	11.97	<38 µm	1.12	1.08	<38 µm	0.12	0.12	13.68		
					1.03			0.11				
				>38 µm	0.11	0.11	>38 µm	0.39	0.40			
					ND			0.41				
138-847C-1H-4, 137	45.34	10.24	10.24	Total	0.78	0.76	Total	0.08	0.09	11.09	11.34	63.02
					0.74			0.09				
	45.33	10.07	10.07	<38 µm	0.53	0.49	<38 µm	0.03	0.03	10.72		
					0.44			ND				
				>38 µm	0.17	0.14	>38 µm	0.00	0.00			
					0.11			0.00				
138-847C-1H-5, 2	46.90	6.08	6.08	Total	0.64	0.59	Total	0.07	0.06	6.73	8.80	71.66
					0.54			0.05				
	49.49	6.02	6.02	<38 µm	0.56	0.51	<38 µm	0.04	0.04	6.71		
					0.46			0.04				
				>38 µm	0.18	0.14	>38 µm	0.01	0.00			
					0.10			0.00				
138-847C-9H-3, 135	47.50	3.95	3.95	Total	1.04	0.99	Total	0.15	0.15	5.09	3.47	75.33
					0.95			0.15				
	63.23	3.88	3.88	<38 µm	0.63	0.60	<38 µm	0.06	0.06	4.82		
					0.57			ND				
				>38 µm	0.28	0.28	>38 µm	0.00	0.00			
					ND			0.01				
138-847B-1H-3, 17	49.30	14.15	14.13	Total	2.02	2.01				16.14	14.97	28.14
		14.11			2.00							
	53.76	13.65	13.67	<38 µm	1.84	1.84				15.58		
		13.69			1.84							
				>38 µm	0.07	0.07						
					0.07							
138-847C-6H-1, 47	50.72	17.52	17.49	Total	3.46	3.46				20.95	16.35	22.63
		17.46			3.46							
	50.66	17.71	17.76	<38 µm	2.67	2.67				21.21		
		17.81			2.67							
				>38 µm	0.81	0.78						
					0.74							
138-847C-6H-1, 62	50.44	14.26	14.28	Total	3.78	3.77				18.05	14.17	22.75
		14.30			3.76							
	50.27	14.56	14.38	<38 µm	2.93	2.91				17.83		
		14.19			2.88							
				>38 µm	0.55	0.55						
					0.55							
138-847D-6H-3, 32	50.27	15.48	15.48	Total	3.03	3.03				18.51	14.80	19.28
		ND			3.03							
	52.88	15.44	15.44	<38 µm	1.97	1.97				18.13		
		15.43			1.97							
				>38 µm	0.72	0.72						
					0.72							
138-847D-6H-3, 47	50.42	16.02	15.99	Total	3.38	3.38				19.37	12.80	25.54
		15.96			3.38							
	50.65	17.21	17.22	<38 µm	2.78	2.78				20.62		
		17.23			2.78							
				>38 µm	0.62	0.62						
					0.62							

[a]Si concentrations for samples treated with the hot Na_2CO_3 leach described in the "Methods" section (this chapter), except that the samples were not ground. All samples were run in duplicate. ND = no data.

[b]Residuals after the first leach were rinsed three times with hot DDW, and one of the residuals for each sample was sieved at 38 µm. Total is the unsplit duplicate.

[c]Si concentrations for samples treated with 17.5 ml of 2N NaOH and placed in a hot water bath for 5 hr.

[d]Si concentrations for four of the samples and the respective splits that were rinsed, dried, and treated with 17.5 ml of 2N NaOH and placed in a hot water bath for 8 hr.

[e]Sum of mean Si concentrations from the sequential extractions for each sample. The sum for samples that were split includes analyses of both the less than and greater than 38-µm portions.

[f]Si concentrations from Table 2.

[g]$CaCO_3$ concentrations from Table 2.

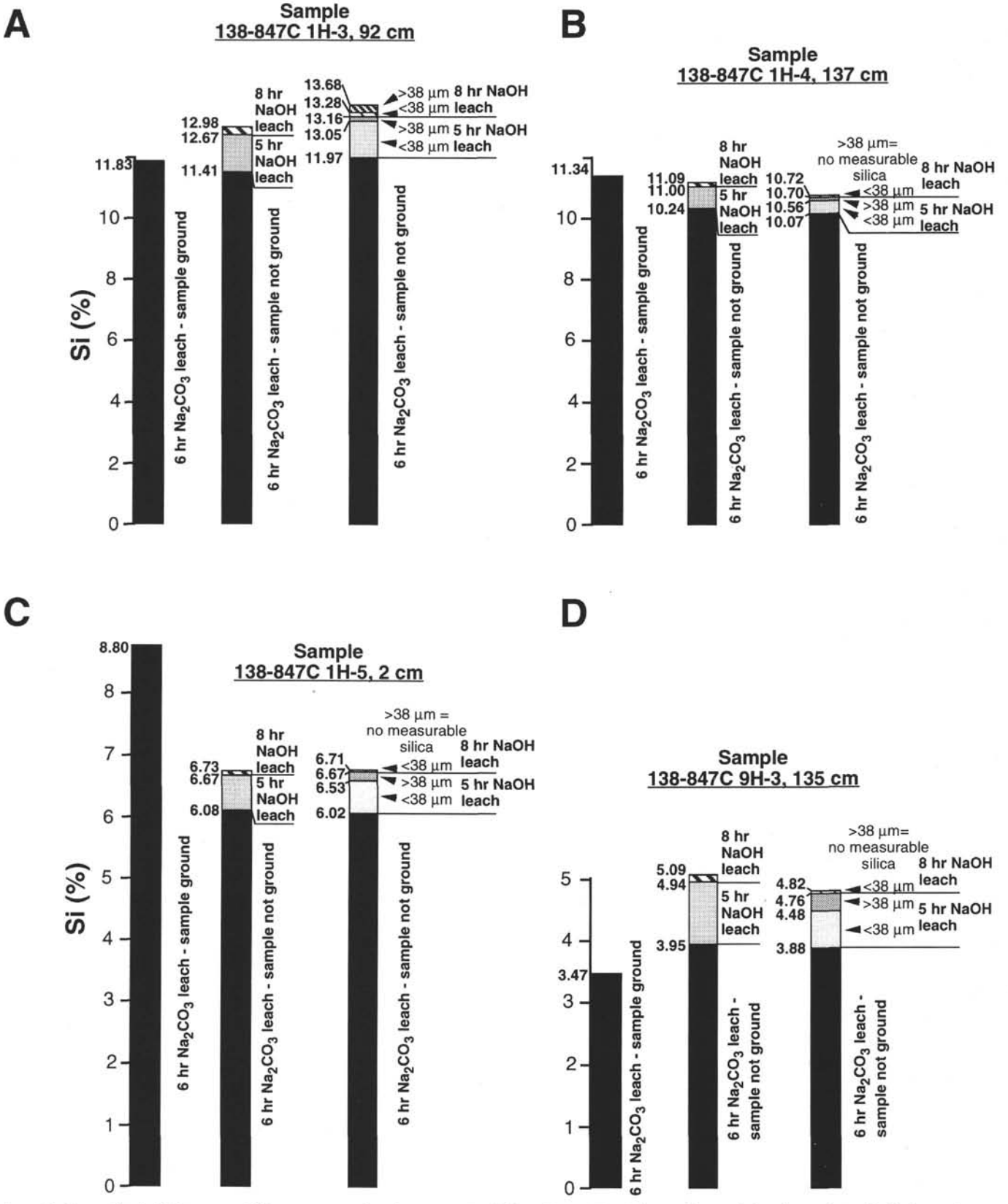

Appendix Figure. Stacked histograms of silicon concentrations in test samples (**A–D**) of the opal leach from carbonate-rich and -poor intervals. Each sample was analyzed in triplicate; one portion was ground and treated using the standard technique. These values are from data listed in Table 2 of this chapter and plotted on the left. Two additional portions were not ground and first treated with a 6-hr Na_2CO_3 leach (solid black bars), then were treated with a 5-hr NaOH leach (dotted patterns), and finally with an 8-hr NaOH leach (stripped patterns). The center plots in all samples are results without sieving the material, whereas the plot on the right is from residuals that were sieved at 38 µm after the first Na_2CO_3 leach. Most of the additional silicon removed from the solids was from the fine fraction. The large difference in silicon percentages between the ground and unground portions of Sample 138-847C-1H-5, 2 cm, is attributed to sediment inhomogeneities.